Self-Avoiding Polygons in (L, M)-Tubes

A Thesis Submitted to the
College of Graduate Studies and Research
in Partial Fulfillment of the Requirements
for the degree of Master of Science
in the Department of Mathematics and Statistics
University of Saskatchewan
Saskatoon

By
Jeremy Eng

Permission to Use

In presenting this thesis in partial fulfilment of the requirements for a Postgraduate degree from the University of Saskatchewan, I agree that the Libraries of this University may make it freely available for inspection. I further agree that permission for copying of this thesis in any manner, in whole or in part, for scholarly purposes may be granted by the professor or professors who supervised my thesis work or, in their absence, by the Head of the Department or the Dean of the College in which my thesis work was done. It is understood that any copying or publication or use of this thesis or parts thereof for financial gain shall not be allowed without my written permission. It is also understood that due recognition shall be given to me and to the University of Saskatchewan in any scholarly use which may be made of any material in my thesis.

Requests for permission to copy or to make other use of material in this thesis in whole or part should be addressed to:

Head of the Department of Mathematics and Statistics
142 McLean Hall
106 Wiggins Road
University of Saskatchewan
Saskatoon, Saskatchewan
Canada
S7N 5E6

Abstract

By studying self-avoiding polygons (SAPs) in (L, M)-tubes (a tubular sublattice of the simple cubic lattice) as a sequence of 2-spans, transfer matrices can be used to obtain theoretical and numerical results for these SAPs. As a result, asymptotic properties of these SAPs, such as pattern densities in a random SAP and the expected span of a random SAP, can be calculated directly from these transfer matrices. These same results can also be obtained for compact polygons, as well as SAPs under the influence of an external force (called compressed or stretched polygons). These results can act as tools for examining the entanglement complexity of SAPs in (L, M)-tubes.

In this thesis, it is examined how transfer matrices can be used to develop these tools. The transfer matrix method is reviewed, and previous transfer matrix results for SAPs in (L, M)-tubes, as well as SAPs subjected to an external force, are presented. The transfer matrix method is then similarly applied to compact polygons, where new results regarding compact polygons are obtained, including proofs for a compact concatenation theorem and for a compact pattern theorem. Also in this thesis, transfer matrices are actually generated (via the computer) for relatively small tube sizes. This is done for the general case of SAPs in (L, M)-tubes, as well as for the compact and external force cases. New numerical results are obtained directly from these transfer matrices, and a new algorithm for generating polygons is also developed from these transfer matrices. Compact polygons are actually generated (via the computer) for relatively small tube sizes and spans by using the developed polygon generation algorithm, and new numerical results for pattern densities and limiting free energies are obtained for stretched and compressed polygons.

Acknowledgements

First and foremost, I would like to thank my supervisor Dr. Chris Soteros for the tremendous amount of support she provided me throughout the two year process of my masters program. Without her knowledge, advice, and guidance, this thesis would have simply not been possible. I would also like to thank my examining committee for taking the time to read my thesis and for their suggestions and comments. This committee includes Dr. Juxin Liu, Dr. Raj Srinivasan, and Dr. Richard Bowles. I would also like to acknowledge the work done by Allan Duffy which I adopted, and I would especially like to thank him for heavily commenting his computer code (which is rare) so I could fully understand it in a timely manner. I greatly appreciate the access I had to the high-performance computers from Compute Canada, which allowed for my higher-order programs to run relatively quickly.

I would like to thank the PotashCorp Kamskénow Science Outreach Program for not only providing me with funding, but also for providing me the unique opportunity of leading fun, high-quality, hands-on science activities with community school students. My special thanks goes to Lana Elias, the director of the program, for making it such an enjoyable experience. I would also like to thank my parents for their unconditional, loving support, as well as my friends and family who kept me sane during my thesis writing process. I am grateful to all of the professors with whom I took at least one class from, and a big thank you goes out to the Department of Mathematics and Statistics' staff for the various tasks they did for me. Lastly, I would like to thank Kevin McGregor, Marla Cheston, and Matthew Schmirler for sharing their knowledge regarding computers and (arguably) more importantly, their friendship.

Contents

List of Tables

List of Figures

Chapter 1

Introduction

This thesis focuses on studying self-avoiding polygons (SAPs) in (L, M)-tubes (a tubular sublattice of the simple cubic lattice) by using transfer matrices. By confining SAPs to an (L, M)-tube, SAPs can only grow in one direction, and therefore, transfer matrices can be used to obtain theoretical and numerical results for SAPs in (L, M)-tubes, which would be otherwise unattainable for non-restricted SAPs. This thesis reviews the transfer matrix method and reviews previous transfer matrix results for polygons in (L, M)-tubes obtained by Soteros in [24]. These results include a pattern theorem for SAPs in (L, M)-tubes, an expression for the expected number of occurrences of a pattern in a random SAP in an (L, M)-tube, and also an expression for the expected span of a random SAP in an (L, M)-tube.

Also in this thesis, transfer matrices are generated for relatively small tube sizes, and new numerical results are obtained directly from the transfer matrices for these small tube sizes. New results regarding compact polygons are also achieved, including proofs for a concatenation theorem and a pattern theorem for compact polygons. A new algorithm which covers how transfer matrices can be used to generate SAPs in (L, M)-tubes is also presented, as well as new numerical results regarding SAPs subjected to an external force. First, we address the question as to why confined SAPs are a topic of interest.

1.1 Motivation

The main motivation behind studying geometrically constrained SAPs is the study of ring polymers which are spatially confined. A *polymer* is a long chain molecule consisting of a large number of repeated units (called monomers), which are held together by chemical bonds[30]. The *functionality* of a monomer is the number of other monomers with which it must bond[17]. A *linear polymer* is a chain of monomers with functionality two, with both end monomers of the polymer having a functionality of one[17]. If instead both end monomers are bonded to each other, then the polymer

is referred to as a *ring polymer*[17].

As an example, if one is not interested in the atomic level, double-stranded Deoxyribonucleic acid (DNA) can be viewed as a polymer based on the axis around which its double helix winds. The DNA's base-pairs of nucleotides can be considered the monomers of the polymer[4]. Bacterial and viral DNA can be found in a closed circular form[31], and human mitochondrial DNA is also a circular molecule[20]. Although human and animal DNA is usually linear, "giant DNA molecules in higher organisms form loop structures held together by protein fasteners in which each loop is largely analogous to closed circular DNA"[31]. Thus circular DNA can be viewed as a ring polymer and linear DNA can form loops that are comparable to ring polymers.

Another example of a polymer is proteins, where the amino acids which make up the protein may be viewed as its monomers.

"Polymers are typically subject to spatial restraints, either as a result of molecular crowding in the cellular medium or of direct spatial confinement"[18]. For example, human DNA, which is approximately 1 m in length, is confined in the cell nucleus, whose diameter is only about 10 μm[18]. Scaling the cell nucleus up to the size of a baseball, it would be equivalent to stuffing approximately 7.5 kilometers of fishing line inside a baseball. As one can imagine, packing an abundance of fishing line into such a small volume may result in quite the tangled fishing line. The same is the case with long polymers subject to confinement.

Since "the conformational and physical properties of confined polymers depend crucially on the dimensionality and width of the confining region"[19], studying spatially confined ring polymers is a topic of interest. One conformational property of a ring polymer is its entanglement complexity. How does the confining region affect how often a ring polymer is knotted? Does confinement change how often one sees certain knot types, and if so, how do the knot types observed change with the confining region? What exactly does it mean for a ring polymer to be knotted? In order to discuss these questions further, some basic knot theory must first be presented, and following this, a detailed outline of the thesis will be given.

1.2 Basic Knot Theory

A mathematical knot is defined as a subset of points in $\mathbb{R}^3$ that are homeomorphic to a circle[6]. A major difference between mathematical knots and the conventional idea of a knot, such as in a shoelace, is that mathematical knots must be closed. That is, there are no ends to tie or untie the

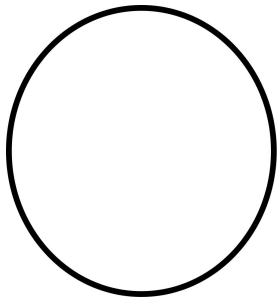

Figure 1.1: The unknot (ϕ).

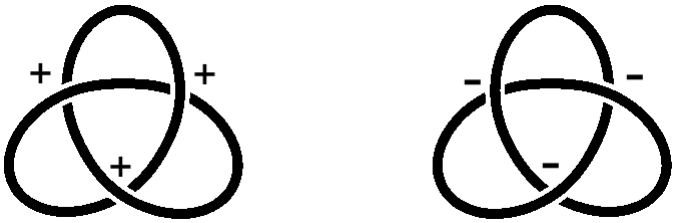

Figure 1.2: The positive trefoil (3_1^+) on the left and the negative trefoil (3_1^-) on the right.

knot. Two knots are considered *equivalent* if one knot can be continuously deformed into the other without crossing itself during the process[10]. Equivalence classes are naturally formed from this definition, and these equivalance classes are referred to as *knot types*.

The simplest knot type is the trivial knot, called the unknot (denoted by ϕ), shown in Figure 1.1. If a knot is not the unknot, then we say it is *knotted*. The simplest nontrivial knot is the trefoil knot (denoted by 3_1). If a knot is equivalent to its mirror image, then we call it *achiral*; if it is not equivalent to its mirror image, then we call it *chiral*. Notice that 3_1 is chiral, and there are two types of trefoils: the positive trefoil and the negative trefoil. A projection of these knots is shown in Figure 1.2, with over and under crossings indicated (this is an example of a knot diagram). These two types of trefoils are not equivalent; therefore, they are considered to be different knot types (denoted by 3_1^+ and 3_1^- respectively). An example of an achiral knot is the figure-8 knot, as shown in Figure 1.3.

This thesis also includes the following chiral knots: the cinquefoil knot (denoted by 5_1), the three-twist knot (denoted by 5_2), and the pretzel knot (denoted by 6_1), all of which can be seen in Figure 1.4. It should be noted that all of the knotted knots presented thus far are *prime knots*. That is, they cannot be decomposed into two or more knotted knots. If a knot is composed of two

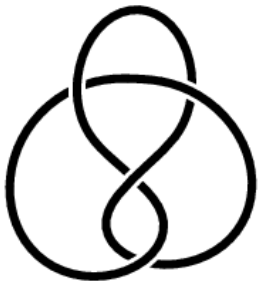

Figure 1.3: The figure-8 knot (4_1).

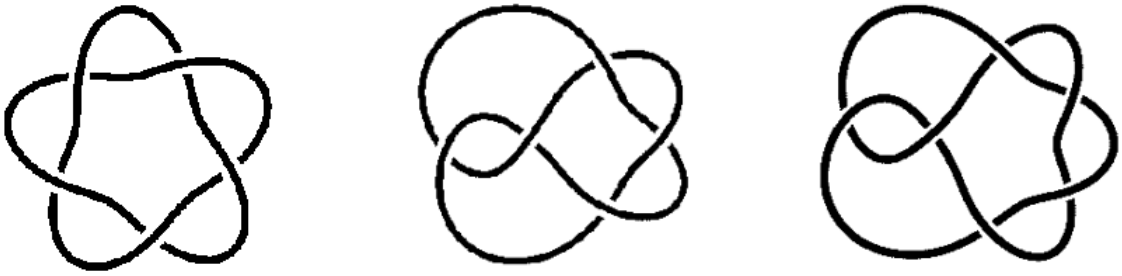

Figure 1.4: From left to right, the cinquefoil knot (5_1), the three-twist knot (5_2), and the pretzel knot (6_1).

or more prime knots, then it is called a *composite knot*. For example, a 3_1^+ may be composed with a 3_1^-, and the resulting knot would be denoted by $3_1^+ \# 3_1^-$, where the symbol # essentially means "composed with". See Figure 1.5 for an example of a composite knot.

It should be noted that it is not always trivial to determine a knot's knot type. For example, the knot pictured in Figure 1.6 can actually be continuously deformed into the unknot. This thesis will not go into detail about knot identification, but it should be noted that the software program

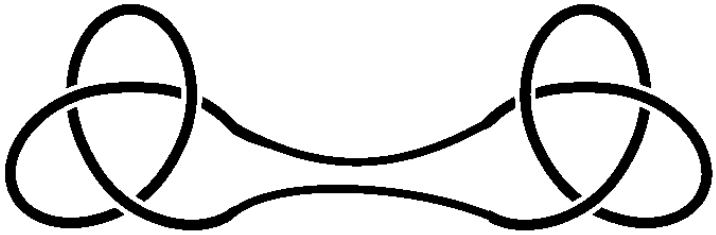

Figure 1.5: A $3_1^+ \# 3_1^-$ knot.

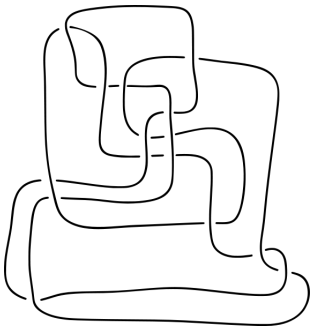

Figure 1.6: This knot is actually an unknot (ϕ).

KnotPlot[23] was used to identify the knot types of the polygons generated in this thesis (covered in Section 4.2).

In the 1960's, Frisch and Wassermann[12], and Delbruck[7] (FWD), conjectured that sufficiently long ring polymers would be knotted, with high probability. This was one of the first questions regarding the entanglement of polymers, and the FWD conjecture was answered using a lattice model. Diao *et. al*[8] have since proved it for off-lattice models. Soteros[24] extended the proof to polygons in the lattice tube, and Atapour *et. al*[3] extended the proof to polygons under an external force. In this thesis, the proof will be extended to compact polygons, and specific details about entanglement complexity will be explored by using transfer matrices.

1.3 Thesis Outline

The remainder of this thesis is outlined as follows. Chapter 2 will explain how linear and ring polymers can be modelled on the simple cubic lattice as, respectively, self-avoiding walks and polygons. Chapter 2 will also review some already established results regarding the entanglement complexity of SAPs in the simple cubic lattice, as well as introduce the definition of an (L, M)-tube, along with some results which pertain to SAPs in an (L, M)-tube. Chapter 3 will explain how transfer matrices can be used in general combinatorial problems, and then an appropriate transfer matrix for SAPs in (L, M)-tubes will be defined. Chapter 3 will then show how this transfer matrix can be used in obtaining a pattern theorem for SAPs in (L, M)-tubes, an expression for the expected number of occurrences of a pattern in a random SAP in an (L, M)-tube, and also an expression for the expected span of a random SAP in an (L, M)-tube. Note that this discussion is based on previous results by Soteros and Duffy in [24] and [9], but the work presented in Chapter 3 is more generalized

and contains more details. Chapter 3 will also briefly explain the computer implementation of the transfer matrix (which was developed by Duffy), which was used to obtain numerical results involving SAPs in (L, M)-tubes. Chapter 4 contains new results which focus on compact polygons in (L, M)-tubes. A new concatenation theorem, pattern theorem, expression for the expected number of occurrences of a pattern, and expression for the expected span for compact polygons is presented for compact polygons. Also contained in Chapter 4 is a new algorithm for using the transfer matrix to generate polygons in an (L, M)-tube. Chapter 5 is devoted to adding an external force into the model and observing how the force affects the limiting free energy (defined in equation (5.6)), as well as the expected number of occurrences of a pattern and the expected span of a polygon. It should be noted that most of the theoretical results from this chapter are a review of Atapour *et al.*'s work in [3], while all of the numerical results new. Appendix A contains the details of the 2-span generation algorithm (developed by Duffy) used in the generation of the transfer matrices, while Appendices B and C contain the details of how sections and column states were given a unique number during the generation process, which was also developed by Duffy.

Chapter 2

Model

Lattice animal models are a set of popular models used for modelling polymers[30]. This thesis will focus on using the three-dimensional integer lattice, also known as the simple cubic lattice. Linear polymers will be modelled by self-avoiding walks (SAWs), and ring polymers will be modelled by self-avoiding polygons (SAPs) (definitions of these terms will be given in Section 2.1). Each SAW or SAP will represent a possible conformation of a linear or ring polymer respectively, with vertices representing monomers and edges representing the chemical bonds which hold the monomers together. As discussed in Chapter 1, circular DNA can be viewed as a ring polymer based on the axis around which its double helix winds. The axis of the double helix can be represented by a curve, and this curve can then be approximated by a lattice polygon (Figure 2.1).

Polymers are almost always immersed in a solvent[30]. Since a good solvent results in it being more favourable for monomers to be surrounded by molecules of the solvent rather than by other monomers[30], the chance of finding a monomer inside a region close to another monomer is very small. This is referred to as the *excluded volume* property[30]. One advantage of modelling polymers as SAWs and SAPs on the simple cubic lattice is that this model possesses the excluded volume property[30], which is reflected in the self-avoiding nature of SAWs and SAPs.

Another advantage to using the simple cubic lattice is that "field theoretic arguments suggest

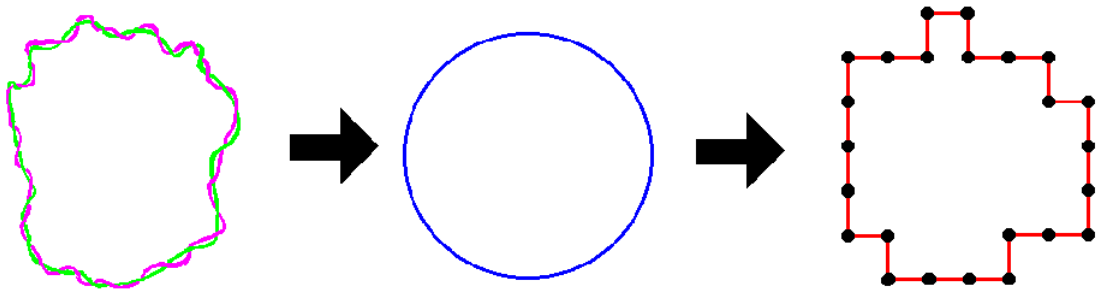

Figure 2.1: Circular DNA can be modelled by a lattice polygon.

that there exist universal quantities ... which will be exactly the same for lattice models and for real polymers"[24]. An example of a universal quantity which is the same for lattice models and for real polymers is the critical exponent ν for the *root-mean-square end-to-end distance*, which is calculated as follows. If a SAW in $\mathbb{Z}^3$ (linear polymer in $\mathbb{R}^3$) consists of $N+1$ vertices (monomers) $(v_0, \ldots, v_N)$, then its *end-to-end distance* R is defined as the euclidean distance from v_0 to v_N (i.e. $R = ||v_N - v_0||$). The *root-mean-square end-to-end distance* R_F for SAWs (linear polymers) with $N+1$ vertices (monomers) is then defined as the root mean square of R:

$$R_F = \sqrt{\langle R^2 \rangle} \sim N^{\nu} \text{ as } N \to \infty, \tag{2.1}$$

where $\langle \cdot \rangle$ averages over all SAWs (linear polymers) with $N+1$ vertices (monomers)[30], and the symbol "$\sim$" is defined right after equation 3.12.

Thus, this allows us to move from $\mathbb{R}^3$ (where real polymers exist) into $\mathbb{Z}^3$, while still maintaining these same universal quantities. Since the simplified $\mathbb{Z}^3$ allows for mathematical analysis which may not be available in $\mathbb{R}^3$, we can obtain mathematical results for $\mathbb{R}^3$ (by using $\mathbb{Z}^3$).

This chapter will first define the simple cubic lattice and review some important results which have already been discovered for SAWs and SAPs in the simple cubic lattice, including their entanglement complexity. A model which introduces confinement contraints on the simple cubic lattice will follow, and a comparison of the two models will be made.

2.1 The Simple Cubic Lattice

In the interest of using consistent notation, the remainder of this chapter, unless noted otherwise, is based on [24]. This notation is considered standard for lattice models of linear and ring polymers.

Definition 2.1 (Simple cubic lattice[3])**.** The *simple cubic lattice*, also known as the *three-dimensional integer lattice*, is defined to be the infinite graph embedded in $\mathbb{R}^3$ with vertex set $\mathbb{Z}^3$ and edge set $\{\{u, v\} | u, v \in \mathbb{Z}^3, ||u - v|| = 1\}$, where $|| \cdot ||$ is the Euclidean norm.

Depending on the context, $\mathbb{Z}^3$ will be used to represent either the three-dimensional integer lattice or its vertex set. Similarily for V, a set of vertices in $\mathbb{Z}^3$, V will be used to represent either the vertex set V or the subgraph of $\mathbb{Z}^3$ induced by this vertex set. That is, V may represent the subgraph with vertex set V and edge set $\{\{u, v\} | u, v \in V, ||u - v|| = 1\}$.

Definition 2.2. An n-edge *self-avoiding walk* (SAW) on the simple cubic lattice, $\mathbb{Z}^3$, is an alternating sequence of $n+1$ distinct vertices and n directed edges, u_0, (u_0, u_1), u_1, (u_1, u_2), u_2, ...,

u_{n-1}, (u_{n-1}, u_n), u_n, such that the vertices $u_i \in \mathbb{Z}^3$ for $i = 0, \ldots, n$, $u_0 = (0, 0, 0)$, and for each $i = 0, \ldots, n-1$, the directed edge (u_i, u_{i+1}) joins two nearest neighbour vertices in $\mathbb{Z}^3$ (i.e. u_{i+1} and u_i differ only in one coordinate with the difference being ± 1).

SAWs are well known as good models for very long linear polymers in equilibrium in dilute solution, and ring polymers in dilute solution have been successfully modelled using self-avoiding polygons[30].

Definition 2.3. A $2n$-edge *self-avoiding polygon* (SAP) in $\mathbb{Z}^3$ is an alternating sequence of $2n$ distinct vertices and $2n$ undirected edges, u_0, $\{u_0, u_1\}$, u_1, $\{u_1, u_2\}$, u_2, ..., u_{2n-1}, $\{u_{2n-1}, u_0\}$, such that for each $i = 0, \ldots, 2n-1$, the vertex $u_i \in \mathbb{Z}^3$ and the edge $\{u_i, u_{i+1}\}$ joins two nearest neighbour vertices in $\mathbb{Z}^3$.

Notice that although the edges of a SAP are not ordered and directed in the definition of a SAP, an ordering and direction can be put on them. First, define the following lexicographic ordering of the vertices in $\mathbb{Z}^3$: given two vertices $v_A = (x_A, y_A, z_A)$ and $v_B = (x_B, y_B, z_B)$ in $\mathbb{Z}^3$, v_A comes before v_B if:

1. $x_A < x_B$, or
2. $x_A = x_B$ and $y_A < y_B$, or
3. $x_A = x_B$ and $y_A = y_B$ and $z_A < z_B$.

Definition 2.4. The *lexicographical ordering of a SAP* is as follows: define the polygon's *first vertex* v_1 to be the first vertex of the polygon following the lexicographic ordering of the polygon's vertices. Notice v_1 will have two edges connected to it, with two corresponding vertices. Of these two vertices, choose the smallest (lexicographically), and call this v_2. Direct the edge from v_1 to v_2 and call this edge the first edge in the ordering of edges of the polygon. The ordering and direction of the remaining edges continues in a cyclic fashion around the polygon.

Definition 2.5. For any SAW or SAP ω, define the *length* of ω, $|\omega|$, to be the number of edges in ω.

Definition 2.6. Define c_n to be the number of n-edge SAWs.

Definition 2.7. Define p_{2n} to be the number of $2n$-edge SAPs, up to translation, or equivalently, the number of $2n$-edge lexicographically ordered SAPs whose first vertex is at the origin.

A natural question that arises after defining c_n and p_{2n} is how difficult are they to determine? Finding exact results for c_n and p_{2n} is a problem with an exponential complexity, and an "efficient" algorithm for calculating c_n and p_{2n} has yet to be discovered[5]. However, there have been results for the growth rate of c_n and p_{2n}. In 1954, Hammersley and Morton proved c_n grows at an exponential rate:

Theorem 2.1 (Hammersley and Morton[15])**.** *The following limit exists:*

$$\kappa := \lim_{n\to\infty} n^{-1} \log c_n. \tag{2.2}$$

κ is known as the *connective constant*[14] for $\mathbb{Z}^3$. The following definition follows from Theorem 2.1:

Definition 2.8.

$$\mu := \lim_{n\to\infty} c_n^{1/n} = e^{\kappa} \tag{2.3}$$

μ is the known as the *growth constant* for SAWs in $\mathbb{Z}^3$.

As for the growth rate of SAPs in $\mathbb{Z}^3$, Hammersley later proved in [13] that the connective constant (and thus also the growth constant) for SAPs in $\mathbb{Z}^3$ is the same as that for SAWs in $\mathbb{Z}^3$:

Theorem 2.2 (Hammersley[13])**.**

$$\lim_{n\to\infty} (2n)^{-1} \log p_{2n} = \kappa. \tag{2.4}$$

Besides their growth rate, another topic of interest for SAPs is their entanglement complexity.

2.1.1 Entanglement Complexity

This sub-section will briefly cover some of the work that has been done regarding the entanglement complexity of SAPs on the simple cubic lattice. One way of measuring the entanglement complexity of a SAP is its knot type. A fundamental result regarding the entanglement complexity of SAPs is obtained using Kesten's Pattern Theorem, which is presented in [16]. However, before Kesten's Pattern Theorem can be presented, we must first introduce the concept of a Kesten Pattern.

Let ω be any n-edge SAW ($n > 0$) consisting of the vertices $\{v_0, \ldots, v_n\}$. Notice ω can be "split" into two SAWs (call them ω_1 and ω_2) by choosing any vertex $v^* \in \omega$. Let ω_1 be the SAW from v_0 to v^* and ω_2 be the SAW from v^* to v_n. Notice that ω_1 or ω_2 may be *empty walks*, defined to be walks

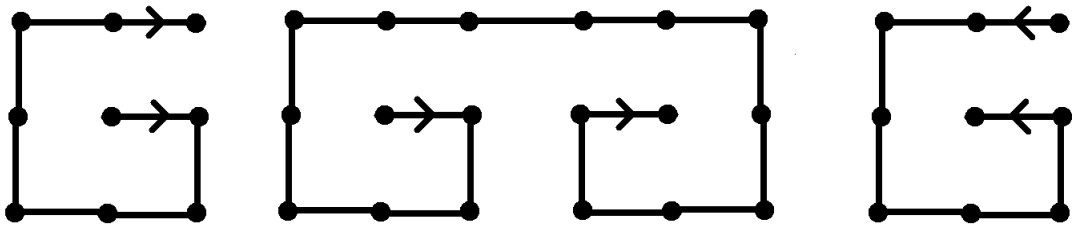

Figure 2.2: An example of three patterns which aren't Kesten Patterns in $\mathbb{Z}^2$. For each of these patterns, there does not exist a SAW in which one of these patterns could occur three times.

with just a single vertex and no edges. We say ω *consists* of ω_1 and ω_2 or ω is the *concatenation* of the SAWs ω_1 and ω_2, and we write $\omega = \omega_1 \circ_w \omega_2$. Similarily, ω can be "split" into three SAWs (ω_1, ω_2, and ω_3) by splitting ω twice. In this case, we can write $\omega_1 \circ_w \omega_2 \circ_w \omega_3$.

Definition 2.9 (Kesten Pattern[2])**.** When we mention SAWs in this definition, we relax the condition in Definition 2.2 that SAWs start at the origin. Also for this definition, the word "pattern" is just a synonym for "SAW". Let $m, n \in \mathbb{Z}^+, m \leq n$, and let ω_p be an m-edge SAW and ω be an n-edge SAW. We say pattern ω_p *appears* in the SAW ω if $\omega = \omega_1 \circ_w \omega_p \circ_w \omega_2$ for some SAWs ω_1 and ω_2. If $|\omega_1| = n_1$ and $|\omega_2| = n_2$, then $n = n_1 + m + n_2$. Note that ω_1 and ω_2 are allowed to be *empty walks*. In particular, we say ω_p has occurred at the *start* (*end*) of ω if ω_1 (ω_2) is an empty walk. We also say ω_p has occurred in the *middle* of ω if both ω_1 and ω_2 are non-empty walks. A pattern ω_{p_k} is called a *Kesten Pattern* if there exists a SAW ω_k such that ω_{p_k} appears at least three times in ω_k.

Note that the "three time appearance" condition prevents patterns similar to those in Figure 2.2. Now if we let $c_n(\omega_p)$ ($c_n(\bar{\omega_p})$) be the number of n-edge SAWs which contain (do not contain) pattern ω_p, then Kesten's Pattern Theorem is as follows:

Theorem 2.3 (Kesten[16])**.** *Let ω_p be any Kesten Pattern, then*

$$\lim_{n\to\infty} n^{-1} \log c_n(\bar{\omega_p}) =: \kappa(\bar{\omega_p}) < \kappa. \tag{2.5}$$

That is, for sufficiently large n, the pattern ω_p occurs in all but exponentially few SAWs.

Using Theorem 2.2 (SAWs and SAPs have the same connective constant), Kesten's Pattern Theorem can be extended to SAPs. First, we must define what it means for a pattern to occur in a polygon. Recall from Definition 2.4 that a lexicographical ordering can be put on any SAP,

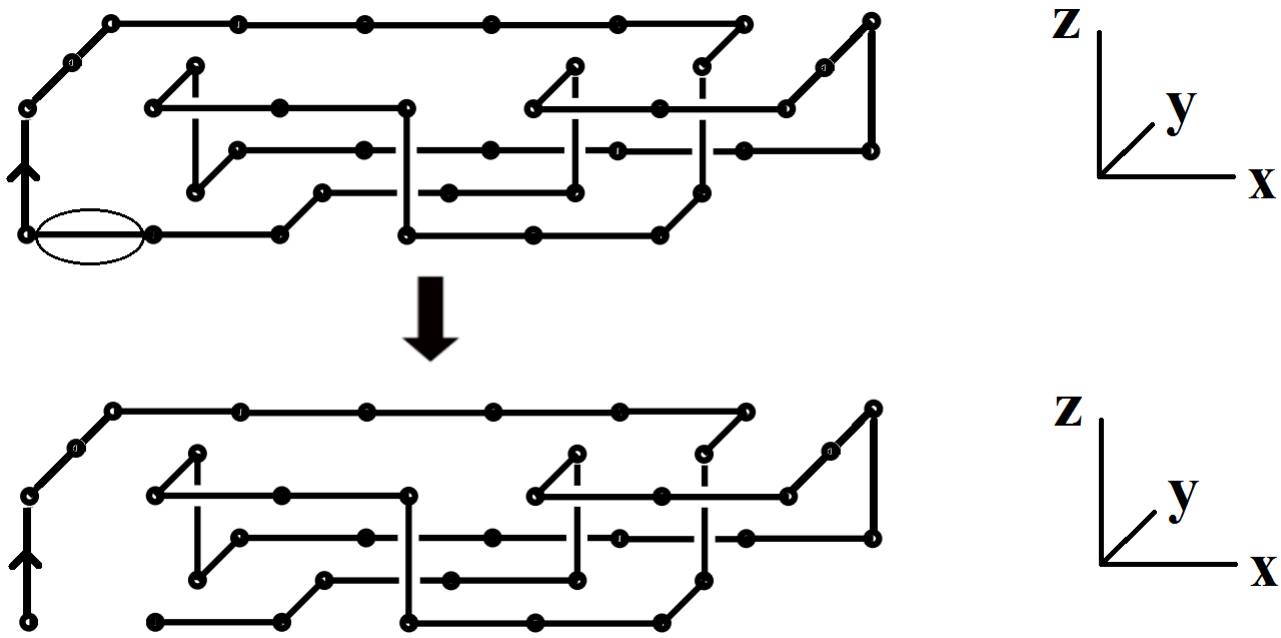

Figure 2.3: Any lexicographically ordered SAP can be represented by a SAW by removing the last edge in the SAP. Here, the edge with the arrow is the SAP's first edge and the circled edge is the SAP's last edge.

and notice that any $2n$-edge SAP can be represented by a $2n-1$ edge SAW by removing the last edge (in the lexicographical ordering of the SAP) from the SAP (See Figure 2.3). Consequently, it is clear that $p_{2n} \leq c_{2n-1}$. We say a pattern ω_p occurs in the polygon ω if ω_p occurs in the SAW obtained by removing the last edge of ω.

If we let $p_{2n}(\omega_p)$ $(p_{2n}(\bar{\omega_p}))$ be the number of $2n$-edge SAPs which contain (do not contain) pattern ω_p, we will similarly have $p_{2n}(\bar{\omega_p}) \leq c_{2n-1}(\bar{\omega_p})$. This leads to the following theorem:

Theorem 2.4 (Sumners, and Whittington[29])**.** *Let ω_p be any Kesten Pattern, then*

$$\lim_{n\to\infty} (2n)^{-1} \log p_{2n}(\bar{\omega_p}) = \kappa(\bar{P}) < \kappa. \tag{2.6}$$

That is, for sufficiently large n, the pattern ω_p occurs in all but exponentially few SAPs.

By constructing a suitable Kesten Pattern which guarantees a knot (such as the pattern in Figure 2.4), the following theorem was also proven in [29].

Theorem 2.5 (Sumners, and Whittington[29])**.** *All except exponentially few sufficiently long self-avoiding polygons on the simple cubic lattice are knotted.*

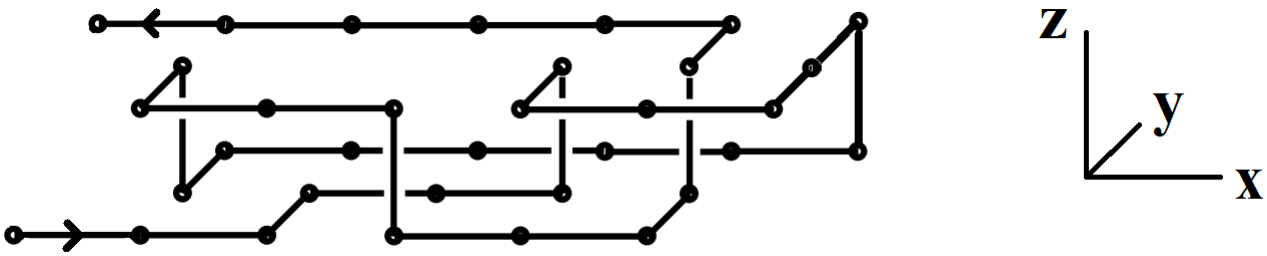

Figure 2.4: An example of a Kesten Pattern which guarantees a knot.

Soteros, Sumners, and Whittington went on to show in [25] that "every knot type is represented by a Kesten Pattern". Applying this to Theorem 2.4 once again, we get the result that all but exponentially few sufficiently long polygons are knotted and are "complex" knots.

So far, we have been working on the simple cubic lattice. This thesis will mainly focus on subgraphs of $\mathbb{Z}^3$, called (L, M)-tubes. Results in these (L, M)-tubes will be compared to the results which have just been covered for the general case of $\mathbb{Z}^3$. Both similarities and differences will be highlighted in the following section.

2.2 (L, M)-Tubes

Definition 2.10. An (L, M)-*tube* (or (L, M)-*rectangular prism*) is defined to be the sublattice of $\mathbb{Z}^3$ induced by the vertex set $\{(x, y, z) \in \mathbb{Z}^3 | x \geq 0, 0 \leq y \leq L, 0 \leq z \leq M\}$.

Definition 2.11. Define $c_n(L, M)$ to be the number of n-edge SAWs confined to an (L, M)-tube.

Definition 2.12. Define $p_{2n}(L, M)$ to be the number of $2n$-edge SAPs confined to an (L, M)-tube, up to translation in the x direction. Equivalently, $p_{2n}(L, M)$ is the number of lexicographically ordered SAPs in an (L, M)-tube whose first vertex is in the $x = 0$ plane.

Unlike the general case in $\mathbb{Z}^3$ where the growth constants for SAWs and SAPs were equal, $p_{2n}(L, M)$ is exponentially smaller than $c_n(L, M)$. This is a consequence of the following two results proven by Soteros and Whittington in [26].

Theorem 2.6 (Soteros and Whittington[26])**.** *The following limit exists:*

$$\kappa(L, M) := \lim_{n \to \infty} n^{-1} \log c_n(L, M). \tag{2.7}$$

Theorem 2.7 (Soteros and Whittington[26]). *The limit in the following inequality exists and satisfies*

$$\lim_{n\to\infty} (2n)^{-1} \log p_{2n}(L, M) =: \kappa_p(L, M) < \kappa(L, M). \tag{2.8}$$

Note that Theorem 2.7 was proven in [26] using a pattern theorem for SAWs in (L, M)-tubes. This pattern theorem for SAWs in (L, M)-tubes was proven by extending the arguments of Kesten's Pattern Theorem (Theorem 2.3) for SAWs in $\mathbb{Z}^d$. However, one consequence of Theorem 2.7 is that it is not possible to prove a pattern theorem for SAPs in (L, M)-tubes in the same way that it was done for SAWs in (L, M)-tubes. That is, one cannot extend Theorem 2.4 to get a pattern theorem for SAPs in (L, M)-tubes because $\kappa_p(L, M) \neq \kappa(L, M)$.

However, a different pattern theorem for SAWs in one-dimensional lattices was established by Alm and Janson in [1] by using transfer matrices. Unlike Kesten's Pattern Theorem, this transfer matrix approach can be extended to SAWs and SAPs in (L, M)-tubes.

In this chapter, a review of the known results for the connective constant and pattern theorems for SAWs in $\mathbb{Z}^3$ and (L, M)-tubes was given, as well as their relationship to SAPs. The following chapter explains what the transfer matrix entails in general and how it can be used for SAPs in (L, M)-tubes. A review of transfer matrix results for SAPs in (L, M)-tube is also given.

Chapter 3

Transfer Matrix Method

Transfer matrices can be used in a wide range of combinatorial problems and their usefulness can be seen in the following example (see [1] and [27] for more examples). In order to explain the transfer matrix method effectively, consider the following general combinatorial problem. Suppose we have an alphabet consisting of four letters: $\{A, B, C, D\}$, and suppose we are interested in how many "words" of a certain length m are possible, with a few restrictions. Suppose C cannot follow A, D cannot follow B, A cannot follow C, and B cannot follow D. This problem can be represented by a directed graph (digraph), which can be seen in Figure 3.1 (each $a_i, 1 \leq i \leq 12$ in Figure 3.1 is the labelling of the arcs, or directed edges). Essentially, given two letters L_1 and L_2, there is a directed arc from L_1 to L_2 if L_2 can follow L_1.

Additionally, suppose that there is some weight associated with each ordered pairing of letters, and suppose the weight of a word is obtained by summing over the weights of the individual letters composing the word. For example, suppose every pairing that starts with A has a weight of 1; starts with B has a weight of 2; start with C has a weight of 3; and starts with D has a weight of 4. One problem of interest is to find the number of words of length m with weight n; call this quantity $d(m, n)$. This has a generating function of the form $F(x, y) = \sum_{m,n} d(m, n) y^m x^n$. Another problem of interest is just to find the number of words with weight n. Call this quantity $d(n) = \sum_{m=0}^{\infty} d(m, n)$, and like for SAWs and SAPs, a quantity of interest is $\lim_{n\to\infty} n^{-1} \log d(n)$, the "connective constant for $d(n)$".

This problem can also be represented by a transfer matrix:

$$G(x) = \begin{bmatrix} x^1 & x^2 & 0 & x^4 \\ x^1 & x^2 & x^3 & 0 \\ 0 & x^2 & x^3 & x^4 \\ x^1 & 0 & x^3 & x^4 \end{bmatrix},$$

where each row or column number corresponds to a letter (row or column i corresponds to the ith letter in the alphabet). The row letter represents the first letter in an ordered pairing, while the

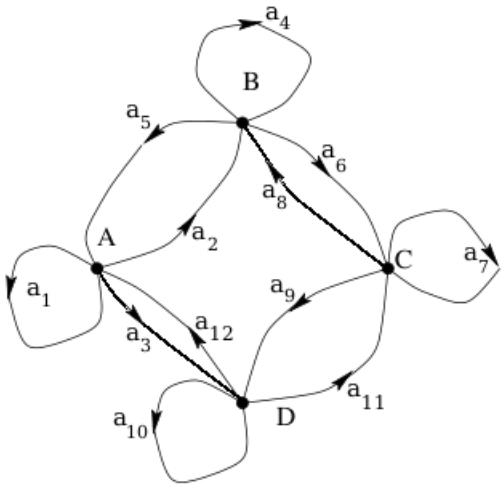

Figure 3.1: A visual depiction of the general combinatorial problem. This is a digraph with vertices $\{A, B, C, D\}$ and arcs $a_i, 1 \leq i \leq 12$.

column letter represents the second letter in an ordered pairing. If a letter L_2 can follow a letter L_1, then the corresponding entry is filled with the contribution to the generating function of the weight of that pairing. If L_2 cannot follow L_1, then the corresponding entry is zero.

This toy example of using "letters" and "words" will be referred to throughout the rest of the chapter to help show how transfer matrix theory can tell us how the generating function $F(x, y)$ can be obtained from the transfer matrix $G(x)$.

3.1 Transfer Matrix Theory

In this section, the theory behind the transfer matrix method is presented. Unless stated otherwise, this section is based on [27].

Definition 3.1. A *directed graph* or *digraph* $\mathcal{D}$ is a triple $(V, \mathcal{A}, \phi)$, where V is a set of vertices, $\mathcal{A}$ is a set of directed arcs, and ϕ is a map from $\mathcal{A}$ to $V \times V$.

If $\phi(b) = (u, v)$, then b is called an arc from u to v, with *initial vertex* $u = \text{int}(b)$ and *final vertex* $v = \text{fin}(b)$. If $u = v$, then b is called a *loop*.

Definition 3.2. A *walk* Γ in $\mathcal{D}$ of length m from vertex $u \in V$ to vertex $v \in V$ is a sequence of m arcs, b_1, b_2, ..., b_m, such that $u = \text{int}(b_1)$, $v = \text{fin}(b_m)$, and $\text{fin}(b_i) = \text{int}(b_{i+1})$ for $1 \leq i < m - 1$. If also $u = v$, then Γ is called a *closed walk* based at u.

Notice that in the toy example, $V = \{A, B, C, D\}$ and "vertices" are "letters". The set $\mathcal{A}$ is the set of arcs between letters which were defined based on the restrictions of which letters could follow each other, and the function $\phi : \mathcal{A} \to V \times V$ just takes an arc and maps it to its associated ordered pair.

Let $w : \mathcal{A} \to \mathbb{C}$ be a *weight function* on $\mathcal{A}$. If $\Gamma = b_1, b_2, \ldots, b_m$ is a walk, then the weight of Γ is defined by $w(\Gamma) = w(b_1)w(b_2)\ldots w(b_m)$. Note that we assume $\mathcal{D}$ is finite, so $V = \{v_1, \ldots, v_p\}$ and $\mathcal{A}$ are finite sets. For any $i, j \in \{1, 2, \ldots, p\}$, define:

$$W_{ij}(m) = \sum_{\Gamma} w(\Gamma), \tag{3.1}$$

where the sum is over all walks Γ in $\mathcal{D}$ of length m from v_i to v_j. For $m = 0$, let $W_{ij}(0) = \delta_{ij}$, where δ_{ij} is defined by

$$\delta_{ij} = \begin{cases} 1 & \text{if } i = j \\ 0 & \text{otherwise} \end{cases}.$$

Now let $W^{(m)} = (W_{ij}(m))$. Notice since $|V| = p$, $W^{(m)}$ is a square $p \times p$ matrix and $W^{(0)} = I_p$, the $p \times p$ identity matrix. Let $W = W^{(1)}$, where W is called the *weighted adjacency matrix* of $\mathcal{D}$, with respect to the weight function w. The following theorem shows that for any $m \in \mathbb{N}$, $W^{(m)}$ can be obtained by evaluating the mth power of the matrix W.

Theorem 3.1 (Stanley[27]). *For any $m \in \mathbb{N}$,*

$$W_{ij}(m) = (W^m)_{i,j}. \tag{3.2}$$

The behaviour of the sequence $(W_{ij}(m))$, $m \in \mathbb{N}$ can be analyzed through its generating function:

$$F_{ij}(\mathcal{D}, y) = \sum_{m \geq 0} W_{ij}(m) y^m = \sum_{m \geq 0} (W^m)_{i,j} y^m. \tag{3.3}$$

The following theorem relates the generating function of the sequence $(W_{ij}(m))$ to the matrix W.

Theorem 3.2 (Stanley[27]). *The generating function $F_{ij}(\mathcal{D}, y)$ is given by*

$$F_{ij}(\mathcal{D}, y) = \frac{(-1)^{i+j} \det(I - yW : j, i)}{\det(I - yW)}, \tag{3.4}$$

where $(H : j, i)$ denotes the matrix obtained by removing the jth row and ith column of H.

Proof. $F_{ij}(\mathcal{D}, y)$ is the (i,j)-entry of the matrix $\sum_{m\geq 0} W^m y^m = (I - yW)^{-1}$. Recall from linear algebra the standard adjugate formula for the inverse of a matrix:

$$(H^{-1})_{i,j} = \frac{(-1)^{i+j}\det(H : j, i)}{\det(H)}. \tag{3.5}$$

Applying it to $(I - yW)^{-1}$, we obtain

$$F_{ij}(\mathcal{D}, y) = ((I - yW)^{-1})_{ij} = \frac{(-1)^{i+j}\det(I - yW : j, i)}{\det(I - yW)}. \tag{3.6}$$

□

Note that for the toy example presented at the beginning of the chapter, if we take:

$$w(a_i) = \begin{cases} x^1 & \text{if } 1 \leq i \leq 3 \\ x^2 & \text{if } 4 \leq i \leq 6 \\ x^3 & \text{if } 7 \leq i \leq 9 \\ x^4 & \text{if } 10 \leq i \leq 12 \end{cases},$$

then $W = G(x)$ and

$$F(x, y) = \sum_{m,n} d(m, n) y^m x^n = \sum_{i,j} F_{ij}(\mathcal{D}, y) = \sum_{i,j} \frac{(-1)^{i+j}\det(I - yG(x) : j, i)}{\det(I - yG(x))}. \tag{3.7}$$

For example, recall $d(n) = \sum_{m=0}^{\infty} d(m, n)$ is the number of words with weight n. Then for $y = 1$,

$$F(x, 1) = \sum_{n=0}^{\infty} \left(\sum_{m=0}^{\infty} d(m, n) \right) x^n = \sum_{n=0}^{\infty} d(n) x^n. \tag{3.8}$$

Notice that since $F(x, 1) = \sum_{n=0}^{\infty} d(n) x^n$ is a power series, it has a radius of convergence of

$$r = \lim_{n\to\infty} d(n)^{-1/n}. \tag{3.9}$$

Taking the logarithm and multiplying both sides by -1, we get

$$-\log(r) = \lim_{n\to\infty} n^{-1} \log d(n) =: \kappa_d, \tag{3.10}$$

which is the connective constant for "words" with weight n.

Since it is also known that $F(x, 1) = \sum_{i,j} \frac{(-1)^{i+j}\det(I - G(x) : j, i)}{\det(I - G(x))}$, the radius of convergence of $F(x, 1)$ can also be found by using the transfer matrix. More specifically, the radius of convergence r is such that $\det(I - G(r)) = 0$. Recall from linear algebra that $\lambda \in \mathbb{R}$ is an eigenvalue of a matrix H if $\det(\lambda I - H) = 0$. Thus, r is such that $G(r)$ has an eigenvalue of one. Notice that Theorem 3.2 shows how a combinatorial generating function can be related to a transfer matrix. Presented next

are important theorems about matrices which allow us to use results about the transfer matrix to explore asymptotic properties of the coefficients of a generating function.

A matrix or vector H is said to be *non-negative* (*non-positive*) if all its elements are non-negative (non-positive), and we write $H \geq 0$ ($H \leq 0$).

Theorem 3.3 (Schaefer[22]). *A non-negative matrix always has a non-negative real eigenvalue r such that the modulus of any other eigenvalue of the matrix does not exceed r. To this maximal eigenvalue corresponds a non-negative eigenvector.*

A *permutation matrix* is a square matrix that has exactly one entry, 1, in each row and each column and has zeros elsewhere. A matrix H is called *reducible* if there is a permutation matrix P such that

$$P^{-1}HP = \begin{bmatrix} X & 0 \\ Y & Z \end{bmatrix},$$

where X and Z are square matrices. Otherwise, we say H is *irreducible*.

Theorem 3.4 (Schaefer[22]). *A matrix H is irreducible if for each i, j there exists a $k \geq 1$ such that $(H^k)_{ij} > 0$.*

The *period* d of an irreducible matrix H is the greatest common divisor (GCD) of the integers k for which $(H^k)_{i,i} > 0$. H is said to be an *aperiodic* matrix if $d = 1$.

A digraph $\mathcal{D} = (V, \mathcal{A}, \phi)$ is called *strongly connected* if for each pair of vertices, v_i and v_j in V, there exists a walk from v_i to v_j.

Let $\mathcal{D} = (V, \mathcal{A}, \phi)$ be a strongly connected digraph with weight function $w : \mathcal{A} \to \mathbb{C}$ such that $w(a) > 0$ for every $a \in \mathcal{A}$. Then W, the weighted adjacency matrix of $\mathcal{D}$, is non-negative and irreducible.

This tells us that in the toy example, since the digraph is strongly connected and the weighted adjacency matrix W is equal to the transfer matrix, $G(x)$ is non-negative and irreducible. Thus, we can apply the following theorems to $G(x)$.

Theorem 3.5 (Perron-Frobenius Theorem[22]). *An irreducible non-negative matrix H always has a positive eigenvalue r that is a simple root of the characteristic polynomial of H. The modulus of any other eigenvalue of H does not exceed r. To the maximal eigenvalue r corresponds a positive eigenvector. Moreover, if H has h eigenvalues of modulus r, then they are all distinct roots of $x^h - r^h = 0$. Furthermore, if H is aperiodic, then r is the only eigenvalue with modulus r.*

Note that the modulus of the maximal eigenvalue of a matrix H is also called the *spectral radius* of H.

Theorem 3.6 (Alm and Janson[1])**.** *Suppose that $G(x) \geq 0$ is a continuously differentiable matrix valued function of $x > 0$, and let $\rho(x)$ be the spectral radius $\rho(G(x))$. If $\rho(x_0) > 0$ is a simple eigenvalue of $G(x_0)$ and $\eta^\top$ and ξ are the corresponding left and right eigenvectors respectively, normalized such that $\eta^\top \xi = 1$, then*

$$\rho'(x_0) = \eta^\top G'(x_0)\xi \tag{3.11}$$

and provided $\rho'(x_0) \neq 0$,

$$\lim_{x \to x_0} (x_0 - x)(\rho(x_0)I - G(x))^{-1} = \frac{1}{\rho'(x_0)}\xi\eta^\top = (\eta^\top G'(x_0)\xi)^{-1}\xi\eta^\top. \tag{3.12}$$

Note that in this thesis, for any two quantities $a(y), b(y)$ that depend on some value y, and for some constant c, we write $a(y) \sim b(y)$ as $y \to c$, if and only if $\lim_{y \to c} \frac{b(y)}{a(y)} = 1$. Equation (3.12) then gives that

$$(x_0 - x)(\rho(x_0)I - G(x))^{-1} \sim (\eta^\top G'(x_0)\xi)^{-1}\xi\eta^\top, \tag{3.13}$$

as $x \to x_0$.

Thus, applying Theorem 3.5 to $G(x)$, the spectral radius $\rho(x)$ of $G(x)$ is a simple root of $\det(\lambda I - G(x))$, $G(x)$ has a strictly positive eigenvector associated with $\rho(x)$, and $\rho(x)$ is the only eigenvalue of modulus $\rho(x)$. Note that $\rho(0) = 0$ and $\rho(x)$ is an unbounded, increasing, continuous function on $[0, \infty)$. Hence, there exists a unique $x_0 > 0$ such that $\rho(x_0) = 1$. From equation (3.4), $F(x, 1)$ has poles only when $\frac{1}{\det(I - G(x))}$ has poles, that is, when 1 is an eigenvalue of $G(x)$. Thus, $F(x, 1)$ has one simple pole when $|x| = x_0$, namely $x = x_0$. Applying Theorem 3.6, we get that as $x \to x_0$,

$$F(x, 1) = (I - G(x))^{-1} \sim (x_0 - x)^{-1}(\eta^\top G'(x_0)\xi)^{-1}\xi\eta^\top, \tag{3.14}$$

where $\eta^\top$ and ξ are the left and right eigenvectors respectively associated with $G(x_0)$, normalized such that $\eta^\top \xi = 1$. Define $\beta = x_0(\eta^\top G'(x_0)\xi)$, differentiate both sides of the above equation n

times with respect to x, set $x = 0$, and divide by $n!$:

$$\begin{aligned}
F(x,1) = \sum_{n=0}^{\infty} d(n)x^n &\sim \frac{x_0\beta^{-1}\xi\eta^\top}{x_0 - x} = \frac{\beta^{-1}\xi\eta^\top}{(1 - x/x_0)} = \beta^{-1}\xi\eta^\top \sum_{n=0}^{\infty}\left(\frac{x}{x_0}\right)^n \\
\sum_{N=n}^{\infty} d(N)N(N-1)\dots(N-n+1)x^{N-n} &\sim \beta^{-1}\xi\eta^\top \sum_{N=n}^{\infty}\left(\frac{1}{x_0}\right)^N N(N-1)\dots(N-n+1)x^{N-n} \\
d(n)n(n-1)\dots(2)(1) &\sim \beta^{-1}\xi\eta^\top \left(\frac{1}{x_0}\right)^n n(n-1)\dots(2)(1) \\
d(n)n! &\sim \beta^{-1}\xi\eta^\top x_0^{-n} n! \\
d(n) &\sim \beta^{-1}\xi\eta^\top x_0^{-n}. \qquad (3.15)
\end{aligned}$$

Thus, we get that there exists $\alpha_d > 0$ such that $d(n) \sim \alpha_d x_0^{-n}$ as $n \to \infty$. Now recall from equation (3.10) that $-\log(x_0) = \kappa_d$, thus we have

$$d(n) \sim \alpha_d e^{(\kappa_d)n} \quad \text{as } n \to \infty, \qquad (3.16)$$

where $\alpha_d = \beta^{-1}\xi\eta^\top$. The following two theorems about matrices will aid us in proving a pattern theorem for "words" in the toy example.

Theorem 3.7 (Schaefer[22])**.** *Increasing any element of a non-negative matrix H does not decrease the maximal eigenvalue. The maximal eigenvalue strictly increases if H is an irreducible matrix.*

Theorem 3.8 (Schaefer[22])**.** *The maximal eigenvalue r' of every principle sub-matrix (obtained by removing one row and one column) of a non-negative matrix H does not exceed the maximal eigenvalue r of H. If H is irreducible, then $r' < r$ always holds.*

Lastly, notice that in the toy example, given any two "words", there exists a *concatenation process* that can "concatenate" (or join) these two words together to create a new valid word. This comes from the fact that the digraph is strongly connected (i.e given any two letters, there exists a walk on the digraph from the first letter to the second letter). Also notice that if any letter L is removed from $\{A, B, C, D\}$, any two words from $\{A, B, C, D\}\backslash L$ can also be concatenated together. To see this, notice that the subgraph induced by the reduced vertex set $\{A, B, C, D\}\backslash L$ is still strongly connected. Finally, for any letter $L \in \{A, B, C, D\}$, define $d(n; \bar{L})$ to be the number of words counted in $d(n) > 0$ that do not contain the letter L. Then a pattern theorem for "words" is as follows:

Theorem 3.9. *Given any letter $L \in \{A, B, C, D\}$, there exists $\alpha_{d_L} > 0$ and κ_{d_L} such that*

$$d(n; \bar{L}) \sim \alpha_{d_L} e^{(\kappa_{d_L})n} \text{as } n \to \infty, \qquad (3.17)$$

with

$$\kappa_{d_L} < \kappa_d. \tag{3.18}$$

Proof. Let $L \in \{A, B, C, D\}$ be any letter, and suppose L is the rth letter in $\{A, B, C, D\}$. Consider the generating function $\bar{F}(x, 1) = \sum_{n \geq 1} d(n; \bar{L})x^n$. Then

$$\bar{F}(x, 1) = \sum_{h=0}^{\infty} \bar{G}(x)^h = (I - \bar{G}(x))^{-1}, \tag{3.19}$$

where $\bar{G}(x)$ is obtained from $G(x)$ by deleting the row and column of $G(x)$ that correspond to letter L (i.e. the rth row and column).

Let $\mathcal{W}_1$ and $\mathcal{W}_2$ be any two words which do not contain the letter L. As shown above, since the subgraph induced by $\{A, B, C, D\}\backslash L$ is still strongly connected, $\mathcal{W}_1$ and $\mathcal{W}_2$ can be concatenated into the word $\mathcal{W}_c = \mathcal{W}_1 \circ_d \mathcal{W}_2$ without using the letter L, so $\mathcal{W}_c$ also does not contain L. Using the same arguments that were used for $G(x)$, $\bar{G}(x)$ can be shown to be a non-negative, irreducible, and aperiodic matrix. Hence, the arguments used to get equation (3.16) apply again so that there exist $\bar{x}_0 > 0$ and $\bar{\alpha}_{d_L} > 0$ such that

$$d(n; \bar{L}) \sim \bar{\alpha}_{d_L}(\bar{x}_0)^{-n} \text{ as } n \to \infty, \tag{3.20}$$

with $e^{\kappa_{d_L}} = (\bar{x}_0)^{-1}$, and the spectral radius $\bar{\rho}(\bar{x}_0)$ of $\bar{G}(\bar{x}_0)$ equals 1.

Now consider the matrix $G_L(x)$ obtained from $G(x)$ by replacing the rth row and column of $G(x)$ by a row and column of zeros. Then the spectral radius $\rho_L(x)$ of $G_L(x)$ equals $\bar{\rho}(x)$. Furthermore, elementwise $G_L(x) \leq G(x)$ and at least one element of $G_L(x)$ is strictly less than the corresponding element of $G(x)$. Thus, Theorem 3.7 implies that $\rho_L(x) < \rho(x)$, and hence, for $x = x_0$, $\rho_L(x_0) < \rho(x_0) = 1$. Therefore, $\bar{x}_0 > x_0$ or equivalently $\kappa_{d_L} < \kappa_d$. □

3.2 Transfer Matrix for SAPs in (L, M)-tubes

In this section, we address the question of how the results in Section 3.1 can be applied to our model of SAPs in (L, M)-tubes. It will be shown how the transfer matrix can be used to prove a pattern theorem for SAPs in (L, M)-tubes (which was first done in [24]). Note that the argument presented here is more generalized than the argument which was presented in [24], and the required concatenation theorem presented here contains more details than the concatenation argument given in [24]. It will also be shown how the transfer matrix can be used to find the expected number of

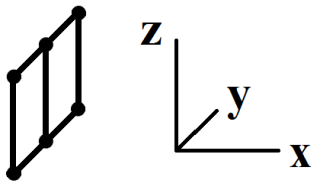

Figure 3.2: An example of a hinge in a $(2, 1)$-tube.

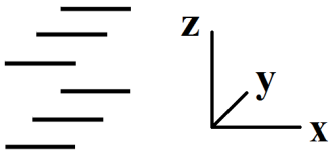

Figure 3.3: An example of a section in a $(2, 1)$-tube.

occurrences of a pattern per edge in a random SAP as $n \to \infty$, as well as the expected span per edge of a random SAP as $n \to \infty$. These results require setting up the proper transfer matrix, which first requires introducing some definitions.

3.2.1 Definitions

Definition 3.3. For any integer $i \geq 0$, the ith *hinge* of an (L, M)-tube, $H_i(L, M)$, is defined to be the subgraph of the tube induced by the vertex set $\{(i, y, z) \in \mathbb{Z}^3 | 0 \leq y \leq L, 0 \leq z \leq M\}$. Depending on the context, a *hinge* may also refer to a set of ordered and directed edges in a hinge. See Figure 3.2 for an example of a hinge.

Definition 3.4. For any integer $i \geq 1$, the ith *section* of an (L, M)-tube, $S_i(L, M)$, is defined to be the set of edges which join $H_{i-1}(L, M)$ to $H_i(L, M)$. Depending on the context, a *section* may also refer to a set of ordered and directed edges in a section. See Figure 3.3 for an example of a section.

Thus, an (L, M)-tube can be thought of as an alternating sequence of hinges and sections. Without loss of generality, we will assume (for the rest of this thesis) that a given SAP in an (L, M)-tube has $H_0(L, M)$ as its first non-empty hinge, and consequently, $S_1(L, M)$ as its first non-empty section.

Definition 3.5. For any integer $m \geq 0$, a SAP ω in an (L, M)-prism is said to have *span* m if all the edges of ω are contained in $H_0(L, M) \cup S_1(L, M) \cup H_1(L, M) \cup \ldots \cup S_m(L, M) \cup H_m(L, M)$, with non-empty hinges $H_0(L, M)$ and $H_m(L, M)$.

Definition 3.6. Let ω be any SAP in an (L, M)-tube with span m. Then for any $k \in \mathbb{Z}$, $2 \leq k \leq m$, we define a *k-span* to be ω's *configuration* in a sublattice of the form $S_i(L, M) \cup H_i(L, M) \cup \ldots \cup H_{i+k-2}(L, M) \cup S_{i+k-1}(L, M)$ for some $i \in \mathbb{Z}$, $1 \leq i \leq m - k + 1$. We say this k-span *occurs* at the i^{th} section of the SAP ω.

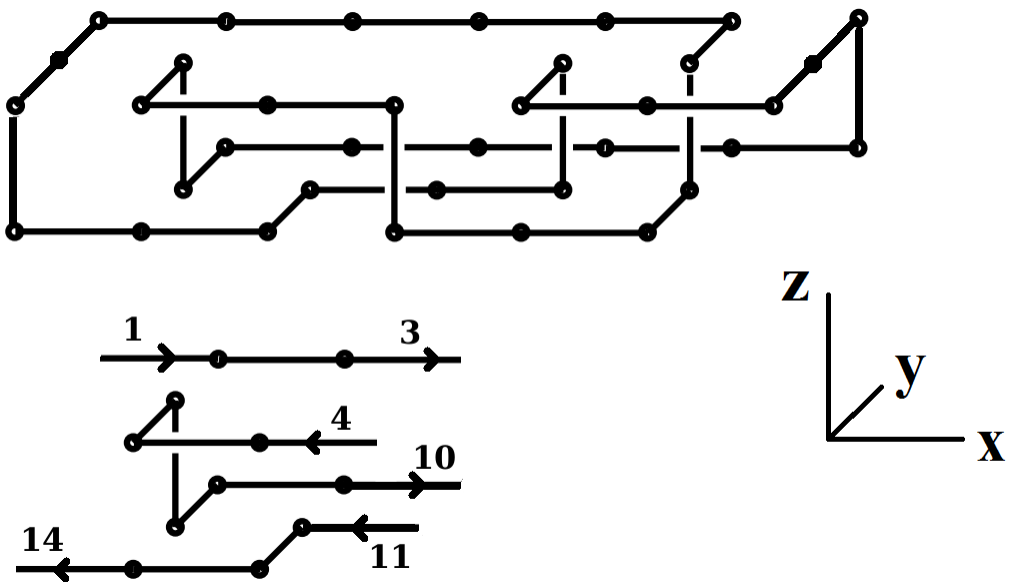

Figure 3.4: An example of a 3-span (bottom) which occurs at the first section of a polygon in a (2,1)-tube (top).

The polygon's *configuration* in such a sublattice of the tube consists of the sublattice, the set of lexicographically ordered and directed edges of the polygon in the sublattice, and if there are $e < 2n$ edges of the polygon in the sublattice, then they are directed and ordered from 1 to e according to their lexicographical ordering in the polygon. For an example of a k-span, see Figure 3.4. Without loss of generality, we will assume (for the rest of this thesis), unless stated otherwise, that a given k-span in an (L, M)-tube has $S_1(L, M)$ as its first section.

Definition 3.7. Let π_1 and π_2 be two k-spans. Then if the configuration of π_1 on $S_2(L, M) \cup H_2(L, M) \cup \ldots \cup H_{k-1}(L, M) \cup S_k(L, M)$ matches the configuration of π_2 on $S_1(L, M) \cup H_1(L, M) \cup \ldots \cup H_{k-2}(L, M) \cup S_{k-1}(L, M)$, then we say π_2 can *follow* π_1.

Definition 3.8. For any integer $k \geq 2$, a k-span π *occurs* in a SAP ω if, when ω is ordered lexicographically, π occurs at some section of ω.

Definition 3.9. For any integer $k \geq 2$, define $\Pi(k)$ to be the set of k-spans that occur in some section of at least one SAP in an (L, M)-tube.

Definition 3.10. For any integer $k \geq 2$ and a given k-span $\pi \in \Pi(k)$, define $p_{2n}(L, M; \bar{\pi})$ to be the number of $2n$-edge SAPs in an (L, M)-tube (up to translation in the x-direction) in which the k-span π does not occur.

Definition 3.11. A hinge H_s is called a *start-hinge* if there exists at least one SAP ω such that when ω is lexicographically ordered, ω has H_s as its first hinge (located at H_0).

Definition 3.12. A hinge H_f is called a *finish-hinge* if there exists at least one SAP ω with span m such that when ω is lexicographically ordered, ω has H_f as its last hinge (located at H_m).

Definition 3.13. Define $\mathcal{H}_s$ to be the set of all start hinges, and define $\mathcal{H}_f$ to be the set of all finish hinges.

Definition 3.14. For any integer $k \geq 2$, given a k-span $\pi \in \Pi(k)$ and a start-hinge $H_s \in \mathcal{H}_s$, we say π can *follow* H_s if there exists a SAP ω such that when ω is lexicographically ordered, H_s is ω's first hinge (located at H_0) and π occurs at ω's first section.

Definition 3.15. For any integer $k \geq 2$, given a k-span $\pi \in \Pi(k)$ and a finish-hinge $H_f \in \mathcal{H}_f$, we say H_f can *follow* π if there exists a SAP ω with span $m \geq k$ such that when ω is lexicographically ordered, H_f is ω's last hinge (located at H_m) and π occurs at ω's $(m-k+1)$th section.

Definition 3.16. A sequence $(H_s, \pi_1, \ldots, \pi_h, H_f)$ of one start-hinge ($H_s \in \mathcal{H}_s$), h k-spans ($\pi_1, \pi_2, \ldots, \pi_h \in \Pi(k)$), and one finish-hinge ($H_f \in \mathcal{H}_f$) is said to be *properly connected* if π_1 can follow H_s, H_f can follow π_h, and π_{i+1} can follow π_i for $i = 1, 2, \ldots, h-1$.

Thus, one can generate all polygons in an (L, M)-tube with span $m \geq k$ by generating all properly connected sequences of $(H_s, \pi_1, \ldots, \pi_h, H_f)$, $h = m-k+1$. Using the definitions from this sub-section, a pattern theorem for SAPs in (L, M)-tubes will be proven in the following section by using the transfer matrix method.

3.3 Pattern Theorem for SAPs in (L, M)-tubes

Let $\mathcal{D}_p$ be a digraph which has a vertex corresponding to each start-hinge, finish-hinge, and k-span and an arc from: each start-hinge to any k-span which can follow it; each k-span to any k-span which can follow it; and each k-span to any finish-hinge which can follow it. Then notice that a properly connected sequence $(H_s, \pi_1, \ldots, \pi_h, H_f)$ corresponds to a walk on the directed graph $\mathcal{D}_p$. In order to apply transfer matrix results, it is important that $\mathcal{D}_p$ has three properties:

(a) finite vertex set,

(b) irreducible on the set of k-spans,

(c) aperiodic on the set of k-spans.

For (a), since the total number of edges in a hinge is finite, there is only a finite number of ways to "fill" the possible edges. Similarily, since the total number of edges in the subgraph induced by the vertex set $\{(x, y, z) \in \mathbb{Z}^3 | 0 \leq x \leq k, 0 \leq y \leq L, 0 \leq z \leq M\}$ is finite, there is only a finite number of ways to "fill" the possible edges.

For (b), $\mathcal{D}_p$ will be irreducible with respect to k-spans if for any pair of k-spans π_A and π_B, there exists a walk on $\mathcal{D}_p$ from π_A to π_B. To see that this holds, we first need the following concatenation theorem for SAPs in (L, M)-tubes. Note that the details of this concatenation theorem are new.

Theorem 3.10. *Let ω_1 and ω_2 be any two polygons in an (L, M)-tube with spans m_1 and m_2 respectively. Notice there is exactly one m_1-span (m_2-span) that occurs at the first section of ω_1 (ω_2). Then ω_1 and ω_2 can always be concatenated (by the process explained below) to form another polygon $\omega_c := \omega_1 \circ_p \omega_2$ which contains both the m_1-span and the m_2-span from ω_1 and ω_2.*

Proof. Choose any edge e_1 from ω_1 in H_{m_1}. Following the lexicographical ordering of SAPs, let $v_{1a} = \text{int}(e_1)$ and $v_{1b} = \text{fin}(e_1)$. Let the edge e_2 be the first edge lexicographically from ω_2, and let $v_{2a} = \text{int}(e_2)$ and $v_{2b} = \text{fin}(e_2)$. Notice that as a consequence of the lexicographical ordering, e_2 must be in H_0 and e_2 must be directed in either the positive y or z direction.

Now if we can translate ω_2 in the positive x-direction, such that when we remove e_1 from ω_1 and e_2 from ω_2, we are able to connect v_{1a} to v_{2b} and v_{2a} to v_{1b} (via two sequences of edges that do not change the m_1-span or the m_2-span), then the resulting orderings of the m_1-span and m_2-span (associated with ω_1 and ω_2 respectively) will be preserved. Thus, it suffices to show that we are able to connect v_{1a} to v_{2b} and v_{2a} to v_{1b} via two sequences of edges (that do not "enter" the m_1-span or m_2-span). This connection will be constructed for two different cases based on which (L, M)-tube we are working in. Case 1 has $L, M > 0$ and Case 2 has $L = 0$ or $M = 0$.

Case 1: Assume $L, M > 0$. Translate ω_2 in the x-direction such that the first hinge of ω_2 is located in the plane $x = m_1 + 3$. Recall that e_2 must be directed in either the positive y or z direction. Without loss of generality, assume e_2 is directed in the positive z-direction. Now initially assume e_1 is directed in the negative z-direction, that is e_1 and e_2 are parallel and in opposite directions. Remove e_1 and e_2; then we can construct two sequences of edges that connect v_{1a} to v_{2b} and v_{2a} to v_{1b} as follows: Starting at v_{1a}, add one edge in the positive x-direction, and then add edges (if necessary) in the positive z-direction until the z-coordinate is greater than or equal to the z-coordinate of v_{2b}. Next, add one edge in the positive x-direction, and then add edges in either

the y or z directions until $v_{2b} - \hat{\imath}$ is reached, while always keeping the z-coordinate greater than or equal to the z-coordinate of v_{2b}. This will ensure this first sequence of edges never intersects with the second sequence of edges. Finally add one edge in the positive x-direction to reach v_{2b}. Thus, we have successfully connected v_{1a} to v_{2b}. Similarily (but in the opposite direction), for the next sequence of edges, start at v_{2a} and add one edge in the negative x-direction, and then add edges (if necessary) in the negative z-direction until the z-coordinate is less than or equal to the z-coordinate of v_{1a}. Next, add one edge in the negative x-direction, and then add edges in either the y or z directions until $v_{1b} + \hat{\imath}$ is reached, while always keeping the z-coordinate less than or equal to the z-coordinate of v_{1b}. As said above, this ensures this second sequence of edges never intersects with the first sequence of edges. Finally add one edge in the negative x-direction to reach v_{1b}. Thus, we have successfully connected v_{2a} to v_{1b} and successfully concatenated ω_1 to ω_2. See Figure 3.5 for an illustration of connecting two edges that are parallel and in opposite directions. It is important to note that by construction, these two sequences of edges do not intersect. This can be seen by looking at each yz-plane, and noticing that the first sequence of edges is always "above" the second sequence of edges ("above" meaning having a larger z-coordinate).

If instead, e_1 is not directed in the negative z-direction (not parallel and in the opposite direction), we show next that we can remove e_1 and connect v_{1a} to v_{1a}^* and v_{1b}^* to v_{1b}, where the edge e_1^* is in the negative z-direction (parallel and in the opposite direction of e_2) with $v_{1a}^* = \text{int}(e_1^*)$ and $v_{1b}^* = \text{fin}(e_1^*)$. Once this is done, by using the same arguments as above, we can remove e_1^* and e_2 and connect v_{1a}^* to v_{2b} and v_{2a}^* to v_{1b} via two sequences of edges that will not change the m_1-span or the m_2-span (from ω_1 and ω_2 respectively).

The required construction to introduce e_1^* is as follows: First, assume e_1 is directed in the positive (negative) y-direction. Remove e_1, and if e_1 was in the positive (negative) y-direction with its z-coordinate > 0, then starting at v_{1a}, add edges in the following directions: positive x, negative z (this creates the edge e_1^*), positive (negative) y, positive z, and negative x, so we are at v_{1b}. If instead, e_1 was in the positive (negative) y-direction with its z-coordinate $= 0$, then starting at v_{1a}, add edges in the following directions: positive x-direction, positive z, positive (negative) y, negative z (this creates the edge e_1^*), and negative x, so we are at v_{1b}. See Figure 3.6 for an illustration of changing an edge directed in the y-direction to an edge directed in the negative z-direction.

If e_1 is instead directed in the positive z-direction, again remove e_1 and create an edge e_1^* by connecting v_{1a} to v_{1a}^* and v_{1b}^* to v_{1b}, but in a different manner: If e_1 has a y-coordinate greater than (equal to) zero, then starting at v_{1a}, add edges in the following directions: positive x, positive

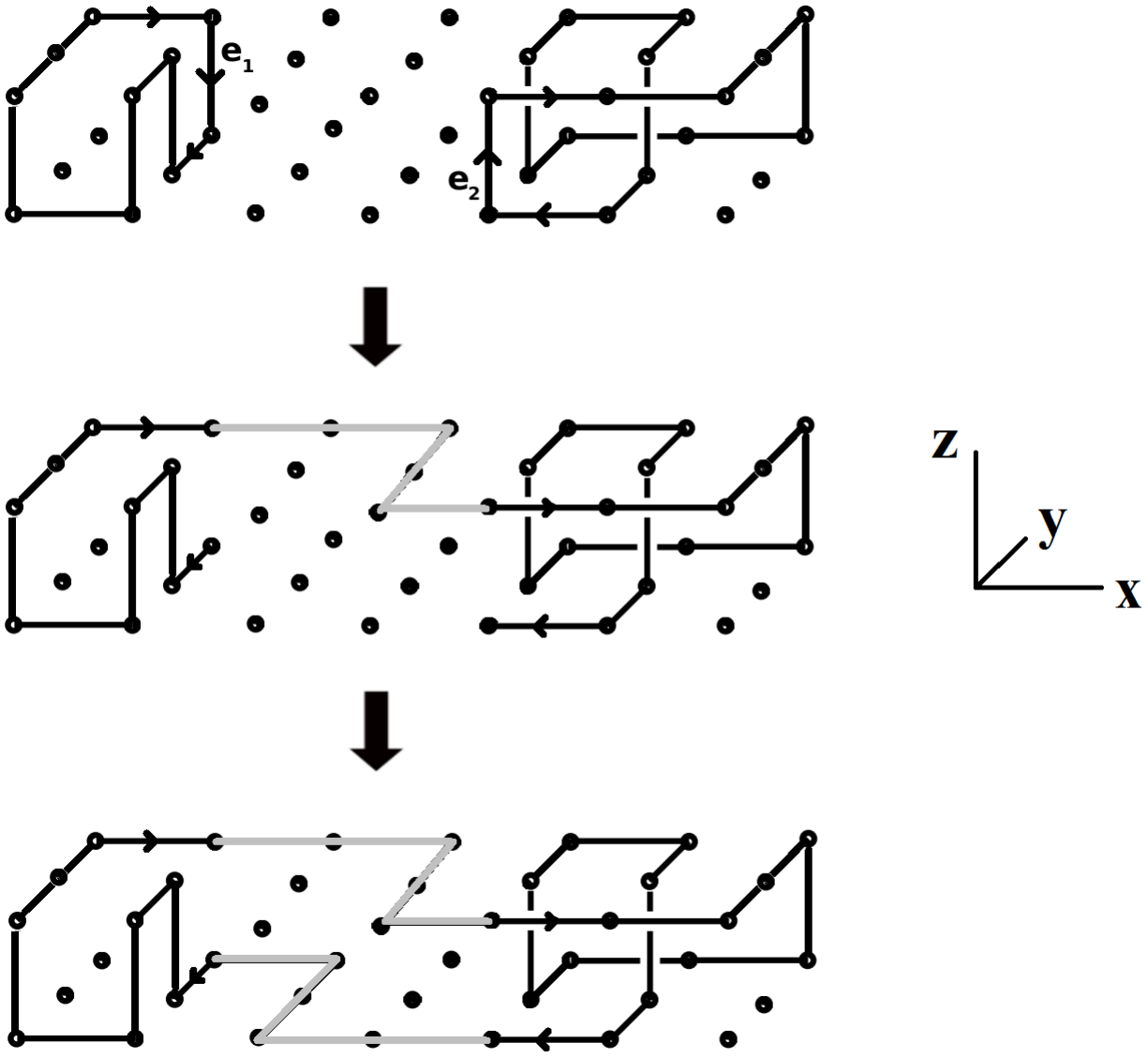

Figure 3.5: An example of the concatenation for Case 1 when e_1 is in the negative z-direction. Note this is a $(2, 1)$-tube.

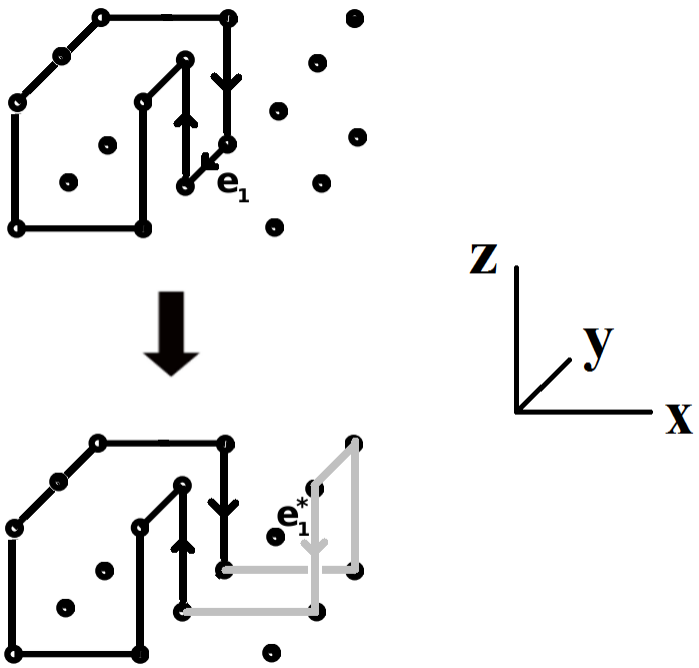

Figure 3.6: An example of creating a new edge e_1^* that is in the negative z-direction, when e_1 is originally in the y-direction. In this case, e_1 is in the negative y-direction, with its z-coordinate equal to zero. Note this is a $(2,1)$-tube.

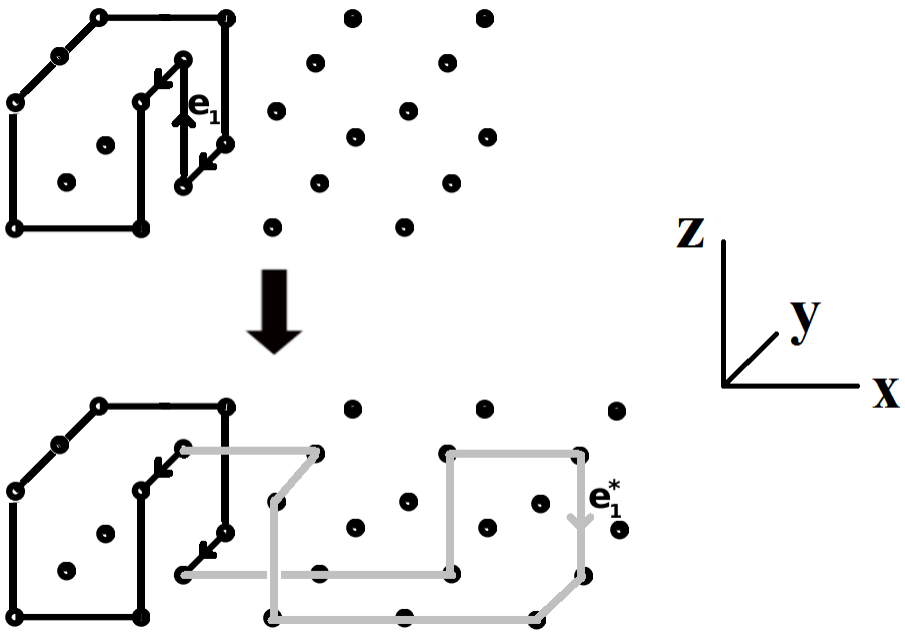

Figure 3.7: An example of creating a new edge e_1^* that is in the negative z-direction, when e_1 is originally in the positive z-direction. In this case, the y-coordinate of e_1 is greater than zero. Note this is a $(2,1)$-tube.

x, positive z, positive x, negative z (this creates the edge e_1^*), negative (positive) y, negative x, negative x, positive z, positive (negative) y, and negative x, so we are at v_{1b}. See Figure 3.7 for an illustration of changing an edge directed in the positive y-direction to an edge directed in the negative y-direction.

Thus, for Case 1, it has been shown that we are able to connect v_{1a} to v_{2b} and v_{2a} to v_{1b} via two sequences of edges (that do not "enter" the m_1-span or m_2-span). Thus, the concatenation theorem is proven for Case 1.

Case 2: Assume without loss of generality that $L = 0$ and $M > 0$, and notice now that e_2 must be in the positive z-direction. If e_1 is in the negative z-direction, we can remove e_1 and e_2 and connect v_{1a} to v_{2b} and v_{2a} to v_{1b} with two sequences of edges similarly to what was done in Case 1. The steps are as follows: Starting at v_{1a}, add one edge in the positive x-direction, and then add edges (if necessary) in the positive z-direction until the z-coordinate is greater than or equal to the z-coordinate of v_{2b}. Next, add one edge in the positive x-direction, and then add edges (if necessary) in the negative z-direction until $v_{2b} - \hat{\imath}$ is reached. Finally add one edge in the positive x-direction to reach v_{2b}. Thus, we have successfully connected v_{1a} to v_{2b}. Similarily (but in the opposite direction), for the next sequence of edges, start at v_{2a} and add one edge in the negative

x-direction, and then add edges (if necessary) in the negative z-direction until the z-coordinate is less than or equal to the z-coordinate of v_{1a}. Next, add one edge in the negative x-direction, and then add edges (if necessary) in the positive z directions until $v_{1b} + \hat{\imath}$ is reached. Finally add one edge in the negative x-direction to reach v_{1b}. Thus, we have successfully connected v_{2a} to v_{1b} and successfully concatenated ω_1 to ω_2. It is important to once again note that by construction, these two sequences of edges do not intersect, and it is repeated that this can be seen by looking at each yz-plane, and noticing that the first sequence of edges is always "above" the second sequence of edges ("above" meaning having a larger z-coordinate).

Notice the situation where e_1 and e_2 are both parallel and directed in the positive z-direction when $L = 0$ and $M > 0$ can never occur. That is, e_1 (or any edge of ω_1 in H_{m_1}) will never be directed in the positive z-direction. To see this, consider ω_1, which is located in the xz-plane between $x = 0$ and $x = m_1$. Note that the first edge of ω_1, call it e^*, must also be directed in the positive z-direction (as a result of lexicographical ordering). Let $v_a^* = \text{int}(e^*)$ and $v_b^* = \text{fin}(e^*)$. Now suppose on the contrary that e_1 is directed in the positive z-direction. Then ω_1 must consist of two sequences of edges (which stay between or on the lines $x = 0$ and $x = m_1$): one sequence from v_b^* to v_{1a} and one sequence from v_{1b} to v_a^*. Since e^* and e_1 are both directed in the positive z-direction, v_a^* lies below v_b^* and v_{1a} lies below v_{1b}. If we first connect say v_b^* to v_{1a} via any sequence of edges, then we have essentially created a border which "splits" the xz-plane ($0 \geq x \geq m_1$ and $0 \geq z \geq M$) into two regions, with v_a^* in the lower region and v_{1b} in the upper region. Notice that starting at a vertex in some region, there is no way to leave the region (via a sequence of edges) without crossing this border. Thus, there is no way to connect v_{1b} to v_a^* without the two sequences of edges intersecting. See Figure 3.8 for an illustration of this impossible case. Hence, there is no SAP that can contain e_1 and e^* and the situation where e_1 and e_2 are both parallel and directed in the positive z-direction when $L = 0$ and $M > 0$ can never occur.

Since the two cases presented are exhaustive, any two polygons in an (L, M)-tube can always be concatenated to form another polygon which contains both the m_1-span and the m_2-span associated with the first and second polygon respectively. □

Now let π_A and π_B be any pair of k-spans. By definition, there exists a polygon ω_A in which π_A occurs, and similarly, there exists a polygon ω_B in which π_B occurs. From Theorem 3.10, ω_A and ω_B can be concatenated into a new polygon ω_C, which has an associated properly connected sequence $(H_s, \pi_1, \ldots, \pi_r, H_f)$. Since π_A occurred in ω_A and π_B occurred in ω_B, and since we know from Theorem 3.10 that the concatenation process will not change any π_A or π_B, it follows that π_A

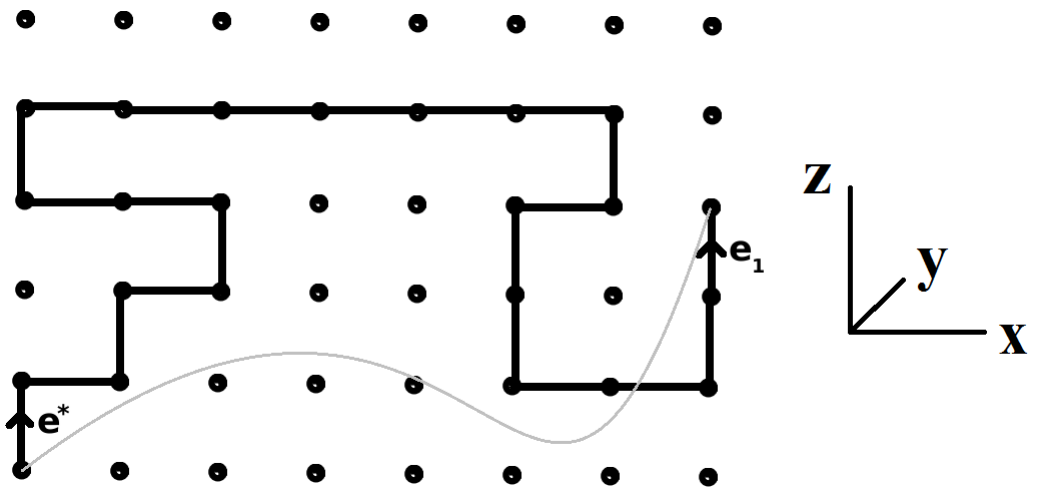

Figure 3.8: An illustration of why it is impossible to have a SAP with two border edges that are parallel and directed in the same direction. Properly connecting two vertices from the edges in any manner essentially creates a border such that the other two vertices that must be connect cannot. Note this is a $(0, 5)$-tube.

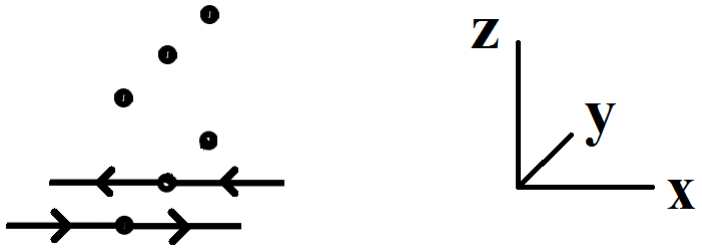

Figure 3.9: An example of a k-span in a $(2, 1)$-tube which can follow itself, with k=2.

and π_B are elements of $(H_s, \pi_1, \ldots, \pi_r, H_f)$, where π_A occurs prior to π_B, as required.

For (c), a sufficient condition for aperiodicity of $\mathcal{D}_p$ with respect to k-spans is the existence of a loop from a k-span to itself. That is, a k-span which can follow itself. Notice that any k-span with just $2k$ edges will be able to follow itself (for an example of a k-span which can follow itself, see Figure 3.9).

The relevant transfer matrix is a matrix-valued function $G(x)$, $x \in \mathbb{C}$, which is a weighted adjacency matrix associated with the subgraph of $\mathcal{D}_p$ generated by the k-spans. $G(x)$ is defined, using the weight exponent function (as done in the toy example), as follows. First label the k-spans

with the integers 1 to $|\Pi(k)|$. Then, $G(x) = (g_{i,j}(x))$ is a $|\Pi(k)| \times |\Pi(k)|$ matrix defined as:

$$g_{i,j}(x) = \begin{cases} x^{e_i} & \text{if } k\text{-span } j \text{ can follow } k\text{-span } i \\ 0 & \text{otherwise,} \end{cases} \tag{3.21}$$

where e_i is the number of edges contained in $S_1(L,M) \cup H_1(L,M)$ of k-span i.

Next, define two additional matrix-valued functions $A(x)$ and $B(x)$ associated with the start-hinges and finish-hinges, respectively. Label the start-hinges with the integers 1 to $|\mathcal{H}_s|$. Then $A(x) = (a_{i,j}(x))$ is a $|\mathcal{H}_s| \times |\Pi(k)|$ matrix defined as:

$$a_{i,j}(x) = \begin{cases} x^{s_i} & \text{if } k\text{-span } j \text{ can follow start-hinge } i \\ 0 & \text{otherwise,} \end{cases} \tag{3.22}$$

where s_i is the number of edges in start-hinge i. Label the finish-hinges with the integers 1 to $|\mathcal{H}_f|$. Then $B(x) = (b_{i,j}(x))$ is a $|\Pi(k)| \times |\mathcal{H}_f|$ matrix defined as:

$$b_{i,j}(x) = \begin{cases} x^{f_{ij}} & \text{if finish-hinge } j \text{ can follow } k\text{-span } i \\ 0 & \text{otherwise,} \end{cases} \tag{3.23}$$

where f_{ij} is the number of edges in $S_2(L,M) \cup H_2(L,M) \cup \ldots \cup H_{k-1}(L,M) \cup S_k(L,M)$ of k-span i plus the number of edges in finish-hinge j.

The first consequence of the transfer-matrix formulation, since (a), (b), and (c) are satisfied, is that not only does the limit in Theorem 2.7 exist, but that there exists $\alpha > 0$ such that

$$p_{2n}(L,M) \sim \alpha e^{\kappa_p(L,M)n} \tag{3.24}$$

as $n \to \infty$. This is done in a similar fashion to our toy example where we used Theorem 3.5 and Theorem 3.6 to show that for the number of "words" with weight n, that $d(n) \sim \alpha_d x_0^{-n}$ as $n \to \infty$. To show how this was achieved for SAPs in (L,M)-tubes, it will be shown next how to relate the generating function for SAPs in (L,M)-tubes to the transfer matrix.

Definition 3.17. For any integer $k \geq 2$, define $p_{2n,k}(L,M)$ to be the number of $2n$-edge polygons counted in $p_{2n}(L,M)$ that have span greater than k, and let $\mathcal{P}_{2n,k}(L,M)$ be the set of all such polygons.

Note that, since k is finite and fixed, there exists $N_k = (L+1)(M+1)(k+1) > 0$ such that $p_{2n,k}(L,M) = p_{2n}(L,M)$ for all $2n > N_k$, and thus, for example, $\lim_{n\to\infty}(2n)^{-1}\log p_{2n,k}(L,M) = \lim_{n\to\infty}(2n)^{-1}\log p_{2n}(L,M) = \kappa_p(L,M)$. Consider the generating function for the sequence $p_{2n,k}(L,M)$,

$$F_k(x) = \sum_n p_{2n,k}(L,M)x^{2n}. \tag{3.25}$$

Notice that for any SAP $\omega \in \mathcal{P}_{2n,k}(L,M)$, there is a properly connected sequence $(H_s, \pi_1, \ldots, \pi_h, H_f)$ associated with ω such that $a_{H_s,\pi_1} \neq 0$, $b_{\pi_h,H_f} \neq 0$, and $g_{i,i+1} \neq 0$ for $1 \leq i \leq h-1$. Also notice that the weight associated with this polygon in $(A(x)G(x)^{h-1}B(x))_{H_s,H_f}$ is:

$$x^{s_{H_s}+f_{\pi_h H_f}+\sum_{i=1}^{h} e_{\pi_i}} = x^{2n}. \tag{3.26}$$

Thus, $F_k(x)$ satisfies the following:

$$\begin{aligned} F_k(x) &= \sum_{h=1}^{\infty} \sum_{i=1}^{|\mathcal{H}_s|} \sum_{j=1}^{|\mathcal{H}_f|} (A(x)G(x)^{h-1}B(x))_{ij} \\ &= \sum_{i=1}^{|\mathcal{H}_s|} \sum_{j=1}^{|\mathcal{H}_f|} (A(x)(I-G(x))^{-1}B(x))_{i,j} \qquad (3.27) \\ &= \sum_{i=1}^{|\mathcal{H}_s|} \sum_{j=1}^{|\mathcal{H}_f|} \sum_{o=1}^{|\Pi(k)|} \sum_{l=1}^{|\Pi(k)|} [A_{i,l}(x)((I-G(x))^{-1}_{l,o}B_{o,j}(x)]. \qquad (3.28) \end{aligned}$$

Using the standard adjugate formula for the inverse of a matrix,

$$((I-G(x))^{-1})_{lo} = \frac{(-1)^{(o+l)} \det(I-G(x);o,l)}{\det(I-G(x))}, \tag{3.29}$$

we have:

$$F_k(x) = \frac{\sum_{i=1}^{|\mathcal{H}_s|} \sum_{j=1}^{|\mathcal{H}_f|} \sum_{o=1}^{|\Pi(k)|} \sum_{l=1}^{|\Pi(k)|} [(-1)^{o+l} A_{i,l}(x) \det(I-G(x);o,l) B_{o,j}(x)]}{\det(I-G(x))}. \tag{3.30}$$

Theorem 3.11 (Soteros[24])**.** *There exists $\alpha > 0$ such that as $n \to \infty$,*

$$p_{2n}(L,M) \sim \alpha e^{\kappa_p(L,M)2n}. \tag{3.31}$$

Proof. Note that the proof given here uses a different (more general) transfer matrix than what Soteros used in [24], but the steps of the proof remain the same. Given any $x > 0$, the irreducibility of the digraph $\mathcal{D}_p$ for the set of k-spans gives that for any pair of k-spans π_i, π_j, there exists an integer h such that $(G(x)^{h-1})_{i,j} > 0$, where h corresponds to the length of a properly connected subsequence of k-spans starting with π_i and ending in π_j. Furthermore, for P_{i^*}, a k-span which can follow itself, $(G(x))_{i^*,i^*} > 0$. Thus, for fixed $x > 0$, $G(x)$ is an irreducible, aperiodic, non-negative matrix, and Theorem 3.5 implies that:

- the spectral radius $\rho(x)$ of $G(x)$ is a simple root of $\det(\lambda I - G(x))$;
- $G(x)$ has a strictly positive eigenvector associated with $\rho(x)$; and

- $\rho(x)$ is the only eigenvalue of modulus $\rho(x)$.

Since $\rho(0)$ and $\rho(x)$ is an unbounded, increasing, continuous function on $[0,\infty)$, there exists a unique $x_0 > 0$ such that $\rho(x_0) = 1$. From equation (3.30), $F_k(x)$ has poles only when $\frac{1}{\det(I-G(x))}$ has poles; that is, when 1 is an eigenvalue of $G(x)$. Thus, $F_k(x)$ has one simple pole when $|x| = x_0$, namely $x = x_0$. In particular, multiplying both sides of equation (3.27), taking $\lim_{x\to x_0}$, and using Theorem 3.6, we have:

$$\begin{aligned}
\lim_{x\to x_0}(x_0^2 - x^2)F_k(x) &= \lim_{x\to x_0}(x_0^2 - x^2)\sum_{i=1}^{|\mathcal{H}_s|}\sum_{j=1}^{|\mathcal{H}_f|}(A(x)(I-G(x))^{-1}B(x))_{i,j} \\
\lim_{x\to x_0}(x_0^2 - x^2)\sum_n p_{2n,k}(L,M)x^{2n} &= \lim_{x\to x_0}(x_0+x)\sum_{i=1}^{|\mathcal{H}_s|}\sum_{j=1}^{|\mathcal{H}_f|}(A(x)(x_0-x)(I-G(x))^{-1}B(x))_{i,j} \\
&= 2x_0\sum_{i=1}^{|\mathcal{H}_s|}\sum_{j=1}^{|\mathcal{H}_f|}(A(x_0)(x_0\beta^{-1}\xi\eta^\top)B(x_0))_{i,j} \\
&= 2x_0^2\beta^{-1}\sum_{i=1}^{|\mathcal{H}_s|}\sum_{j=1}^{|\mathcal{H}_f|}(A(x_0)\xi\eta^\top B(x_0))_{i,j}. \qquad (3.32)
\end{aligned}$$

For ease of notation, let $\sum_{i=1}^{|\mathcal{H}_s|}\sum_{j=1}^{|\mathcal{H}_f|}(A(x_0)\xi\eta^\top B(x_0))_{i,j} = C(x_0)$. Equation (3.32) implies that as $x \to x_0$,

$$\begin{aligned}
\sum_n p_{2n,k}(L,M)x^{2n} &\sim 2x_0^2\beta^{-1}C(x_0)(x_0^2-x^2)^{-1} \\
&\sim 2\beta^{-1}C(x_0)(1-x^2/x_0^2)^{-1} \\
&\sim 2\beta^{-1}C(x_0)\sum_{n=0}^{\infty}(x^2/x_0^2)^n \\
&\sim 2\beta^{-1}C(x_0)\sum_{n=0}^{\infty}x_0^{-2n}(x^2)^n \qquad (3.33)
\end{aligned}$$

where $\beta = x_0\eta^\top G'(x_0)\xi$, and $\eta^\top$ and ξ are, respectively, strictly positive left and right eigenvectors of $G(x_0)$ associated with $\rho(x_0) = 1$ and normalized so that $\eta^\top\xi = 1$ (note that $G'(x)$ denotes the derivative of $G(x)$ with respect to x). Thus, as was done in equation (3.15), differentiating both sides of the above equation n times with respect to x, setting $x = 0$, and dividing by $n!$ implies that for $2n > N_k$:

$$p_{2n}(L,M) = p_{2n,k}(L,M) \sim \alpha(x_0^2)^{-n} \text{ as } n \to \infty, \qquad (3.34)$$

where

$$\alpha = 2\beta^{-1}C(x_0) > 0. \tag{3.35}$$

From Theorem 2.7, $e^{\kappa_p(L,M)} = x_0^{-1}$, and hence, the theorem is proved. □

The next consequence of the transfer matrix formulation is a pattern theorem. Given a k-span π, we prove results about $p_{2n,k}(L, M; \bar{\pi})$, the number of SAPs counted in $p_{2n,k}(L, M) > 0$ that do not contain k-span π. First, we must define another category of k-spans. That is, we say a k-span π is *protected* with respect to the concatenation process (in the proof of Theorem 3.10) if the concatenation of any pair of SAPs in an (L, M)-tube that do not contain π results in a SAP that still does not contain π.

Theorem 3.12 (Soteros[24])**.** *Given any integer $k \geq 2$ let π be a k-span that is protected (with respect to the concatenation process). Then there exists $\alpha_\pi > 0$ and $\kappa_\pi(L, M) > 0$ such that for $2n > N_k$,*

$$p_{2n}(L, M; \bar{\pi}) = p_{2n,k}(L, M; \bar{\pi}) \sim \alpha_\pi e^{\kappa_\pi(L,M)2n} \text{ as } n \to \infty \tag{3.36}$$

with

$$\kappa_\pi(L, M) < \kappa_p(L, M) \tag{3.37}$$

Proof. Note once again that the proof given here uses a different (more general) transfer matrix than what Soteros used in [24], but the steps of the proof remain the same. For any integer $k \geq 2$, let $\pi \in \Pi(k)$ be any protected k-span, and suppose π is the rth k-span in the ordered list of $\Pi(k)$. Consider the generating function $\bar{F}_k(x) = \sum_{n\geq 1} p_{2n,k}(L, M; \bar{\pi})x^{2n}$. Then

$$\begin{aligned} \bar{F}_k(x) &= \sum_{h=1}^{\infty} \sum_{i=1}^{|\mathcal{H}_s|} \sum_{j=1}^{|\mathcal{H}_f|} (\bar{A}(x)\bar{G}(x)^{h-1}\bar{B}(x))i, j \\ &= \sum_{i=1}^{|\mathcal{H}_s|} \sum_{j=1}^{|\mathcal{H}_f|} (\bar{A}(x)(I - \bar{G}(x))^{-1}\bar{B}(x))i, j \end{aligned} \tag{3.38}$$

where $\bar{G}(x)$ is obtained from $G(x)$ by deleting the row and column of $G(x)$ that correspond to pattern π (i.e. the rth row and column), and $\bar{A}(x)$ and $\bar{B}(x)$ are defined as follows: $\bar{A}(x)$ ($\bar{B}(x)$) is defined to be the matrix obtained from $A(x)$ ($B(x)$) by deleting its rth column (row). Let ω_1 and ω_2 be any two SAPs which do not contain the k-span π. Since π is protected, if ω_1 and ω_2 are concatenated into the SAP $\omega_c = \omega_1 \circ_p \omega_2$, then ω_c does not contain π. With this, arguments

analogous to those used by Soteros and Whittington in [26] for the proof of Theorem 2.7 lead now to the existence of the following limit:

$$\lim_{n\to\infty} (2n)^{-1} \log p_{2n,k}(L, M; \bar{\pi}) =: \kappa_\pi(L, M). \tag{3.39}$$

Furthermore, using the same arguments that were used for $G(x)$, $\bar{G}(x)$ can be shown to be a non-negative, irreducible, and aperiodic matrix (if π happens to be the k-span used to establish aperiodicity previously, then use a different k-span with $2k$-edges to establish periodicity). Hence, the arguments used in the proof of Theorem 3.11 apply again so that there exist $\bar{x}_0 > 0$ and $\alpha_\pi > 0$ such that

$$p_{2n,k}(L, M; \bar{\pi}) \sim \alpha_\pi (\bar{x}_0)^{-2n} \text{ as } n \to \infty, \tag{3.40}$$

with $e^{\kappa_\pi(L,M)} = (\bar{x}_0)^{-1}$ and the spectral radius $\bar{\rho}(\bar{x}_0)$ of $\bar{G}(\bar{x}_0)$ equals 1. Now note that since $n \to \infty$, we have the following result which does not include the restriction on the span of the SAP:

$$p_{2n}(L, M; \bar{\pi}) \sim \alpha_\pi e^{\kappa_\pi(L,M)2n} \text{ as } n \to \infty. \tag{3.41}$$

Now consider the matrix $G_\pi(x)$ obtained from $G(x)$ by replacing the rth row and column of $G(x)$ by a row and column of zeros. Then the spectral radius $\rho_\pi(x)$, of $G_\pi(x)$ equals $\bar{\rho}(x)$. Furthermore, elementwise $G_\pi(x) \leq G(x)$ and at least one element of $G_\pi(x)$ is strictly less than the corresponding element of $G(x)$. Thus, Theorem 3.7 implies that $\rho_\pi(x) < \rho(x)$, and hence for $x = x_0$, $\rho_\pi(x_0) < \rho(x_0) = 1$. Therefore, $\bar{x}_0 > x_0$ or equivalently $\kappa_\pi(L, M) < \kappa_p(L, M)$. □

Note that if k-span $\pi \in \Pi(k)$ is not protected, then we expect that other concatenation constructions (which may depend on π) that avoid creating π can be defined. These modifications should lead to the same resulting pattern theorem.

The pattern theorem tells us that all but exponentially few sufficiently large SAPs contain a given suitable k-span π. If we let the given k-span guarantee that the polygon is knotted (see Figure 3.10 for such a k-span), then the result that all but exponentially few sufficiently large SAPs in an (L, M)-tube are knotted follows.

The transfer-matrix formulation also allows us to prove results about the expected number of times a k-span π occurs as a function of the length of a SAP in an (L, M)-tube, i.e. results about the density of π.

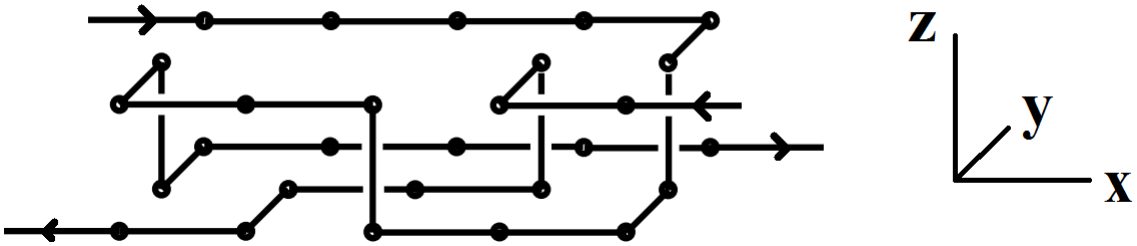

Figure 3.10: This 6-span in a $(2,1)$-tube is a "tight" trefoil, meaning that any SAP which contains this 6-span will be knotted.

3.4 Expected Number of Occurrences Per Edge of a k-span in a Random $2n$-edge SAP (as $n \to \infty$)

This section is based on [9], where Duffy applied Alm and Janson's work on one-dimensional SAWs in [1] to SAPs in (L, M)-tubes to find the expected number of occurrences per edge of a k-span in a random $2n$-edge SAP (as $n \to \infty$) in an (L, M)-tube. Here, for any integer $k \geq 2$, we are assuming that for large enough n ($2n > N_k$), each SAP of length $2n$ in an (L, M)-tube is equally likely. That is, if we let $W_{2n,k}$ be a random $2n$-edge SAP in an (L, M)-tube with span greater than k, then the probability mass function (pmf) of $W_{2n,k}$ is

$$\mathrm{P}(W_{2n,k} = \omega) = \frac{1}{p_{2n,k}(L, M)}, \tag{3.42}$$

for every $\omega \in \mathcal{P}_{2n,k}(L, M)$. Let $\mathrm{E}_{2n,k}(\cdot)$ be the expected value with respect to this pmf. That is, the expected value is taken over all polygons in the set $\mathcal{P}_{2n,k}(L, M)$. So given a function f on a random polygon $W_{2n,k}$, we have

$$\mathrm{E}_{2n,k}(f(W_{2n,k})) = \sum_{\omega \in \mathcal{P}_{2n,k}(L,M)} f(\omega) \left(\frac{1}{p_{2n,k}(L, M)} \right). \tag{3.43}$$

Now consider the case where $k = 2$ and we are working with 2-spans, and consider the 3-span made up of 2-span u followed by 2-span v, assuming that v can follow u. Let $\psi_{uv}(\omega)$ be the number of times the 3-span uv occurs in a SAP ω. Following the proof of [1, Theorem 7], let $\widetilde{G}(x;t) = (\widetilde{g}_{r,l}(x;t))$ be the matrix with elements:

$$\widetilde{g}_{r,l}(x;t) = \begin{cases} x^{e_r} e^t & \text{if } r = u \text{ and } l = v \\ x^{e_r} & \text{otherwise,} \end{cases}$$

where e_r is the number of edges in the first section and hinge of the rth 2-span. Thus we have $\widetilde{G}(x;0) = G(x)$, where $G(x)$ is the transfer matrix defined in Section 3.3. Define

$$\widetilde{\Lambda}(x) = \frac{\partial}{\partial t}(\widetilde{G}(x;0)) = (\widetilde{\lambda}_{r,l}(x)), \tag{3.44}$$

with

$$\widetilde{\lambda}_{r,l}(x) = \begin{cases} x^{e_r} = x^{e_u} & \text{if } r = u \text{ and } l = v \\ 0 & \text{otherwise.} \end{cases}$$

For ease of notation, let ψ_{uv} represent the random variable $\psi_{uv}(W_{2n,2})$. It then follows that:

$$\begin{aligned} \sum_n \mathrm{E}_{2n,2}\left(e^{\psi_{uv}t}\right) p_{2n,2}(L,M)x^{2n} &= \sum_n \sum_{\omega \in \mathcal{P}_{2n,2}(L,M)} e^{\psi_{uv}(\omega)t}\left(\frac{1}{p_{2n,2}(L,M)}\right) p_{2n,2}(L,M)x^{2n} \\ &= \sum_n \sum_{\omega \in \mathcal{P}_{2n,k}(L,M)} e^{\psi_{uv}(\omega)t}x^{2n} \end{aligned} \tag{3.45}$$

Recall from equation (3.26) that any SAP $\omega \in \mathcal{P}_{2n,k}(L,M)$ can be represented by a properly connected sequence $(H_s, \pi_1, \ldots, \pi_h, H_f)$, and that the weight associated with ω in $(A(x)G(x)^{h-1}B(x))_{H_s,H_f}$ is:

$$x^{s_{H_s}+f_{\pi_h H_f}+\sum_{i=1}^h e_{\pi_i}} = x^{2n}. \tag{3.46}$$

Similarily, the weight associated with ω in $(A(x)\widetilde{G}(x;t)^{h-1}B(x))_{H_s,H_f}$ is:

$$e^{\psi_{uv}(\omega)t}x^{s_{H_s}+f_{\pi_h H_f}+\sum_{i=1}^h e_{\pi_i}} = e^{\psi_{uv}(\omega)t}x^{2n}. \tag{3.47}$$

Hence, we can rewrite equation (3.45) as:

$$\begin{aligned} \sum_n \mathrm{E}_{2n,2}\left(e^{\psi_{uv}t}\right) p_{2n,2}(L,M)x^{2n} &= \sum_{h=1}^{\infty}\sum_{i=1}^{|\mathcal{H}_s|}\sum_{j=1}^{|\mathcal{H}_f|}\left[A(x)\widetilde{G}(x;t)^{h-1}B(x)\right]_{ij} \\ &= \sum_{i=1}^{|\mathcal{H}_s|}\sum_{j=1}^{|\mathcal{H}_f|}\left[A(x)(I-\widetilde{G}(x;t))^{-1}B(x)\right]_{ij} \end{aligned} \tag{3.48}$$

Taking derivatives with respect to t on both sides and evaluating at $t = 0$ implies:

$$\sum_n \mathrm{E}_{2n,2}(\psi_{uv})p_{2n,2}(L,M)x^{2n} = \sum_{i=1}^{|\mathcal{H}_s|}\sum_{j=1}^{|\mathcal{H}_f|}\left[A(x)(I-G(x))^{-1}\widetilde{\Lambda}(x)(I-G(x))^{-1}B(x)\right]_{ij}. \tag{3.49}$$

Recall from Theorem 3.6 that $\lim_{x\to x_0}(x_0-x)(I-G(x))^{-1} = x_0\beta^{-1}\xi\eta^\top$. Thus, multiplying both sides of the above equation by $(x_0^2-x^2)^2$, taking $\lim_{x\to x_0}$, and using Theorem 3.6, we have:

$$\begin{aligned}
\lim_{x\to x_0}(x_0^2-x^2)^2\sum_n \mathrm{E}_{2n,2}(\psi_{uv})p_{2n,2}(L,M)x^{2n} &= 4x_0^2\sum_{i=1}^{|\mathcal{H}_s|}\sum_{j=1}^{|\mathcal{H}_f|}\Big[A(x_0)(x_0\beta^{-1}\xi\eta^\top)\widetilde{\Lambda}(x_0)(x_0\beta^{-1}\xi\eta^\top)B(x_0)\Big]_{i,j}\\
&= 4x_0^4\beta^{-2}\sum_{i=1}^{|\mathcal{H}_s|}\sum_{j=1}^{|\mathcal{H}_f|}\Big[A(x_0)\xi\eta^\top\widetilde{\Lambda}(x_0)\xi\eta^\top B(x_0)\Big]_{i,j}\\
&= 4x_0^4\beta^{-2}\sum_{i=1}^{|\mathcal{H}_s|}\sum_{j=1}^{|\mathcal{H}_f|}\Big[A(x_0)\xi\eta_u x_0^{e_u}\xi_v\eta^\top B(x_0)\Big]_{i,j}\\
&= 4x_0^4\beta^{-2}(\eta_u x_0^{e_u}\xi_v)\sum_{i=1}^{|\mathcal{H}_s|}\sum_{j=1}^{|\mathcal{H}_f|}\Big[A(x_0)\xi\eta^\top B(x_0)\Big]_{i,j}\\
&= 4x_0^4\beta^{-2}(\eta_u x_0^{e_u}\xi_v)C(x_0), \qquad (3.50)
\end{aligned}$$

since $\eta^\top\widetilde{\Lambda}(x_0)\xi = \eta_u x_0^{e_u}\xi_v$. Therefore, we have that as $x\to x_0$,

$$\begin{aligned}
\sum_n \mathrm{E}_{2n,2}(\psi_{uv})p_{2n,2}(L,M)x^{2n} &\sim 4x_0^4\beta^{-2}(\eta_u x_0^{e_u}\xi_v)C(x_0)(x_0^2-x^2)^{-2}\\
&\sim 4\beta^{-2}(\eta_u x_0^{e_u}\xi_v)C(x_0)(1-x^2/x_0^2)^{-2}\\
&\sim 4\beta^{-2}(\eta_u x_0^{e_u}\xi_v)C(x_0)\sum_{n=0}^{\infty}(n+1)(x^2/x_0^2)^n\\
&\sim 4\beta^{-2}(\eta_u x_0^{e_u}\xi_v)C(x_0)\sum_{n=0}^{\infty}(n+1)x_0^{-2n}x^{2n}. \qquad (3.51)
\end{aligned}$$

Differentiating both sides of the above equation n times with respect to x, setting $x=0$, and dividing by $n!$, we obtain

$$\mathrm{E}_{2n,2}(\psi_{uv})p_{2n,2}(L,M) \sim 4\beta^{-2}(\eta_u x_0^{e_u}\xi_v)C(x_0)(n+1)x_0^{-2n}. \qquad (3.52)$$

Solving for $\mathrm{E}_{2n,2}(\psi_{uv})$ and recalling equations (3.34) and (3.35), we get:

$$\begin{aligned}
\mathrm{E}_{2n,2}(\psi_{uv}) &\sim \frac{4\beta^{-2}(\eta_u x_0^{e_u}\xi_v)C(x_0)(n+1)x_0^{-2n}}{p_{2n,k}(L,M)}\\
&\sim \frac{4\beta^{-2}(\eta_u x_0^{e_u}\xi_v)C(x_0)(n+1)x_0^{-2n}}{2\beta^{-1}C(x_0)x_0^{-2n}}\\
&\sim \frac{2(\eta_u x_0^{e_u}\xi_v)(n+1)}{\beta}. \qquad (3.53)
\end{aligned}$$

Thus, we have:

$$\lim_{n\to\infty}\frac{\mathrm{E}_{2n}(\psi_{uv})}{2n} = \frac{\eta_u x_0^{e_u}\xi_v}{\beta}, \qquad (3.54)$$

which gives us an expression for the expected number of occurrences per edge of a 3-span in a random $2n$-edge SAP (as $n \to \infty$).

If we let $\psi_u(\omega)$ be the number of times the 2-span u occurs in a SAP ω, then similar to the previous argument, one can derive the following expression for the expected number of occurrences per edge of a 2-span in a random $2n$-edge SAP (as $n \to \infty$):

$$\lim_{n\to\infty} \frac{\mathrm{E}_{2n}(\psi_u)}{2n} = \frac{\eta_u \xi_u}{\beta}. \tag{3.55}$$

To derive an equation for the probability that a 2-span v follows 2-span u, we note that by using equivalent arguments to those leading to [1, equation (7.3)], the probability that a 2-span v follows 2-span u is asymptotically:

$$x_0^{e_u} \frac{\xi_v}{\xi_u}. \tag{3.56}$$

As stated in [1], this has the interpretation that given 2-span u occurs in a section, the probability that the next 2-span is 2-span j is asymptotically $x_0^{e_u} \frac{\xi_v}{\xi_u}$. Thus, we can model the occurrences of 2-spans by a Markov chain, with states $\Pi(2)$ and probability transition matrix $P = (p_{uv})$, where

$$p_{uv} = x_0^{e_u} \frac{\xi_v}{\xi_u}. \tag{3.57}$$

We can now calculate the expected number of times an arbitrary k-span occurs (per edge) as follows. Suppose a k-span consists of $h = k - 1$ 2-spans $(\pi_1, \pi_2, ..., \pi_h)$. Then all that is needed is to multiply the expected number of times 2-span π_1 occurs by the probability that π_2 follows π_1, multiplied by the probability that π_3 follows π_2 and so forth. The resulting expression is:

$$\begin{aligned} \lim_{n\to\infty} \frac{\mathrm{E}_{2n}(\psi_{\pi_1\pi_2\ldots\pi_h})}{2n} &= \left(\frac{\eta_{\pi_1}\xi_{\pi_1}}{\beta}\right)\left(x_0^{e_{\pi_1}}\frac{\xi_{\pi_2}}{\xi_{\pi_1}}\right)\left(x_0^{e_{\pi_2}}\frac{\xi_{\pi_3}}{\xi_{\pi_2}}\right)\cdots\left(x_0^{e_{\pi_{h-1}}}\frac{\xi_{\pi_h}}{\xi_{\pi_{h-1}}}\right) \\ &= \frac{\eta_{\pi_1} x_0^{e_{\pi_1}+e_{\pi_2}+\cdots e_{\pi_{h-1}}} \xi_{\pi_h}}{\beta}, \end{aligned} \tag{3.58}$$

which gives us an expression for the expected number of occurrences per edge of a k-span that consists of the $h = k - 1$ 2-spans $(\pi_1, \pi_2, ..., \pi_h)$, in a random $2n$-edge SAP (as $n \to \infty$).

3.5 Expected Span Per Edge of a Random $2n$-edge SAP (as $n \to \infty$)

This section is also based on [9], where Duffy once again applied Alm and Janson's work on one-dimensional SAWs in [1] to SAPs in (L, M)-tubes to find the expected span per edge of a random $2n$-edge SAP (as $n \to \infty$) in an (L, M)-tube. Let $\widehat{G}(x; t)$ be the matrix defined by

$$\widehat{G}(x; t) = G(x)e^t, \tag{3.59}$$

where $G(x)$ is the transfer matrix in Section 3.3. Thus, we have $\widehat{G}(x;0) = G(x)$, and we define

$$\widehat{\Lambda}(x) = \frac{\partial}{\partial t}(\widehat{G}(x;0)) = G(x). \tag{3.60}$$

If for any polygon ω, we let $m(\omega)$ be the span of ω, and for ease of notation, we let m represent the random variable $m(W_{2n,2})$, then it follows that:

$$\begin{aligned}\sum_n \mathrm{E}_{2n,2}\left(e^{mt}\right) p_{2n,2}(L,M)x^{2n} &= \sum_n \sum_{\omega\in\mathcal{P}_{2n,2}(L,M)} e^{m(\omega)t}\left(\frac{1}{p_{2n,2}(L,M)}\right) p_{2n,2}(L,M)x^{2n} \\ &= \sum_n \sum_{\omega\in\mathcal{P}_{2n,k}(L,M)} e^{m(\omega)t}x^{2n} \end{aligned} \tag{3.61}$$

Recall once again from equation (3.26) that any SAP $\omega \in \mathcal{P}_{2n,k}(L,M)$ can be represented by a properly connected sequence $(H_s, \pi_1, \ldots, \pi_h, H_f)$, and that the weight associated with ω in $(A(x)G(x)^{h-1}B(x))_{H_s,H_f}$ is:

$$x^{s_{H_s}+f_{\pi_h H_f}+\sum_{i=1}^{h} e_{\pi_i}} = x^{2n}. \tag{3.62}$$

Also, since a polygon with h 2-spans has a span of $h+1$, we can rewrite equation (3.61) as:

$$\begin{aligned}\sum_n \mathrm{E}_{2n,2}(e^{mt})p_{2n,2}(L,M)x^{2n} &= \sum_{h=1}^{\infty}\sum_{i=1}^{|\mathcal{H}_s|}\sum_{j=1}^{|\mathcal{H}_f|}\left[A(x)G(x)^{h-1}B(x)\right]_{ij} e^{(h+1)t} \\ &= \sum_{h=1}^{\infty}\sum_{i=1}^{|\mathcal{H}_s|}\sum_{j=1}^{|\mathcal{H}_f|}\left[A(x)\widehat{G}(x;t)^{h-1}B(x)\right]_{ij} e^{2t} \\ &= \sum_{i=1}^{|\mathcal{H}_s|}\sum_{j=1}^{|\mathcal{H}_f|}\left[A(x)(I-\widehat{G}(x;t))^{-1}B(x)\right]_{ij} e^{2t}. \end{aligned} \tag{3.63}$$

Taking derivatives with respect to t on both sides and evaluating at $t=0$ implies:

$$\begin{aligned}\sum_n \mathrm{E}_{2n,2}(m)p_{2n,2}(L,M)x^{2n} &= \sum_{i=1}^{|\mathcal{H}_s|}\sum_{j=1}^{|\mathcal{H}_f|}\left[A(x)(I-G(x))^{-1}\widehat{\Lambda}(x)(I-G(x))^{-1}B(x)\right]_{ij} + \\ &\quad 2\sum_{i=1}^{|\mathcal{H}_s|}\sum_{j=1}^{|\mathcal{H}_f|}\left[A(x)(I-G(x))^{-1}B(x)\right]_{ij} \end{aligned} \tag{3.64}$$

Recall from Theorem 3.6 that $\lim_{x\to x_0}(x_0-x)(I-G(x))^{-1} = x_0\beta^{-1}\xi\eta^\top$. Thus, multiplying both sides of the above equation by $(x_0^2-x^2)^2$, taking $\lim_{x\to x_0}$, and using Theorem 3.6, we have:

$$\begin{aligned}
\lim_{x\to x_0}(x_0^2-x^2)^2\sum_n \mathrm{E}_{2n,2}(m)p_{2n,2}(L,M)x^{2n} &= 4x_0^2\sum_{i=1}^{|\mathcal{H}_s|}\sum_{j=1}^{|\mathcal{H}_f|}\Big[A(x_0)(x_0\beta^{-1}\xi\eta^\top)\widehat{\Lambda}(x_0)(x_0\beta^{-1}\xi\eta^\top)B(x_0)\Big]_{i,j}\\
&= 4x_0^4\beta^{-2}\sum_{i=1}^{|\mathcal{H}_s|}\sum_{j=1}^{|\mathcal{H}_f|}\Big[A(x_0)\xi\eta^\top G(x_0)\xi\eta^\top B(x_0)\Big]_{i,j}\\
&= 4x_0^4\beta^{-2}\sum_{i=1}^{|\mathcal{H}_s|}\sum_{j=1}^{|\mathcal{H}_f|}\Big[A(x_0)\xi\eta^\top\xi\eta^\top B(x_0)\Big]_{i,j}\\
&= 4x_0^4\beta^{-2}\sum_{i=1}^{|\mathcal{H}_s|}\sum_{j=1}^{|\mathcal{H}_f|}\Big[A(x_0)\xi\eta^\top B(x_0)\Big]_{i,j}\\
&= 4x_0^4\beta^{-2}C(x_0), \qquad (3.65)
\end{aligned}$$

since $\eta^\top$ and ξ are eigenvectors of $G(x_0)$ and $\eta^\top\xi = 1$. Therefore, we have that as $x\to x_0$,

$$\begin{aligned}
\sum_n \mathrm{E}_{2n,2}(m)p_{2n,2}(L,M)x^{2n} &\sim 4x_0^4\beta^{-2}C(x_0)(x_0^2-x^2)^{-2}\\
&\sim 4\beta^{-2}C(x_0)(1-x^2/x_0^2)^{-2}\\
&\sim 4\beta^{-2}C(x_0)\sum_{n=0}^{\infty}(n+1)(x^2/x_0^2)^n\\
&\sim 4\beta^{-2}C(x_0)\sum_{n=0}^{\infty}(n+1)x_0^{-2n}x^{2n}. \qquad (3.66)
\end{aligned}$$

Differentiating both sides of the above equation n times with respect to x, setting $x=0$, and dividing by $n!$, we obtain

$$\mathrm{E}_{2n,2}(m)p_{2n,2}(L,M) \sim 4\beta^{-2}C(x_0)(n+1)x_0^{-2n}. \qquad (3.67)$$

Solving for $\mathrm{E}_{2n,2}(m)$, recalling equations (3.34) and (3.35), we get:

$$\begin{aligned}
\mathrm{E}_{2n,2}(m) &\sim \frac{4\beta^{-2}C(x_0)(n+1)x_0^{-2n}}{p_{2n,2}(L,M)}\\
&\sim \frac{4\beta^{-2}C(x_0)(n+1)x_0^{-2n}}{2\beta^{-1}C(x_0)x_0^{-2n}}\\
&\sim \frac{2(n+1)}{\beta}. \qquad (3.68)
\end{aligned}$$

Thus, we have:

$$\lim_{n\to\infty}\frac{\mathrm{E}_{2n}(m)}{2n} = \beta^{-1}, \qquad (3.69)$$

which gives us an expression for the expected span per edge of a random $2n$-edge SAP (as $n \to \infty$). Note that in Section 3.7, the expected span per edge was found for SAPs in tube sizes of $(1,0)$ to $(10,0)$; $(1,1)$ to $(4,1)$; and $(2,2)$. The results can be found in Tables 3.1 and 3.2.

It should be noted that similar arguments can be used for any function like $\psi_{ij}(\omega)$ or $m(\omega)$ which is "additive" with 2-spans, to obtain the asymptotic expected value of the additive functional. However, this will not be covered in this thesis.

3.6 Computer Implementation of the Transfer Matrix

This section will cover how to program the implementation of the transfer matrix method for SAPs in (L,M)-tubes. It will go through the algorithms that were used in order to generate a proper transfer matrix, as well as the algorithms that were needed to get a dominant eigenvalue equal to one. This whole process relies on generating the set of all possible valid sections and 2-spans in an (L,M)-tube, thus the algorithm for generating these will also be included in this section.

3.6.1 Generating Valid Sections and 2-spans

Given a fixed (L,M)-tube, notice that there are a finite number of unique sections and 2-spans. In order to generate our transfer matrix, we must first generate all "valid" sections and 2-spans in a given tube size. A section (2-span) is valid if it occurs in at least one SAP in an (L,M)-tube. This section will give an overview of the algorithm developed by Duffy in [9] for generating all valid sections and 2-spans. The details of the algorithm are located in Appendix A.

Essentially, all 2-spans were generated by creating all SAWs that could occur in a 2-span with some essential constraints. Because a 2-span is part of a closed polygonal walk, the generated 2-spans must be able to be "closed off" on both the left and right sides of the hinge of the 2-span (see Figure 3.11 for an example of a valid 2-span). Without loss of generality, the SAW used to generate the 2-spans started on the left, and every possible entering point on the left for the SAW is considered. Since the SAW starts on the left, the SAW must travel to the right of the hinge at least once and then return to the left of the hinge at least once. The end of the SAW must also end on the left, since that is where it started (so it can be closed off). Every time the SAW leaves the hinge to the right, it could be imagined as continuing the SAW outside of the 2-span, further down the tube. However, it must eventually re-enter the 2-span in order to reconnect to the start point of the SAW on the left (see Figure 3.12 for an illustration of this). When the SAW leaves to the left

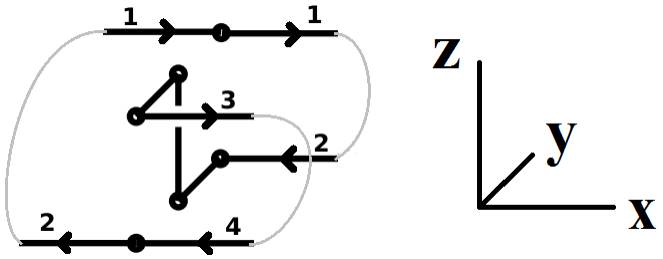

Figure 3.11: An example of a valid 2-span in a $(2, 1)$-tube (with . Notice that the left and right sides can be closed off.

Figure 3.12: When the SAW leaves to the right, it can be imagined to be continuing the SAW down the tube to the right. However, it must always re-enter the 2-span in order to reconnect to the start point on the left of the 2-span.

of the hinge, it can either connect to the start point (at which point the 2-span is complete), or it can re-enter the 2-span and then once again eventually leave to the left (see Figure 3.13). Because of this, a check is needed to see if a valid 2-span was generated at this point.

3.6.2 Storing 2-Spans and the Transfer Matrix

During the generation process described in the previous section, a template of a 2-span was used to keep track of the current 2-span being generated. The template kept track of which edges were traversed during the SAW, as well as the order in which the edges were traversed. The template also kept track of the number of edges in the first section and hinge in the 2-span template, as this information is needed for the transfer matrix defined in Section 3.2. When the SAW leaves to the left and we have a valid 2-span, the 2-span template's information is recorded. Essentially, each section is uniquely assigned a number based on which edges are in the section and the order in which the edges were traversed in the generation process. The 2-span information is stored by recording the first section's distinct number, the second section's distinct number, and the number

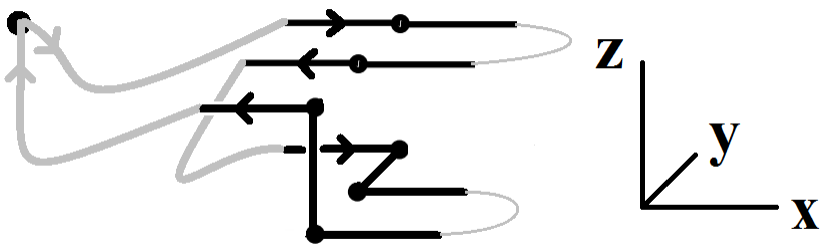

Figure 3.13: When the SAW leaves to the left, it may either connect to the start point, or it may re-enter the 2-span and then once again eventually leave to the left to connect to the start point.

of edges in the first section and hinge of the 2-span template. Note that when $L = 0$ or $M = 0$, the sections were labelled a bit differently to save some memory. In such cases, sections may be referred to as *column states*; but for convenience, the word "section" may also mean "column state". For information on how sections and column states were uniquely labelled based on their edges, see Appendix B and Appendix C. Essentially, each section is uniquely assigned a number based on which edges are in the section and the order in which the edges were traversed in the generation process.

Once all of the 2-spans were generated, each of the 2-spans were ordered based on the two sections which make up the 2-spans. The 2-spans are then arranged in numerical order, such that the first section number of 2-span i is less than or equal to the first section number of 2-span $i + 1$. When there is more than one 2-span with a given first section number, the 2-spans are then ordered according to their second section numbers. Notice that while generating all possible 2-spans, we also generated all possible sections. Also notice that we know which 2-spans can connect to which 2-spans (overlapping section), as well as which sections can connect to which sections (they create a valid 2-span).

So now, since we have generated and stored all possible 2-spans (sections), and we know which 2-spans connect to which 2-spans, and also know how many edges are in the first section and hinge of each of these 2-spans, we have all of the information needed to create the 2-span transfer matrix. Since this matrix will be relatively large and very sparse, the transfer matrix is just stored abstractly in these generated 2-spans. Thus, we can perform any of the necessary matrix calculations that we need by simply accessing the appropriate 2-span information.

3.6.3 Finding x_0, $\eta^\top$, and ξ From the Transfer Matrix

Once the transfer matrix is "stored," the next step is to find the value of x_0, that is the value of x such that the spectral radius of $G(x)$ is equal to one. This was done by using the power method, along with the false position method. The process of finding x_0, as well as $\eta^\top$ and ξ (the left and right eigenvectors associated with $G(x_0)$), is covered in this subsection.

The Power Method

The power method is a numerical method used in mathematics to find the spectral radius ρ (the eigenvalue with the largest magnitude) of a matrix, as well as the eigenvector associated with ρ. It works on the assumption that the eigenvalue with modulus ρ has multiplicity one. The power method is an iterative process that continues until convergence. Given a matrix H that satisfies the assumption that the eigenvalue with modulus ρ has multiplicity one, the power method proceeds as follows:

- Choose an initial vector v_0 that is strictly positive.
- Iterate for $n = 1, 2, 3, \ldots$:

$$v_n = \frac{1}{\gamma_n} H v_{n-1}, \tag{3.70}$$

  where γ_n is the component of the vector Hv_{n-1} with the maximum modulus.

- Choose some convergence tolerance $\epsilon > 0$, and iterate until $|\gamma_n - \gamma_{n-1}| < \epsilon$.

Under these conditions, the sequence $(\gamma_1, \gamma_2, \gamma_3, \ldots)$ converges to ρ, and the sequence of vectors $(v_0, v_1, v_2, \ldots)$ converges to the right eigenvector ξ, corresponding to ρ.

The left eigenvector $\eta^\top$ of a matrix H is found similarly: Choose an initial vector $u_0^\top$ that is strictly positive, and then iterate for $n = 1, 2, 3, \ldots$:

$$u_n^\top = \frac{1}{\zeta_n} u_{n-1}^\top H, \tag{3.71}$$

where ζ_n is the component of the vector $u_{n-1}^\top H$ with the maximum modulus. Then the sequence $(\zeta_1, \zeta_2, \zeta_3, \ldots)$ also converges to ρ, and the sequence of vectors $(u_0^\top, u_1^\top, u_2^\top, \ldots)$ converges to the left eigenvector $\eta^\top$, corresponding to ρ.

Note that a tolerance of $\epsilon = 10^{-6}$ was used in the computer implementation of the transfer matrix. The power method was used along with the false position method to find x_0.

The False Position Method

The false position method is an iterative, bracketed, root-finding method. Since we are looking for the value of x that gives $G(x)$ a spectral radius of one, and we know that we can use the power method to find the dominant eigenvalue of any matrix, we can combine the false position method with the power method to find x_0.

To understand the False Position Method, assume we have a continuous function $f(x)$ that has one unique root. That is, there is a unique x^* such that $f(x^*) = 0$. The false position method initially needs two "brackets" x_a, x_b such that the correct root (x^*) lies between the brackets. That is either $f(x_a) > 0$ and $f(x_b) < 0$, or $f(x_a) < 0$ and $f(x_b) > 0$. Without loss of generality, assume $f(x_a) > 0$ and $f(x_b) < 0$. The false position method calculates the function at both of these brackets ($f(x_a)$ and $f(x_b)$), and then obtains its next guess by "drawing a line" between the two points associated with the brackets ($(x_a, f(x_a)$ and $(x_b, f(x_b))$. The next guess x_1 is chosen from where the line crosses zero. Then if $f(x_1) > 0$, replace x_a with x_1, or if $f(x_1) < 0$, replace x_b with x_1. Notice the root is still bracketed with the new set of brackets. For some chosen tolerance $\delta > 0$, continue this iterative process until $|f(x_{n^*})| < \delta$ is achieved. Thus, $x^* = x_{n^*}$. Note that a tolerance of $\delta = 10^{-7}$ was used in the computer implementation of the transfer matrix.

Applying the false position method to the power method, we set $f(x)$ to be the spectral radius $\rho(x)$ obtained by using the power method on the matrix $G(x)$, minus one. That is given x_n, $f(x_n)$ will be the spectral radius of $G(x_n)$ minus one. Thus, when $f(x_n) = 0$, $\rho(x_n) = 1$. From Theorem 3.5, x_0 is unique, and thus $f(x_n)$ has one unique root. Hence, x_0 can be obtained by combining the false position method along with the power method.

3.7 Numerical Results

This section contains numerical results obtained from the computer implementation of the transfer matrix. Table 3.1 contains results for the two-dimensional tube sizes ranging from $(0, 1)$ to $(0, 10)$. Table 3.2 contains results for the three-dimensional tube sizes of $(1, 1)$, $(2, 1)$, $(3, 1)$, $(4, 1)$, and $(2, 2)$. Note that x_0 decreases as the tube size increases, and therefore, the connective constant increases as the tube size increases. Refer to Chapter 5 when the force is zero for more results about k-span densities and expected span results.

Table 3.1: Numerical Results for $L = 0$, $M > 0$.

Tube Size	Column States	α	β	x_0
(0,1)-tube	1	1.000000	1.000000	1.000000
(0,2)-tube	3	$2.500000\ 10^{-1}$	2.500000	0.707107
(0,3)-tube	8	$3.042050\ 10^{-3}$	2.841143	0.594616
(0,4)-tube	20	$5.967867\ 10^{-4}$	3.107643	0.536749
(0,5)-tube	50	$1.562115\ 10^{-4}$	3.330234	0.501896
(0,6)-tube	126	$4.972553\ 10^{-5}$	3.523772	0.478782
(0,7)-tube	322	$1.826577\ 10^{-5}$	3.696418	0.462427
(0,8)-tube	834	$7.490957\ 10^{-6}$	3.853173	0.450302
(0,9)-tube	2,187	$3.353797\ 10^{-6}$	3.997338	0.440989
(0,10)-tube	5,797	$1.613301\ 10^{-6}$	4.131236	0.433634

Table 3.2: Numerical Results for $L > 0$, $M > 0$.

Tube Size	Sections	2-Spans	α	β	x_0
(1,1)-tube	20	108	$2.097520\ 10^{-3}$	2.951241	0.547397
(2,1)-tube	814	9,702	$2.330946\ 10^{-4}$	3.621382	0.437382
(3,1)-tube	44,484	963,096	$4.160686\ 10^{-5}$	4.105161	0.388795
(4,1)-tube	4,065,078	129,413,546	$1.001093\ 10^{-5}$	4.486078	0.361863
(2,2)-tube	426,456	12,095,392	$2.515882\ 10^{-5}$	4.343681	0.366126

Chapter 4

Compact Polygons

This chapter is devoted to compact polygons in (L, M)-tubes. Studying compact polygons is motivated by ring polymers which are tightly packed into a small space. Such a ring polymer can be modeled by a compact polygon, as a compact polygon reflects the lack of movement freedom which compressed ring polymers experience. An example of such a polymer is DNA packed into a viral capsid, or more specifically into the head of a bacteriophage[18]. Also, experiments have shown that proteins fold from an unknotted state into a knotted state, in which case the protein has a tight configuration[28]. Proteins with a tight configuration can also be modelled as compact polygons[11].

A new concatenation theorem for compact polygons is presented here, and a pattern theorem for compact polygons will be proven in this chapter. This chapter will also explain how the 2-span information obtained from Section 3.6 is used to develop a new algorithm for efficiently generating polygons in (L, M)-tubes. Lastly, results for generated compact polygons and their knot types are presented.

4.1 Pattern Theorem for Compact SAPs in (L, M)-tubes

A pattern theorem for compact polygons will once again be proved by using the transfer matrix method, as was done in Section 3.3. This will involve defining compact polygons, defining compact k-spans, developing and proving a concatenation theorem for compact polygons, and showing irreducibility and aperiodicity (if possible) on the set of compact k-spans. First, we define what it means for a polygon in an (L, M)-tube to be compact.

Definition 4.1. A SAP ω with span m in an (L, M)-tube is considered *compact* if ω contains V, where $V = \{(x, y, z) \in \mathbb{Z}^3 | 0 \leq x \leq m, 0 \leq y \leq L, 0 \leq z \leq M\}$.

Figure 4.1 contains an example of a compact polygon. We then call a k-span π *compact* if there exists a compact polygon ω such that π occurs at some section of ω. Once compact polygons

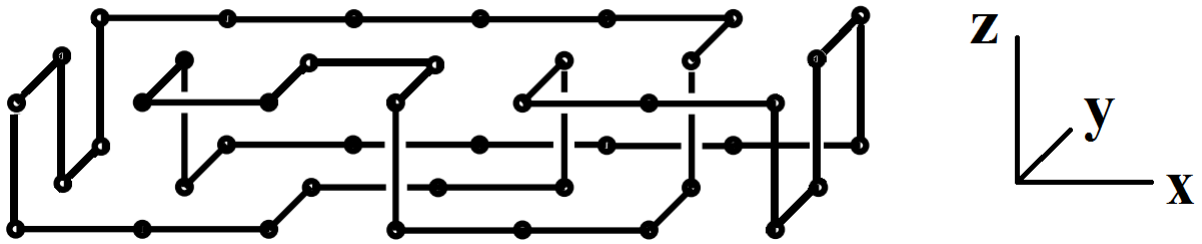

Figure 4.1: A compact polygon with span 6 in a $(2, 1)$-tube.

and compact k-spans are defined, we can present the following concatenation theorem for compact polygons.

Theorem 4.1. *Let ω_1 and ω_2 be two compact polygons in an (L, M)-tube, with spans m_1 and m_2 respectively. Notice there is exactly one compact m_1-span (m_2-span) that occurs at the first section of ω_1 (ω_2). Then ω_1 and ω_2 can always be concatenated (by the process explained below) to form another compact polygon $\omega_c := \omega_1 \circ_c \omega_2$ which contains the compact m_1-span and compact m_2-span from ω_1 and ω_2 respectively.*

Proof. In order to prove by construction that there always exists an appropriate concatenation, we must first introduce the idea of a sequence of directed edges *zig-zagging*. Note that a sequence of directed edges may also be referred to as a SAW. Essentially, a zig-zagging SAW is just a SAW that follows a certain set of rules. Zig-zagging will be defined to occur in $\mathbb{Z}^2$, in a certain direction, between two lines. Without loss of generality, let us look at an example. Suppose we are working in the yz-plane. If the SAW is zig-zagging in the positive y-direction, between the lines $z = a$ and $z = b$, then starting at some point (y_0, z_0), the SAW abides to the following set of rules:

1. If possible (without violating self-avoidance), travel in the positive z-direction until it is no longer possible, without going past $z = b$. If it is not possible to travel in the positive z-direction from the start, then travel in the negative z-direction until it is no longer possible, without going past $z = a$.
2. Take one step in the positive y-direction.
3. Repeat steps 1 and 2 until no more movement is possible.

The idea of zig-zagging will be used to create compact "hinge patterns" while creating a compact concatenation. See Figure 4.2 for an illustration of zig-zagging.

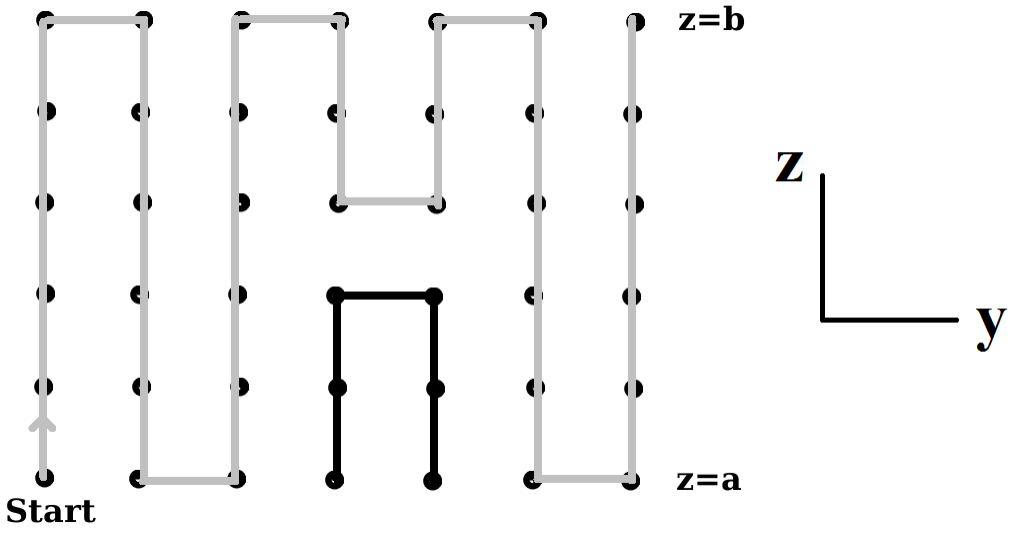

Figure 4.2: The gray SAW is zig-zagging in the positive y-direction between $z = a$ and $z = b$. Notice that the SAW may have already visited some vertices before the zig-zagging begins (black edges).

Also to make the proof simpler, we first define four special hinges. Note that $\hat{\imath}$, $\hat{\jmath}$, and $\hat{k}$ are the unit vectors in the x, y, and z directions respectively, and the hinges defined here are a set of undirected edges (which may be directed later on) which exist in a hinge of the (L, M)-tube. We say a hinge pattern is *compact* in an (L, M)-tube if the hinge pattern contains all vertices in a hinge of the (L, M)-tube. Also notice that hinge patterns are defined in the yz-plane. In order to define these four compact hinge patterns efficiently, first define a SAP $\omega_h(L, M)$ which exists in the hinge (yz-plane) of a (L, M)-tube, where L is odd, as follows: Let the sequence of edges in $\omega_h(L, M)$ start at (y, z)=$(0, 1)$. Zig-zag in the y-direction between $z = 1$ and $z = M$. In more detail, starting at $(0, 1)$, the SAW will take $M - 1$ steps in the positive z-direction until they reach the border of the tube at $(0, M)$. That is, the SAW will travel from $(0, 1) \to (0, 2) \to \ldots \to (0, M)$. Next, the y-coordinate is increased by one, as an edge from $(0, M)$ to $(1, M)$ is added. Following this edge, the SAW will take another $M - 1$ steps back in the negative z-direction from $(1, M)$ to $(1, 1)$. This zig-zagging between $z = 1$ and $z = M$ continues until y can no longer be increased (because of the restraint of the tube). Notice that since L is odd, the zig-zagging will run out of room when $z = 1$ (at the point $(L, 1)$). Once the SAW reaches $(L, 1)$, add an edge from $(L, 1)$ to $(L, 0)$, and then the SAW takes L steps in the negative y direction, from $(L, 0)$ to $(0, 0)$. Finally, close the polygon up by adding the edge from $(0, 0)$ to $(0, 1)$. See Figure 4.3 for an example of $\omega_h(L, M)$.

Next, define the following four compact hinge patterns (see Figures 4.4, 4.5, 4.6, and 4.7 for

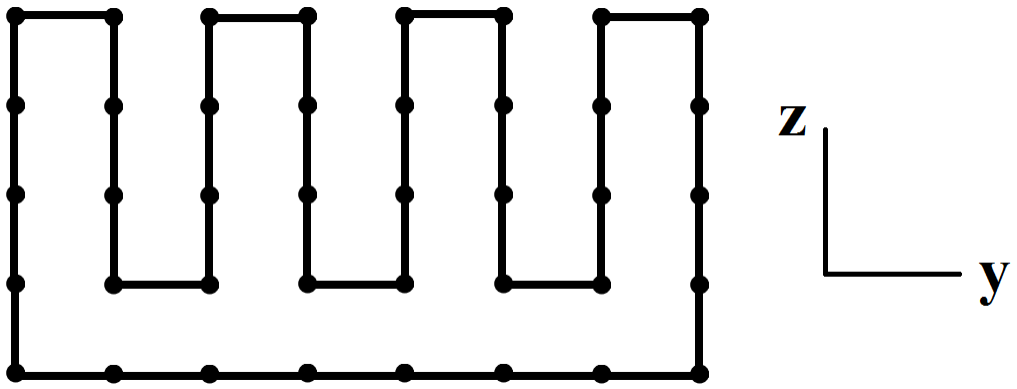

Figure 4.3: ω_h in a $(7,4)$-tube. Notice that L must be odd for ω_h to exist.

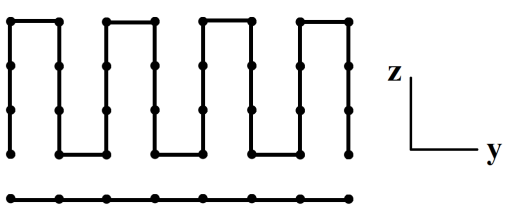

Figure 4.4: Hinge A in a $(7,4)$-tube.

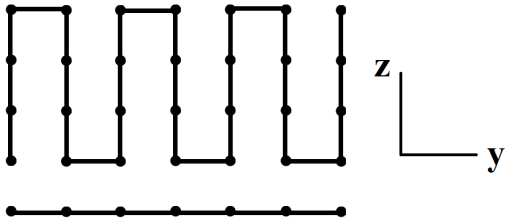

Figure 4.5: Hinge B in a $(6,4)$-tube.

examples of these four hinges):

Hinge A (H_A): This hinge pattern will only be defined when L is odd. Obtain this hinge pattern by deleting the edges $(0,0) \to (0,1)$ and $(L,0) \to (L,1)$ from $\omega_h(L,M)$.

Hinge B (H_B): This hinge pattern will only be defined when L is even. Notice $L-1$ is odd, so $\omega_h(L-1,M)$ is defined. Obtain this hinge pattern by first deleting the edges $(0,0) \to (0,1)$ and $(L-1,0) \to (L-1,1)$ from $\omega_h(L-1,M)$. Then add the edges $(L-1,0) \to (L,0)$, $(L-1,1) \to (L,1)$, and the edges from $(L,1) \to (L,M)$.

Hinge C (H_C): This hinge pattern will only be defined when L is odd. Obtain this hinge pattern by deleting the edges $(0,0) \to (1,0)$ and $(L,0) \to (L,1)$ from $\omega_h(L,M)$.

Hinge D (H_D): This hinge pattern will only be defined when L is even. Notice $L-1$ is odd, so $\omega_h(L-1,M)$ is defined. Obtain this hinge pattern by first deleting the edges $(0,0) \to (1,0)$ and $(L-1,0) \to (L-1,1)$ from $\omega_h(L-1,M)$. Then add the edges $(L-1,0) \to (L,0)$, $(L-1,1) \to (L,1)$, and the edges from $(L,1) \to (L,M)$.

Now, we will concatenate ω_1 and ω_2 while preserving order. Assume $L, M > 0$. Since ω_2 is compact, the vertex $(0,0,0)$ is occupied by ω_2, and at least one of the two polygon edges incident

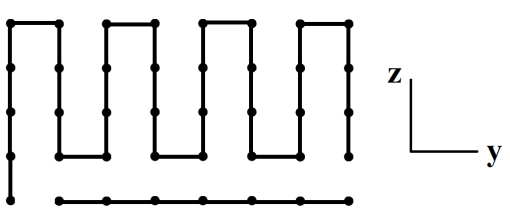

Figure 4.6: Hinge C in a $(7, 4)$-tube.

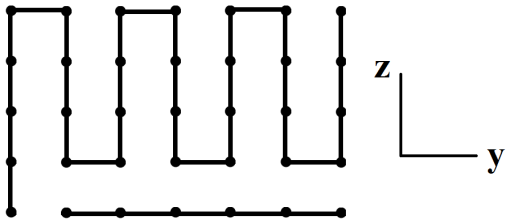

Figure 4.7: Hinge D in a $(6, 4)$-tube.

on $(0, 0, 0)$ lies in $H_0(L, M)$. As a result of the lexicographical ordering, one of the two possible edges in $H_0(L, M)$ incident on v_{1b} is ω_2's first edge, and it must be directed in the positive y or z direction. Without loss of generality, we will assume the edge directed in the positive z-direction is present and is the first edge (if it is not, then simply switch the labels of y and z; L and M; H_B and H_D; H_A and H_C; and H_E and H_F for the rest of this proof). Therefore, there is an edge, call it e_2, from $v_{2a} := (0, 0, 0)$ to $v_{2b} := (0, 0, 1)$.

Since ω_1 is also compact, the vertex $(m_1, 0, 0)$ is occupied by ω_1, and at least one of the two polygon edges incident on $(m_1, 0, 0)$ lies in H_{m_1}. We will call this edge e_1, and define $v_{1a} = \text{int}(e_1)$ and $v_{1b} = \text{fin}(e_1)$. There are two possible edges for e_1 (y-direction or z-direction), each with two possible directions (positive or negative), so there are four cases. The idea behind the next part (Part 1) of the proof is to show that for two of the cases (positive y and negative z), given a tube size, there exists a concatenation. Then Part 2 will show that the other two cases can be converted into one of the first two cases (similar to what was done in the proof of Theorem 3.10, where the concatenation was done for general SAPs). However, because of the compact requirement, the way they are converted will have to change, depending on the tube size.

Part 1

In Part 1, we will show that if e_1 is in either the positive y or negative z direction, then ω_1 and ω_2 can always be concatenated to form another compact polygon which contains the m_1-span and m_2-span from ω_1 and ω_2 respectively. First let $v_{1a} = (m_1, 0, 1)$ and $v_{1b} = (m_1, 0, 0)$, so e_1 is in the negative z-direction. If we simply translate ω_2 $m_1 + 1$ steps in the positive x-direction, delete e_1 and e_2, and then connect v_{1a} to v_{2b} (via one edge from $(m_1, 0, 1)$ to $(m_1 + 1, 0, 1)$) and connect v_{2a} to v_{1b} (via one edge from $(m_1 + 1, 0, 0)$ to $(m_1, 0, 0)$), then we have succesfully formed another compact polygon which contains the m_1-span and m_2-span from ω_1 and ω_2 respectively. See Figure 4.8 for an illustration of this process. Note that for the case where $L = 0$ or $M = 0$, we may assume without loss of generality that $L = 0$ and $M > 0$. Then e_2 must be in the positive z-direction and e_1 must be in the negative z-direction (using the same reasoning that was used in the general concatenation

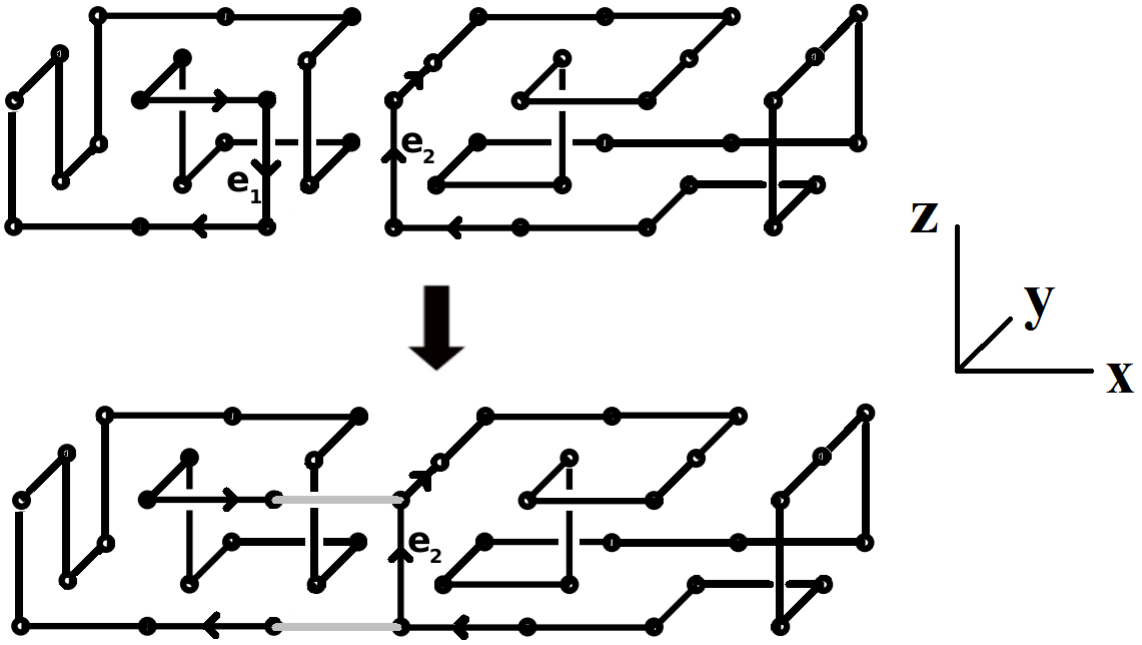

Figure 4.8: A simple compact concatenation in a $(2,1)$-tube for the case where e_1 and e_2 are parallel and in the opposite direction.

theorem (Theorem 3.10)). Thus, as was just shown, ω_1 and ω_2 can always be concatenated to form another compact polygon which contains the m_1-span and m_2-span from ω_1 and ω_2 respectively.

Back to the case where $L, M > 0$. If instead, $v_{1a} = (m_1, 0, 0)$ and $v_{1b} = (m_1, 1, 0)$, so e_1 is in the positive y-direction, then concatenate ω_1 and ω_2 as follows. First translate ω_2 $m_1 + 3$ steps in the positive x-direction. If L is odd, place H_C in the plane $x = m_1 + 1$, place H_A in the plane $x = m_1 + 2$, and delete the edges e_1 and e_2. Then connect v_{1a} to H_C (via one edge from $(m_1, 0, 0)$ to $(m_1 + 1, 0, 0)$) and connect H_C to v_{1b} (via one edge from $(m_1 + 1, 1, 0)$ to $(m_1, 1, 0)$). Connect H_C to H_A (via one edge from $(m_1 + 1, L, 1)$ to $(m_1 + 2, L, 1)$) and connect H_A to H_C (via one edge from $(m_1 + 2, L, 0)$ to $(m_1 + 1, L, 0)$). Lastly, connect H_A to v_{2b} (via one edge from $(m_1 + 2, 0, 1)$ to $(m_1 + 3, 0, 1)$) and connect v_{2a} to H_A (via one edge from $(m_1 + 2, 0, 0)$ to $(m_1 + 3, 0, 0)$). If instead L is even, place H_D in the plane $x = m_1 + 1$, place H_B in the plane $x = m_1 + 2$, and delete the edges e_1 and e_2. Then connect v_{1a} to H_D (via one edge from $(m_1, 0, 0)$ to $(m_1 + 1, 0, 0)$) and connect H_D to v_{1b} (via one edge from $(m_1 + 1, 1, 0)$ to $(m_1, 1, 0)$). Connect H_D to H_B (via one edge from $(m_1 + 1, L, M)$ to $(m_1 + 2, L, M)$) and connect H_B to H_D (via one edge from $(m_1 + 2, L, 0)$ to $(m_1 + 1, L, 0)$). Lastly, connect H_B to v_{2b} (via one edge from $(m_1 + 2, 0, 1)$ to $(m_1 + 3, 0, 1)$) and connect v_{2a} to H_B (via

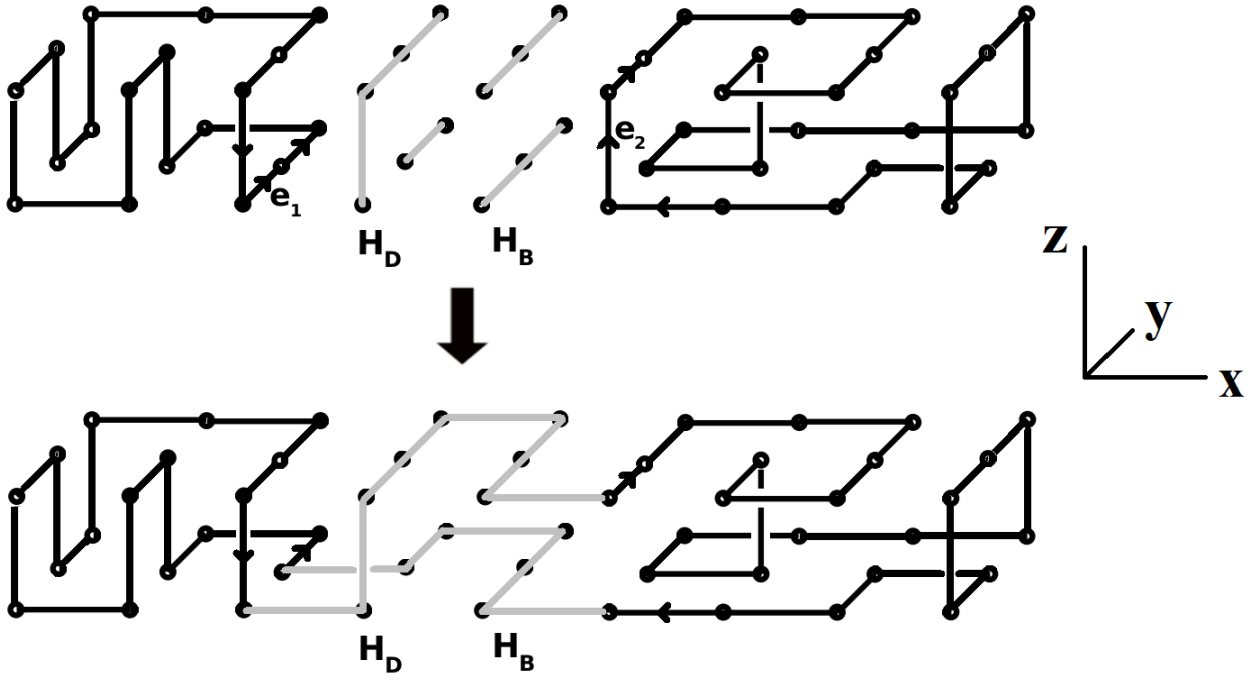

Figure 4.9: A compact concatenation in a $(2,1)$-tube for the case where e_1 is in a positive direction and perpendicular to e_2.

one edge from $(m_1+2,0,0)$ to $(m_1+3,0,0)$). Thus, we have succesfully formed another compact polygon which contains the m_1-span and m_2-span from ω_1 and ω_2 respectively. See Figure 4.9 for an illustration of this process.

Part 2

In Part 2, we will show that the other two cases (e_1 is in either the negative y or positive z direction) can be converted into one of the previous two cases. This is done by creating a new compact polygon ω_1' with span $m_1' > m_1$, which also contains the m_1-span from ω_1, but the difference being that ω_1' will have an edge incident on $(m_1',0,0)$ that is either in the positive y or negative z direction. Thus, we can apply Part 1 to ω_1' to form a compact polygon which contains both the m_1-span and m_2-span from ω_1 and ω_2 respectively.

Assume $v_{1a} = (m_1,0,0)$ and $v_{1b} = (m_1,0,1)$, so e_1 is in the positive z-direction. If L is odd, place $\omega_h(L,M)$ in the plane $x = m_1+1$, and delete e_1 and the edge $(m_1+1,0,0)$ to $(m_1+1,0,1)$ from $\omega_h(L,M)$. Then connect v_{1a} to $\omega_h(L,M)$ (via one edge from $(m_1,0,0)$ to $(m_1+1,0,0)$), and connect $\omega_h(L,M)$ to v_{1b} (via one edge from $(m_1+1,0,1)$ to $(m_1,0,1)$). By construction, this new polygon ω_1' with span $m_1' = m_1+1$ has the edge e_1' from $(m_1+1,0,0)$ to $(m_1+1,1,0)$ in the positive y direction. Hence, we can apply Part 1 to ω_1' to form a compact polygon which contains both the

m_1-span and m_2-span from ω_1 and ω_2 respectively.

If L is even and M is odd, rotate $\omega_h(L, M)$ 90° clockwise in the yz-plane (so the edges initially on the y-axis are now on the z-axis). Place this rotated polygon $\omega_r(L, M)$ in the plane $x = m_1 + 1$, and delete e_1 and the edge $(m_1 + 1, 0, 0)$ to $(m_1 + 1, 0, 1)$ from $\omega_r(L, M)$. Then connect v_{1a} to $\omega_r(L, M)$ (via one edge from $(m_1, 0, 0)$ to $(m_1 + 1, 0, 0)$), and connect $\omega_r(L, M)$ to v_{1b} (via one edge from $(m_1 + 1, 0, 1)$ to $(m_1, 0, 1)$). By construction, this new polygon ω_1' with span $m_1' = m_1 + 1$ has the edge e_1' from $(m_1 + 1, 0, 0)$ to $(m_1 + 1, 1, 0)$ in the positive y direction. Hence, we can apply Part 1 to ω_1' to form a compact polygon which contains both the m_1-span and m_2-span from ω_1 and ω_2 respectively.

If L and M are both even, then change ω_1 into ω_1' as follows. Delete e_1, and then starting at v_{1a}, connect to v_{1b} by adding the following directed edges. Add two edges in the positive x-direction, zig-zag in the positive z-direction between $y = 0$ and $y = L$, add one edge in the negative x-drection, zig-zag in the negative y-direction between $z = 0$ and $z = M$, and then add one final edge in the negative x-direction to connect to v_{1b}. By construction, this new polygon ω_1' with span $m_1' = m_1 + 2$ has the edge e_1' from $(m_1 + 2, 0, 0)$ to $(m_1 + 2, 1, 0)$ in the positive y direction. Hence, we can apply Part 1 to ω_1' to form a compact polygon which contains both the m_1-span and m_2-span from ω_1 and ω_2 respectively.

Thus, the case where e_1 is in the positive z-direction has been covered. Notice that starting with e_1 in the positive z-direction, we always (for any combination of L, M odd or even) created a new polygon ω_1' with e_1' in the positive y-direction. By symmetry, it can also be shown that if e_1 is in the negative y-direction, we can always create a new polygon ω_1' with e_1' in the negative z-direction (details not given). Using Part 1 once again on ω_1', we can form a compact polygon which contains both the m_1-span and m_2-span from ω_1 and ω_2 respectively. □

We can also call a start-hinge H_s (finish-hinge H_f) *compact* if there exists a compact polygon ω with H_s (H_f) as its start-hinge (finish-hinge). Now let $\mathcal{D}_c$ be a digraph which has a vertex corresponding to each compact start-hinge, finish-hinge, and k-span; and an arc from each compact start-hinge to any compact k-span which can follow it; each compact k-span to any compact k-span which can follow it; and each compact k-span to any compact finish-hinge which can follow it. Then notice that a properly connected sequence $(H_s, \pi_1, \ldots, \pi_h, H_f)$ corresponds to a walk on the directed graph $\mathcal{D}_c$. As in the general case, in order to apply transfer matrix results, it is important that $\mathcal{D}_c$ has three properties:

(a) finite vertex set,

(b) irreducible on the set of compact k-spans,

(c) aperiodic on the set of compact k-spans.

For (a), since $\mathcal{D}_p$ had a finite vertex set, and we are now focusing on the subset of vertices from $\mathcal{D}_p$ which correspond to start-hinges, finish-hinges, and k-spans which are compact, $\mathcal{D}_c$ also has a finite vertex set.

For (b), $\mathcal{D}_c$ will be irreducible with respect to compact k-spans if for any pair of compact k-spans π_A and π_B, there exists a walk on $\mathcal{D}_c$ from π_A to π_B. To see that this holds, recall that by definition, there exists a compact polygon ω_A in which π_A occurs, and similarly, there exists a compact polygon ω_B in which π_B occurs. From Theorem 4.1, ω_A and ω_B can be concatenated into a new compact polygon ω_C, which has an associated properly connected sequence $(H_s, \pi_1, \ldots, \pi_r, H_f)$. Since π_A occurred in ω_A and π_B occurred in ω_B, and since we know from Theorem 3.10 that the concatenation process will not change any π_A or π_B, it follows that π_A and π_B are elements of $(H_s, \pi_1, \ldots, \pi_r, H_f)$, where π_A occurs prior to π_B, as required.

For (c), a sufficient condition for aperiodicity of $\mathcal{D}_c$ with respect to compact k-spans is the existence of a loop from a compact k-span to itself. That is, a compact k-span which can follow itself. Notice that for an (L, M)-tube with $(L+1)(M+1)$ even, any compact k-span with $(L+1)(M+1)k$ edges will be able to follow itself. An example of a compact k-span which can follow itself is given in Figure 4.10. For the case where $(L+1)(M+1)$ is odd, there is no compact k-span which can follow itself. In this case, there are only k-spans which can follow themselves in two "steps," or in two sections. That is, a k-span π can follow itself in two steps if there exists some k-span π^* such that there is a properly connected sequence which contains the sequence (π, π^*, π). See Figure 4.11 for such an example. So when $(L+1)(M+1)$ is odd, $\mathcal{D}_c$ is periodic with a period of two.

Similar to Section 3.3, for $(L+1)(M+1)$ even, a transfer matrix $G_c(x)$, start-hinge matrix $A_c(x)$, and finish-hinge matrix $B_c(x)$ for the compact case can be created in the same manner, but now by using the compact start-hinges, end-hinges, and k-spans. Thus, for any integer $k \geq 2$, the generating function for compact polygons with span greater than k and $(L+1)(M+1)$ even is:

$$\begin{aligned} F_k^c(x)_{even} &= \sum_{h=1}^{\infty} \sum_{i=1}^{|\mathcal{H}_s^c|} \sum_{j=1}^{|\mathcal{H}_f^c|} (A_c(x) G_c(x)^{h-1} B_c(x))_{ij} \\ &= \sum_{i=1}^{|\mathcal{H}_s^c|} \sum_{j=1}^{|\mathcal{H}_f^c|} (A_c(x)(I - G_c(x))^{-1} B_c(x))_{i,j}, \end{aligned} \tag{4.1}$$

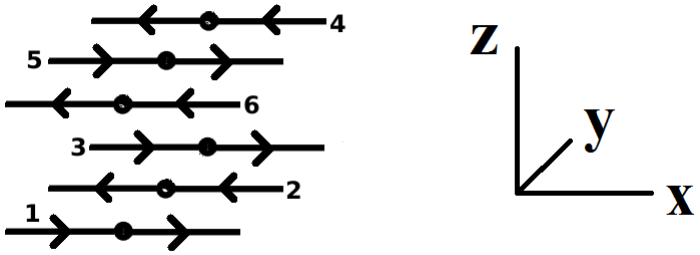

Figure 4.10: An example of a compact k-span in a $(2,1)$-tube which can follow itself, with k=2.

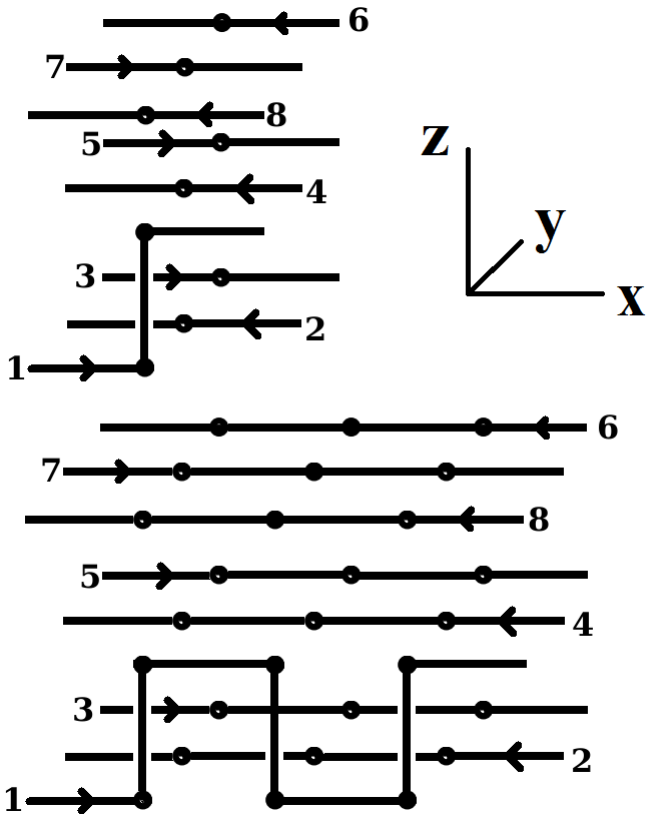

Figure 4.11: An example of a compact k-span (top) in a $(2,2)$-tube which can follow itself in two steps (bottom), with k=2.

where $\mathcal{H}_s^c$ is the set of compact start-hinges and $\mathcal{H}_f^c$ is the set of compact finish-hinges.

If instead $(L+1)(M+1)$ is odd, we must be more careful. Since a SAP must have an even number of edges, a compact polygon in an (L, M)-tube with span m must have $(L+1)(M+1)(m+1)$ even. So if $(L+1)(M+1)$ is odd, $m+1$ must be even (m must be odd), and so SAPs in this case can only have odd span. It can be shown that if $(L+1)(M+1)$ is odd, two mutually exclusive classes of k-spans are naturally formed. One class (call it class one) can only occur at odd sections of a polygon, while the other class (call it class two) can only occur at even sections of a polygon. The details of the existence of these two mutually exclusive classes is given in Appendix D. Suppose the number of class one k-spans is $N_1 > 0$ and the number of class two k-spans is $N_2 > 0$. Note that compact start-hinges will only be able to be followed by k-spans which are in class one. As a result of these two classes, we can reorder the rows and columns of $G_c(x)$ such that $G_c(x)$ can be rewritten as a block matrix:

$$G_c(x) = \begin{bmatrix} 0_{N_1 \times N_1} & G_{12}(x) \\ G_{21}(x) & 0_{N_2 \times N_2} \end{bmatrix},$$

where $G_{12}(x)$ ($G_{21}(x)$) has rows corresponding to k-spans in class one (two) and columns corresponding to k-spans in class two (one). The matrix $0_{i \times j}$ is the $i \times j$ matrix consisting of all zeros. Thus, $G_c^2(x)$ can be written as

$$G_c^2(x) = \begin{bmatrix} G_1(x) & 0_{N_1 \times N_2} \\ 0_{N_2 \times N_1} & G_2(x) \end{bmatrix},$$

where $G_1(x) = G_{12}(x)G_{21}(x)$ and $G_2(x) = G_{21}(x)G_{12}(x)$. Thus, $G_1(x)$ is a square matrix with rows and columns corresponding to the k-spans in class one, and $G_2(x)$ is a square matrix with rows and columns corresponding to the k-spans in class two.

The columns of $A_c(x)$ can also be reordered such that column l of $A_c(x)$ and row l of $G_c^2(x)$ correspond to the same k-span. Thus, since start-hinges can only be followed by k-spans in class one, $A_c(x)$ can be rewritten as

$$A_c(x) = \begin{bmatrix} A_c^*(x) & 0_{|\mathcal{H}_s^c| \times N_2} \end{bmatrix}.$$

Similarly, the rows of $B_c(x)$ can also be reordered such that row l of $B_c(x)$ and column l of $G_c^2(x)$ correspond to the same k-span. Now notice that if k is odd, finish-hinges can only follow k-spans which are in class one, and if k is even, finish-hinges can only follow k-spans which are in

class two. Thus, $B_c(x)$ can be rewritten as

$$B_c(x) = \begin{cases} \begin{bmatrix} B_1(x) \\ 0_{N_2 \times |\mathcal{H}_f^c|} \end{bmatrix} & \text{if } k \text{ is odd} \\ \\ \begin{bmatrix} 0_{N_1 \times |\mathcal{H}_f^c|} \\ B_2(x) \end{bmatrix} & \text{if } k \text{ is even} \end{cases}.$$

If we define $B_c^*(x)$ as:

$$B_c^*(x) = \begin{cases} B_1(x) & \text{if } k \text{ is odd} \\ G_{12}(x)B_2(x) & \text{if } k \text{ is even} \end{cases},$$

then the generating function for compact polygons with span greater than k and $(L+1)(M+1)$ odd is:

$$\begin{aligned} F_k^c(x)_{odd} &= \sum_{i=1}^{|\mathcal{H}_s^c|} \sum_{j=1}^{|\mathcal{H}_f^c|} (A_c(x)(I + G_c^2(x) + G_c^4(x) + G_c^6(x) + \cdots)(G_c(x)^{\sigma_k})B_c(x))_{ij} \\ &= \sum_{h=1}^{\infty} \sum_{i=1}^{|\mathcal{H}_s^c|} \sum_{j=1}^{|\mathcal{H}_f^c|} (A_c(x)G_c^2(x)^{h-1}(G_c(x)^{\sigma_k})B_c(x))_{ij} \\ &= \sum_{h=1}^{\infty} \sum_{i=1}^{|\mathcal{H}_s^c|} \sum_{j=1}^{|\mathcal{H}_f^c|} (A_c^*(x)G_1(x)^{h-1}B_c^*(x))_{ij} \\ &= \sum_{i=1}^{|\mathcal{H}_s^c|} \sum_{j=1}^{|\mathcal{H}_f^c|} (A_c^*(x)(I - G_1(x))^{-1}B_c^*(x))_{i,j}, \end{aligned} \tag{4.2}$$

where

$$\sigma_k = \begin{cases} 0 & \text{if } k \text{ is odd} \\ 1 & \text{if } k \text{ is even} \end{cases}.$$

Notice the compact concatenation theorem shows that $G_1(x)$ is irreducible (with respect to taking two steps on the set of k-spans in class one), and $G_1(x)$ is aperiodic since there exists a compact k-span in class one which can follow itself in two steps (see Figure 4.11 for an example).

We can now achieve a pattern theorem for compact SAPs by following the same process which was done in Section 3.3. Let $p_{2n}^c(L, M)$ be the number of $2n$-edge compact SAPs in an (L, M)-tube, and define the connective constant for compact polygons in an (L, M)-tube to be:

$$\kappa_p^c(L, M) := \lim_{n \to \infty} (2n)^{-1} \log(p_{2n}^c(L, M)). \tag{4.3}$$

Then we get the following theorem for compact polygons (which is equivalent to Theorem 3.11 for the non-compact case).

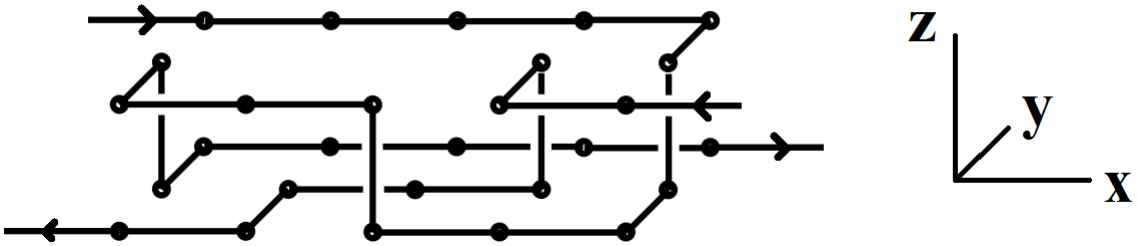

Figure 4.12: This compact 6-span in a $(2,1)$-tube guarantees that any SAP which contains it will be knotted.

Theorem 4.2. *There exists $\alpha_c > 0$ such that as $n \to \infty$,*

$$p^c_{2n}(L,M) \sim \alpha_c e^{\kappa^c_p(L,M)2n}. \tag{4.4}$$

The proof of this theorem is done in a similar manner to the proof for Theorem 3.11, and, once again following Section 3.3, the compact polygon pattern theorem is as follows.

Theorem 4.3. *Given any integer $k \geq 2$ let π be a compact k-span that is protected (with respect to the compact concatenation process). Then there exists $\alpha^c_\pi > 0$ and $\kappa^c_\pi(L,M) > 0$ such that for $2n > N_k$,*

$$p^c_{2n}(L,M;\bar{\pi}) = p^c_{2n,k}(L,M;\bar{\pi}) \sim \alpha^c_\pi e^{\kappa^c_\pi(L,M)2n} \text{ as } n \to \infty \tag{4.5}$$

with

$$\kappa^c_\pi(L,M) < \kappa^c_p(L,M) \tag{4.6}$$

Note that if the compact k-span $\pi \in \Pi_c(k)$ is not protected, then we expect that other concatenation constructions (which may depend on π) that avoid creating π can be defined. These modifications should lead to the same resulting pattern theorem for compact polygons.

The pattern theorem for compact polygons tells us that all but exponentially few sufficiently large compact SAPs contain a given suitable k-span π. If we let the given compact k-span guarantee the SAP is knotted (see Figure 4.12), then we have the following theorem.

Theorem 4.4. *All but exponentially few sufficiently large compact self-avoiding polygons in an (L,M)-tube are knotted.*

Table 4.1: Numerical Results for the Compact Polygon Case with $L > 0$, $M > 0$.

Tube Size	Sections	2-Spans	α	β	x_0
(1,1)-tube	16	56	$6.603902\ 10^{-3}$	4.000000	0.719471
(2,1)-tube	658	4,504	$6.606032\ 10^{-4}$	5.999997	0.643553
(3,1)-tube	35,004	387,740	$1.352603\ 10^{-4}$	7.999984	0.613786
(4,1)-tube	3,176,798	47,253,296	$3.349597\ 10^{-5}$	10.00000	0.597403
(2,2)-tube*	183,860	3,082,080	$5.405694\ 10^{-5}$	8.945637	0.596566

The compact polygon transfer matrix was also generated (in a similar manner to what was done in Section 3.6). Table 4.1 contains numerical results for the compact case. *Note that because the $(2,2)$-tube has $(L+1)(M+1)$ odd, the numerical results must be calculated differently (as shown previously), and its numerical results were still being verified at the time this thesis was written.

Also note that the transfer-matrix formulation for compact polygons also allows us to prove results about the expected number of occurrences of a compact k-span in a random $2n$-edge compact SAP in the same way it was done in to Section 3.4. Thus, the expression from equation 3.58 remains the same:

$$\lim_{n\to\infty} \frac{\mathrm{E}_{2n}(\psi_{\pi_1\pi_2\ldots\pi_h})}{2n} \quad = \quad \frac{\eta_{\pi_1} x_0^{e_{\pi_1}+e_{\pi_2}+\cdots e_{\pi_{h-1}}} \xi_{\pi_h}}{\beta}, \tag{4.7}$$

where $\eta^\top$ and ξ are, respectively, the left and right eigenvectors of the compact transfer matrix. The expected span expression can also be obtained in the same way it was done in Section 3.5. The expected span expression also remains the same:

$$\lim_{n\to\infty} \frac{\mathrm{E}_{2n}(m)}{2n} = \beta^{-1}, \tag{4.8}$$

where β is obtained from the transfer matrix associated with compact polygons. Notice from Table 4.1 that for the tube sizes of $(1,1)$, $(2,1)$, and $(3,1)$, this is consistent with the fact that the span m of a $2n$-edge compact polygon in an (L,M)-tube is

$$m = \frac{2n}{(L+1)(M+1)} - 1. \tag{4.9}$$

4.2 Polygon Generation

This section will cover the algorithm the 2-span information obtained in Section 3.6 can be used to efficiently generate polygons in a given tube size with a certain span. Results for compact polygons that were actually generated will also be included in this section.

4.2.1 Polygon Generation Using 2-spans and Start/Finish-hinges

The valid 2-spans generated in Section 3.6 were also used to generate polygons. As discussed in Section 3.2, a SAP in an (L, M)-tube with span $m \geq 2$ can be represented by a properly connected sequence $(H_s, \pi_1, \ldots, \pi_h, H_f)$, $h = m - 1$, where H_s is a start-hinge, H_f is a finish-hinge, and $\pi_1, \ldots, \pi_h$ are 2-spans such that π_1 can follow H_s, H_f can follow π_h, and π_{i+1} can follow π_i, $i = 1, \ldots, h-1$. Thus, if we are interested in generating all SAPs in an (L, M)-tube with span m, all we need to do is generate all properly connected sequences $(H_s, \pi_1, \ldots, \pi_h, H_f)$, $h = m - 1$.

This was done on the computer by first storing each start/finish-hinge and 2-span as a set of ordered SAWs. This way, the polygon (sequence of edges) could be obtained by connecting each of the ordered SAWs from the properly connected sequence. The generation process was then as follows:

1. Loop through and start with each start-hinge.
2. For each start-hinge, loop through and add each 2-span that can follow the given start-hinge.
3. For the 2-span just added, loop through and add each 2-span that can follow the given 2-span that was just added.
4. Continue looping through and adding 2-spans to the previous 2-span until the desired span is reached. For a polygon with span m, there are $h = m - 1$ 2-spans that need to be added.
5. Loop through and add each finish-hinge that can follow the last (hth) 2-span.
6. Lexicographically find the first edge, and follow the SAWs from the properly connected sequence to record the polygon.

4.2.2 Compact Polygon Generation Results

Compact polygons in the $(2, 1)$-tube were generated up to span 8, and for the $(3, 1)$-tube, compact polygons were generated up to span 5. Only compact polygons were generated because even with relatively small tube sizes and spans, the number of unique polygons is very large. Since there was an interest in generating knotted polygons, the compact restriction reduced the number of generated polygons. This allowed us to explore relatively larger tube sizes and spans which would not have been possible in the general non-compact case due to memory and storage restraints of the computer. Thus, only compact start/finish-hinges and compact 2-spans were used in the polygon generation process. The knot types of these generated compact polygons were then identified by

Table 4.2: Compact Polygon Generation Results.

Tube	Span	Total	3_1^+	3_1^-	4_1	5_1^+	5_1^-	5_2^+	5_2^-	6_1^+	6_1^-	$3_1^+\#3_1^-$
(2,1)	2	324	0	0	0	0	0	0	0	0	0	0
(2,1)	3	4,580	0	0	0	0	0	0	0	0	0	0
(2,1)	4	64,558	0	0	0	0	0	0	0	0	0	0
(2,1)	5	908,452	0	0	0	0	0	0	0	0	0	0
(2,1)	6	12,788,368	144	144	0	0	0	0	0	0	0	0
(2,1)	7	180,011,762	4,302	4,302	0	0	0	0	0	0	0	0
(2,1)	8	2,533,935,102	96,620	96,620	72	0	0	0	0	0	0	0
(3,1)	2	4,580	0	0	0	0	0	0	0	0	0	0
(3,1)	3	232,908	58	58	0	0	0	0	0	0	0	0
(3,1)	4	11,636,834	5,710	5,710	16	0	0	0	0	0	0	0
(3,1)	5	578,377,118	458,980	458,980	3,216	32	32	70	70	2	2	36

using the software knotpolt[23]. Table 4.2 shows a summary of the generated compact polygons and their knot types.

While compact polygons model compressed ring polymers by allowing only the compact subset of polygons, one may perhaps be instead interested in a model which prefers these compact polygons, but does not completely disallow non-compact polygons. On the other hand, one may be interested in a model which prefers "stretched" polygons, or polygons which have many empty vertices. This brings us to Chapter 5, where this preference for certain types of polygons is modelled by an external force applied to the polygon.

Chapter 5

Compressed and Stretched Polygons

In this chapter, polygons confined to an (L, M)-tube and under the influence of an external force are examined. SAPs subject to an external force have been studied in [11], [21], and more recently in [3], on which this chapter is based. In [3], theoretical upper and lower bounds on the *free energy* (to be defined later in Section 5.2) for $2n$-edge SAPs in an (L, M)-tube under the influence of a force are found. Also in [3], a pattern theorem is proved for SAPs in (L, M)-tubes (using similar techniques to those that were used in subsection 3.3) by using the transfer matrix method. In this chapter, we consider polygons subjected to an external force, and the theoretical upper and lower bounds of [3] will be verified directly from transfer matrix calculations for a wide range of forces. The relationship between the expected span per edge of a random $2n$-edge polygon (as $n \to \infty$) and force is also examined, as well as the relationship between the expected number of occurrences per edge of a k-span in a random $2n$-edge polygon (as $n \to \infty$) and force.

5.1 Force Model

We assume that a force f parallel to the x-axis, perpendicular to and incident on the plane $x = m$, is applied to a single ring polymer modelled by a SAP with span m. If $f > 0$, then the force is called a *tensile* or *stretching* force, tending to stretch the polygon in the x-direction. On the other hand, if $f < 0$, then the force is called a *compressing* force, tending to push the planes $x = 0$ and $x = m$ together. For convenience, regardless of the sign of f, we will call the polygons under the influence of a finite force f *stretched polygons*. See Figure 5.1 for an example of a SAP subject to an external force.

The generating function of this model is defined to be

$$F(x, f) = \sum_{n,m} p_{2n,m}(L, M) x^{2n} e^{fm}, \tag{5.1}$$

where $p_{2n,m}(L, M)$ denotes the number of $2n$-edge SAPs in an (L, M)-tube with span m. The

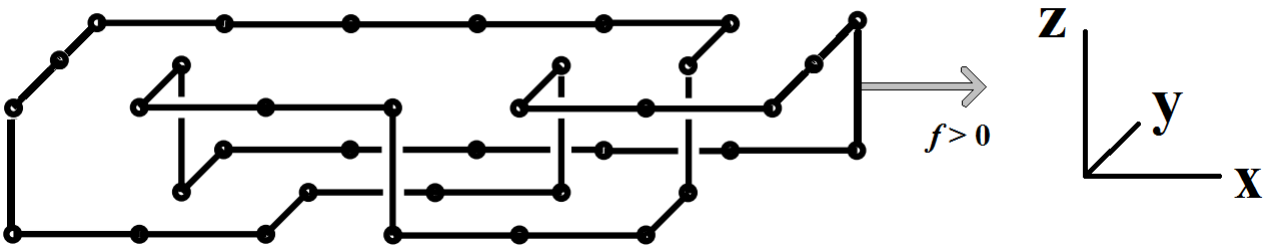

Figure 5.1: A SAP subject to any external force f, parallel to the x-axis.

corresponding transfer matrix which includes force in the model is defined as $G(x,f) = (g_{i,j}(x,f))$, with:

$$g_{i,j}(x,f) = \begin{cases} x^{e_i}e^f & \text{if } k\text{-span } j \text{ can follow } k\text{-span } i \\ 0 & \text{otherwise,} \end{cases} \tag{5.2}$$

where e_i is the number of edges contained in $S_1(L,M) \cup H_1(L,M)$ of k-span i. Notice that this is the same transfer matrix that was used in Section 3.3 (defined in equation (3.21)), except it is now multiplied by e^f. Recall that a polygon consisting of h k-spans has a span of $m = h + k - 1$. Adopting the same start-hinge matrix ($A(x)$) and finish-hinge matrix ($B(x)$) that were previously used (in Section 3.3), for any integer $k \geq 2$, the generating function for a polygon with span greater than k, subjected to an external force can be written as:

$$\begin{aligned} F_k(x,f) &= \sum_{h=1}^{\infty}\sum_{i=1}^{|\mathcal{H}_s|}\sum_{j=1}^{|\mathcal{H}_f|}(A(x)G(x)^{h-1}B(x))_{ij}e^{(h+k-1)f} \\ &= \sum_{h=1}^{\infty}\sum_{i=1}^{|\mathcal{H}_s|}\sum_{j=1}^{|\mathcal{H}_f|}(A(x)G(x,f)^{h-1}B(x))_{ij}e^{kf} \\ &= \sum_{i=1}^{|\mathcal{H}_s|}\sum_{j=1}^{|\mathcal{H}_f|}(A(x)(I-G(x,f))^{-1}B(x))_{i,j}e^{kf} \end{aligned} \tag{5.3}$$

Also notice that:

$$F(x,f) = \sum_n \left(\sum_m p_{2n,m}(L,M)e^{fm}\right)x^{2n} = \sum_n \hat{Z}_{2n}(L,M;f)x^{2n}, \tag{5.4}$$

where $\hat{Z}_{2n}(L,M;f)$, known as the canonical partition function, is defined to be the number of weighted $2n$-edge SAPs, weighted by e^{fm}. In this model, the probability of any random $2n$-edge, span m SAP ($\omega_{2n,m}$) is taken to be

$$P(X = \omega_{2n,m}) = \frac{e^{fm}}{\hat{Z}_{2n}(L,M;f)}. \tag{5.5}$$

Notice that for $f >> 0$, $2n$-edge SAPs with a larger span will be more likely than $2n$-edge SAPs with a smaller span. On the other hand, for $f << 0$, $2n$-edge SAPs with a smaller span will be more likely than $2n$-edge SAPs with a larger span.

5.2 Bounds on the Limiting Free Energy as a Function of Force

The *limiting free energy* for $2n$-edge SAPs in an (L, M)-tube subject to a force is defined as follows:

Theorem 5.1 (Atapour et al.[3]). *The following limit exists:*

$$\kappa_p(L, M; f) := \lim_{n\to\infty} (2n)^{-1} \log \hat{Z}_{2n}(L, M; f). \tag{5.6}$$

By using the same arguments that were used in obtaining equation (3.10), we can find $\kappa_p(L, M; f)$ for fixed f by using the transfer matrix $G(x, f)$. Thus, we have $\kappa_p(L, M; f) = -\log(x_0(f))$, where for fixed f, $G(x_0(f), f)$ yields a spectral radius of one. The following theorem are the bounds on $\kappa_p(L, M; f)$ that were proved in [3].

Theorem 5.2 (Atapour et al.[3]). *For $f \geq 0$,*

$$f/2 \leq \kappa_p(L, M; f) \leq \kappa_p(L, M) + f/2, \tag{5.7}$$

and for $f < 0$,

$$\kappa_p(L, M; f) \leq \kappa_p(L, M). \tag{5.8}$$

Recall $\kappa_p(L, M)$ is the connective constant for $2n$-edge SAPs in an (L, M)-tube (defined in Theorem 2.7). In addition to these bounds found in [3], a new lower bound on $\kappa_p(L, M; f)$ for $f < 0$ can be found by using results from the compact case as follows. Recall $\hat{Z}_{2n}(L, M; f) = \sum_m p_{2n,m}(L, M)e^{fm}$. Notice that if we have a compact polygon with span m^c in an (L, M)-tube, then $(L + 1)(M + 1)(m^c + 1) = 2n$. Solving for m^c, we obtain $m^c = m^c(n) = \frac{2n}{(L+1)(M+1)} - 1$ for a compact polygon. Then if we look at the subset of $2n$-edge SAPs with span $m^c(n)$ that were counted in $p_{2n,m}(L, M)$ and call this count $p_{2n,m^c(n)}(L, M)$, then we have

$$p_{2n,m^c(n)}(L, M)e^{fm} \leq \sum_m p_{2n,m}(L, M)e^{fm} = \hat{Z}_{2n}(L, M; f). \tag{5.9}$$

Using this, taking the log of both sides of the above inequality, dividing by $2n$, and letting $n \to \infty$, we obtain:

$$\frac{f}{(L + 1)(M + 1)} + \kappa_p^c(L, M) \quad \leq \quad \kappa_p(L, M; f), \tag{5.10}$$

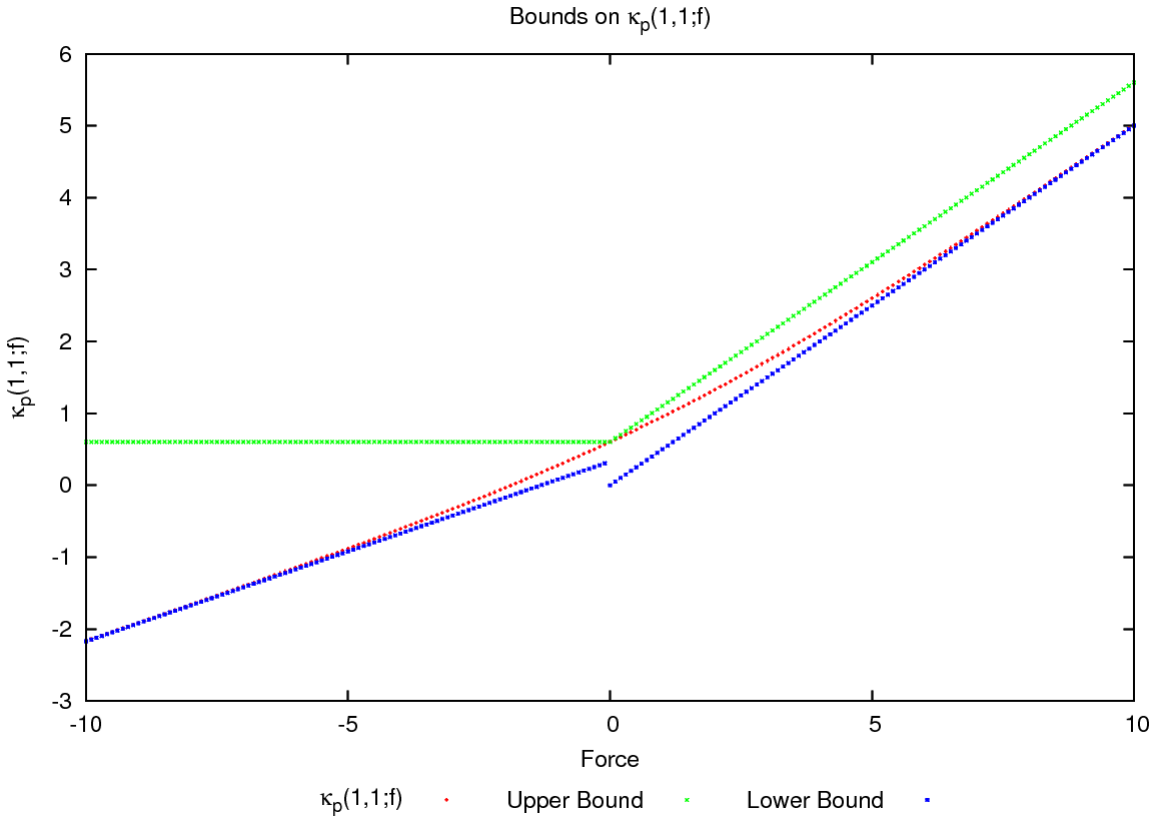

Figure 5.2: $\kappa_p(1,1;f)$, along with its bounds for varying force.

where $\kappa_p^c(L,M)$ is the connective constant for compact polygons in an (L,M)-tube (defined in equation (4.3)).

For (L,M)-tube sizes of $(2,0)$ to $(8,0)$, $\kappa_p(L,M;f)$ was found for fixed values of f, for $-15 \leq f \leq 15$. For (L,M)-tube sizes of $(1,1)$, $(2,1)$, $(3,1)$, and $(2,2)$, $\kappa_p(L,M;f)$ was found for fixed values of f, for $-10 \leq f \leq 10$. Note that the lower bound for $f < 0$ in the $(2,2)$ case is still being verified, since $\kappa_p^c(2,2)$ is still being verified. For all of these tube sizes, the bounds in Theorem 5.2, as well as the bound in equation (5.10) were satisfied. See Figures 5.2, 5.3, 5.4, and 5.5 for graphs of $\kappa_p(L,M;f)$ and its bounds in tube sizes of $(1,1)$, $(2,1)$, $(3,1)$, and $(2,2)$.

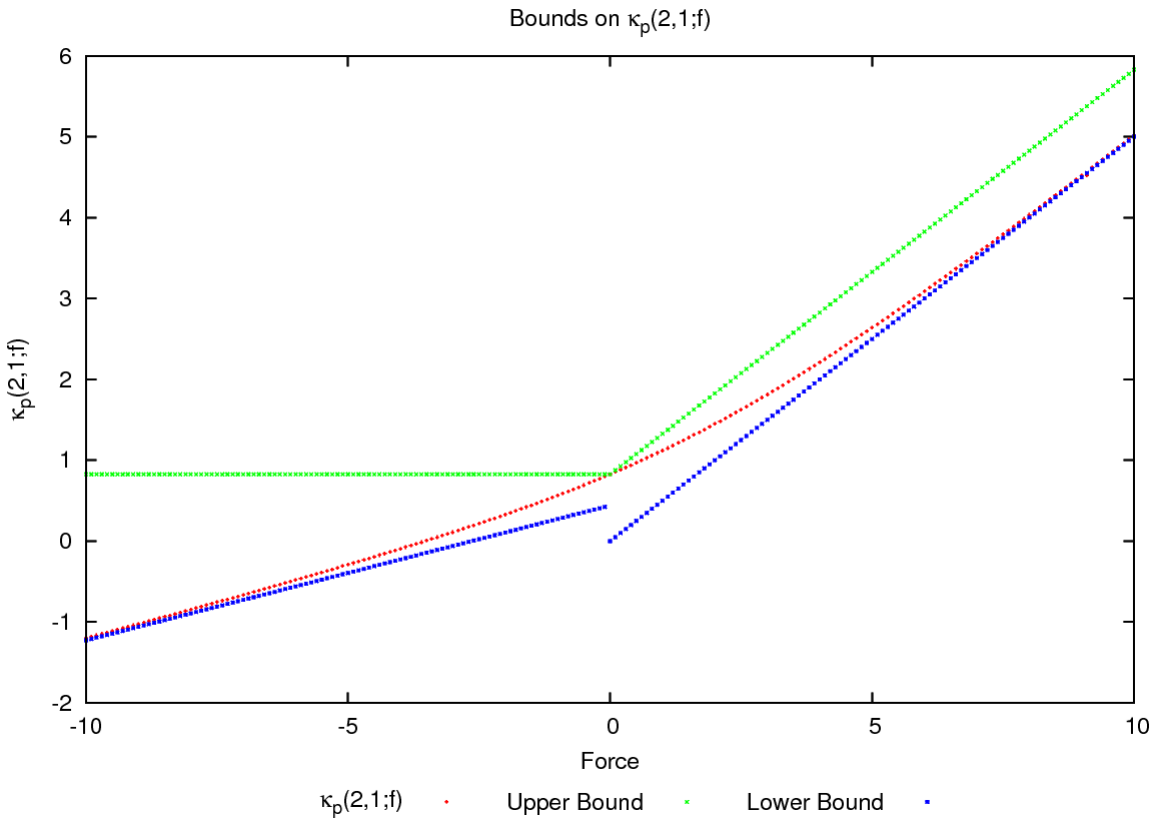

Figure 5.3: $\kappa_p(2,1;f)$, along with its bounds for varying force.

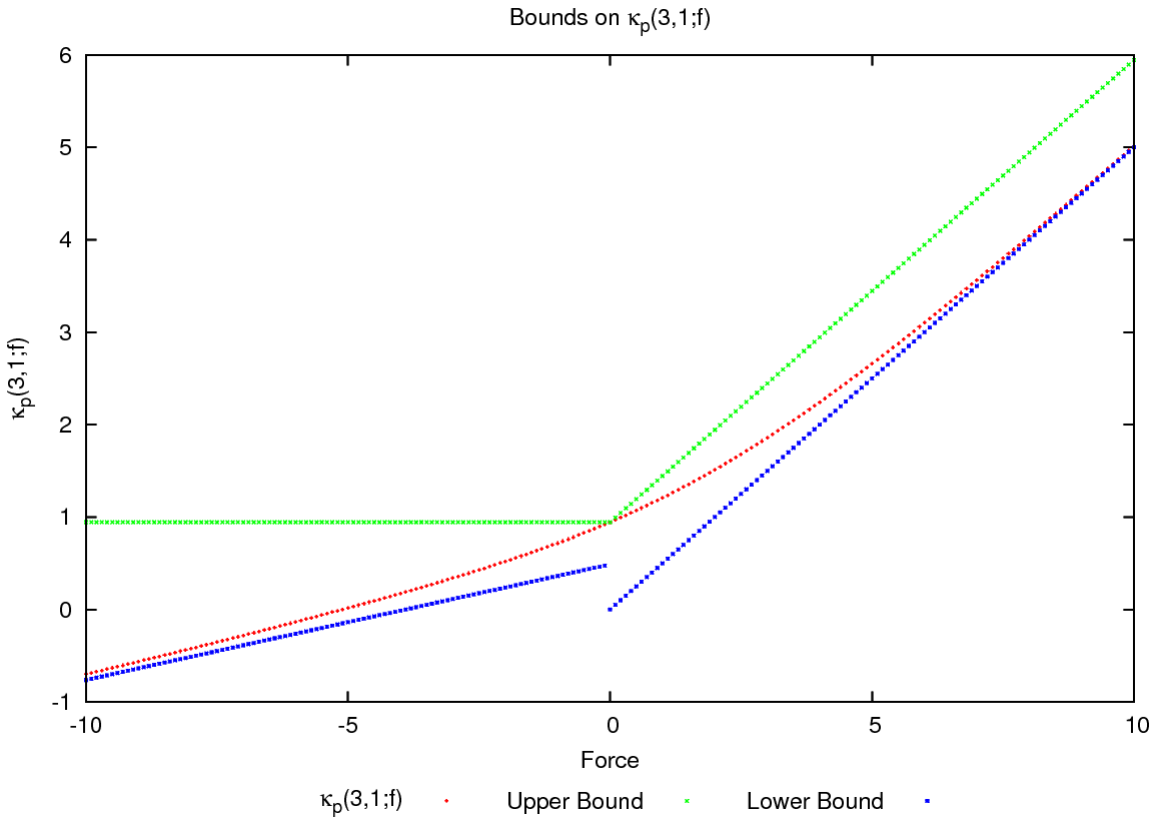

Figure 5.4: $\kappa_p(3,1;f)$, along with its bounds for varying force.

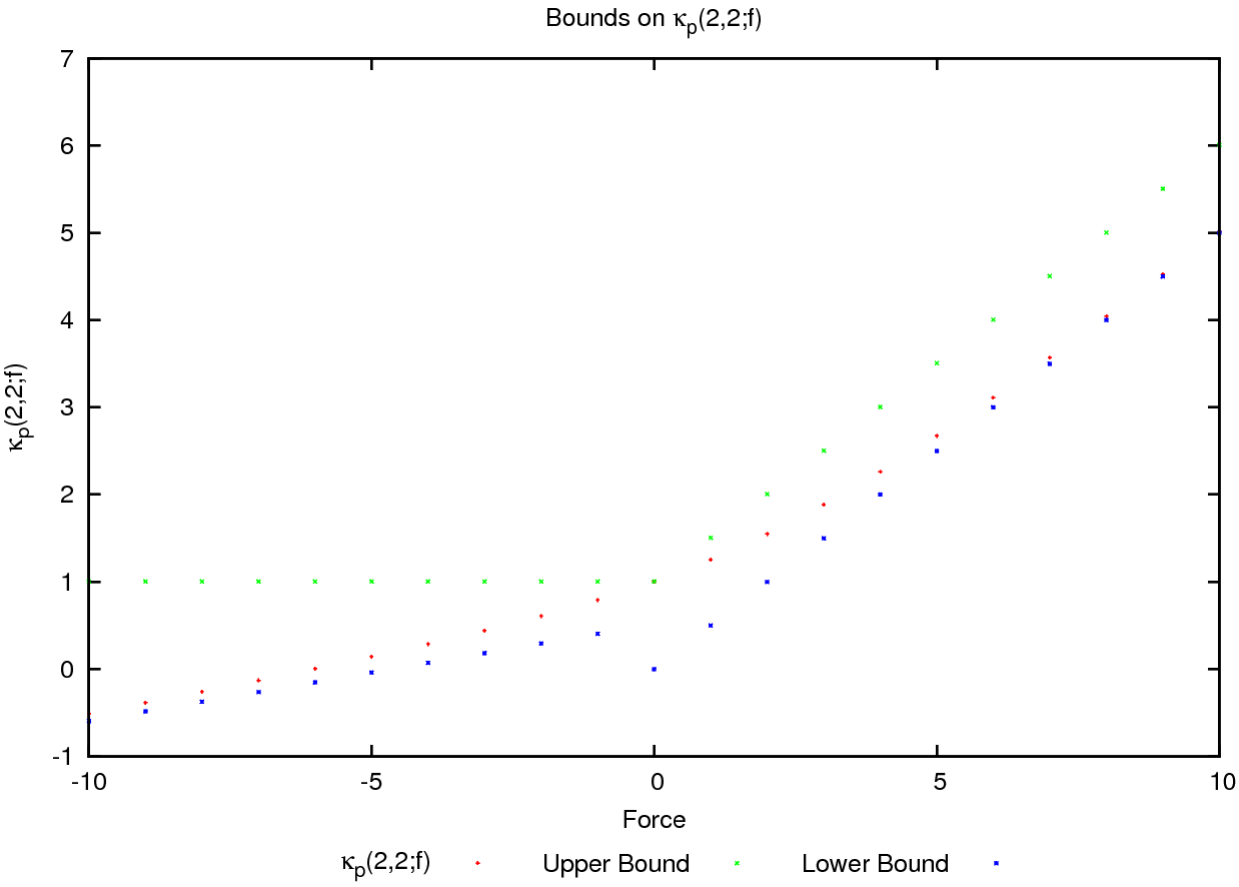

Figure 5.5: $\kappa_p(2, 2; f)$, along with its bounds for varying force.

5.3 Expected Number of Occurrences Per Edge of a k-span in a Random $2n$-edge SAP (as $n \to \infty$), Subject to an External Force

For the model which includes an external force f, the corresponding transfer matrix is defined in equation (5.2). For fixed f, this is equivalent to multiplying the original transfer matrix $G(x)$ by the constant e^f. Thus, by using $G(x, f)$ instead of $G(x)$ and following the arguments leading up to equation (3.58), we obtain:

$$\begin{aligned}\lim_{n\to\infty} \frac{\mathrm{E}_{2n}(\psi_{\pi_1\pi_2\ldots\pi_h})}{2n} &= \left(\frac{\eta(f)_{\pi_1}\xi(f)_{\pi_1}}{\beta_f}\right)\left(x_0(f)^{e_{\pi_1}} e^f \frac{\xi(f)_{\pi_2}}{\xi(f)_{\pi_1}}\right)\cdots\left(x_0(f)^{e_{\pi_{h-1}}} e^f \frac{\xi(f)_{\pi_h}}{\xi(f)_{\pi_{h-1}}}\right) \\ &= \frac{\eta(f)_{\pi_1} x_0(f)^{e_{\pi_1}+e_{\pi_2}+\cdots e_{\pi_{h-1}}} e^{f(h-1)} \xi(f)_{\pi_h}}{\beta_f}, \qquad (5.11)\end{aligned}$$

where $\eta(f)^\top$ and $\xi(f)$ are, respectively, the left and right eigenvectors of $G(x, f)$, and $\beta_f = x_0(f)(\eta(f)^\top G'(x_0(f))\xi(f))$. Thus, equation 5.11 gives the expected number of occurrences per edge of a k-span, that consists of the $h = k - 1$ 2-spans $(\pi_1, \pi_2, ..., \pi_h)$, in a random $2n$-edge SAP (as $n \to \infty$), subject to an external force f.

In Section 3.6, the transfer matrix was implemented on the computer, and values such as $x_0(f)$, β_f, $\eta(f)^\top$, and $\xi(f)$ were found directly from the transfer matrix. The expected number of occurrences of some certain 2-spans were found in a $(2, 1)$-tube, with $-10 \le f \le 10$. See Figure 5.6 for which 2-spans were used.

Notice in Figure 5.6 how different 2-spans are affected differently by the force. An "elongated" 2-span like 2-span #1 has its expected number of occurrences increase quickly as the force increases. A 2-span like 2-span #48 which is not really "compressed" or "elongated" has a peak to its expected number of occurrences at a certain force. A "compressed" 2-span like 2-span #726 has every vertex filled and contains relatively a lot of edges. Its expected number of occurrences decrease as the force increases.

Also, using the computer implemenation of the transfer matrix, three "tight" trefoil 6-spans also had their expected number of occurrences calculated directly from the transfer matrix. See Figure 5.7 for a picture of these three 6-spans and for how the expected number of occurrences change with force for these tight trefoil 6-spans. Notice that since they are "tight," they have relatively lots of edges, and thus their expected number of occurrences decrease as force increases.

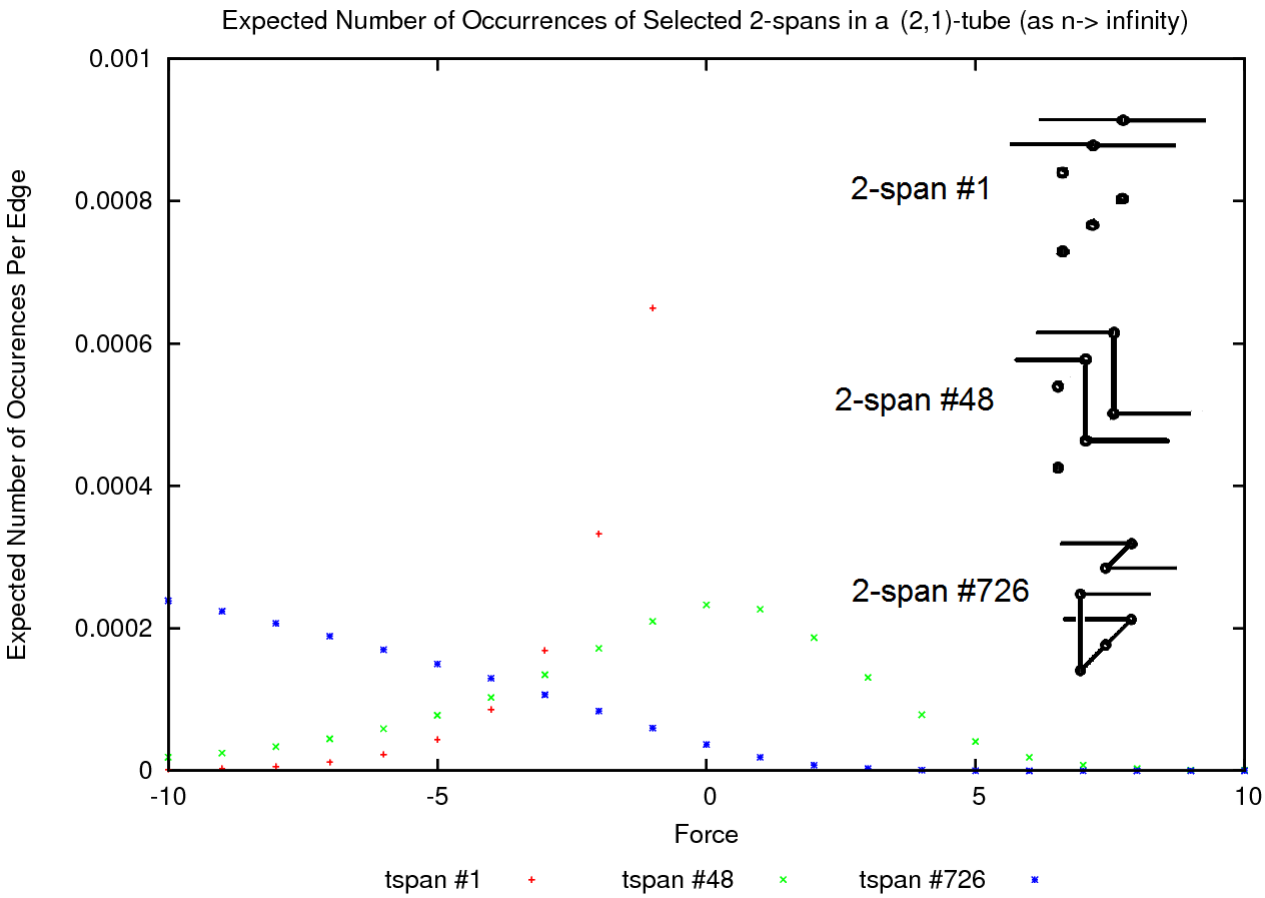

Figure 5.6: Expected number of occurrences per edge of selected 2-spans in a $(2, 1)$-tube, as a function of force.

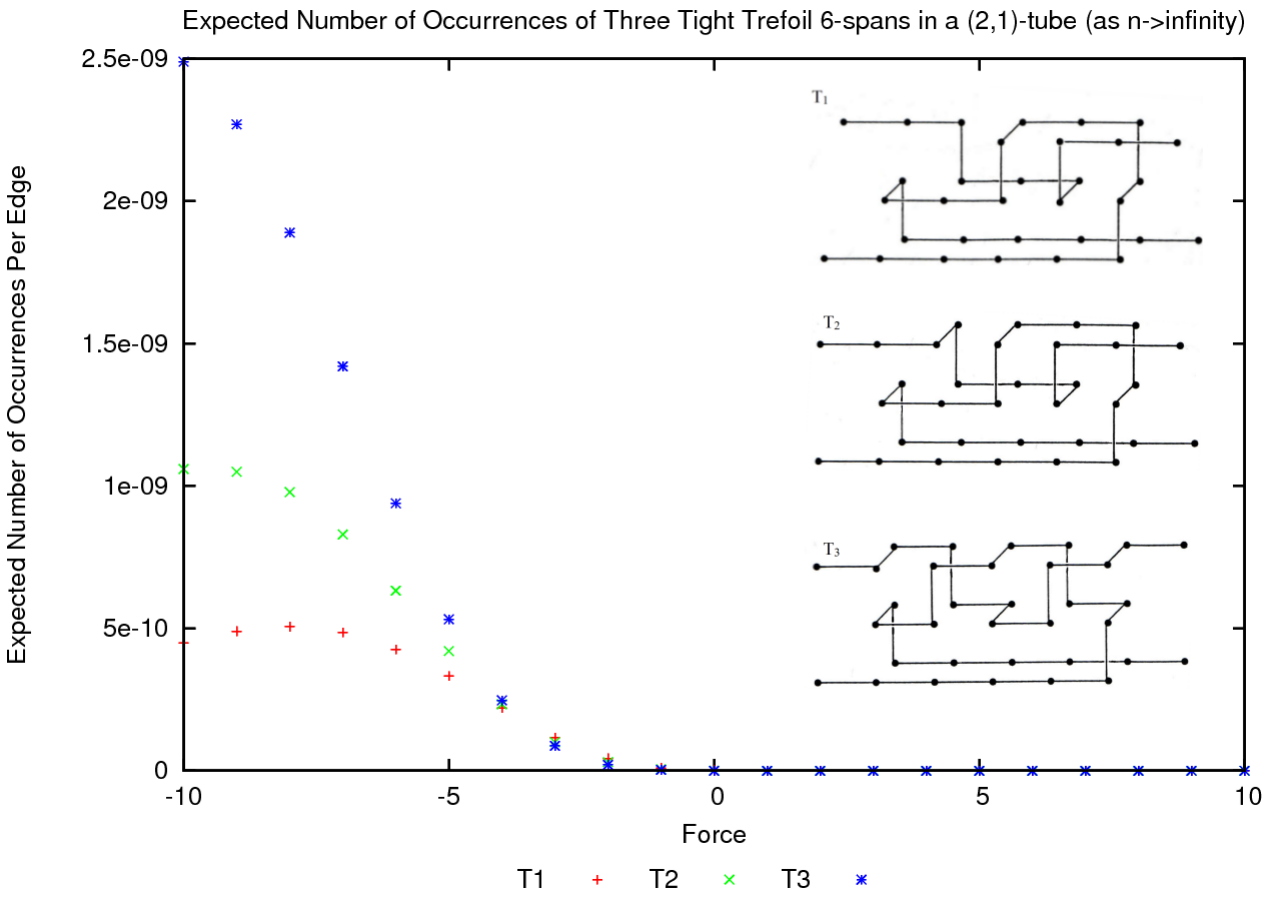

Figure 5.7: Expected number of occurrences per edge of three tight trefoil 6-spans in a $(2, 1)$-tube, as a function of force.

5.4 Expected Span Per Edge of a Random $2n$-edge SAP (as $n \to \infty$), Subject to an External Force

First, as was done in section 3.3, define:

$$C(x_0, f) = \sum_{i=1}^{|\mathcal{H}_s|} \sum_{j=1}^{|\mathcal{H}_f|} \Big[A(x_0)\xi(f)\eta(f)^\top B(x_0) \Big]_{i,j}. \tag{5.12}$$

Then, as was done in the previous section, by using $G(x, f)$ instead of $G(x)$ and following the arguments leading up to equation (3.68), we obtain:

$$\begin{aligned} \mathrm{E}_{2n,2}(m) &\sim \frac{4\beta_f^{-2} C(x_0, f)(n+1)(x_0(f)e^f)^{-2n}}{2\beta_f^{-1} C(x_0, f)(x_0(f)e^f)^{-2n}} \\ &\sim \frac{2(n+1)}{\beta_f}, \end{aligned} \tag{5.13}$$

as $x \to x_0(f)$. Thus, we have

$$\begin{aligned} \lim_{n\to\infty} \mathrm{E}_{2n}(m) &= \left(\frac{1}{\beta_f}\right) 2n \\ \lim_{n\to\infty} \frac{\mathrm{E}_{2n}(m)}{2n} &= \beta_f^{-1}, \end{aligned} \tag{5.14}$$

which gives us an equivalent expression for the expected span per edge of a random $2n$-edge SAP (as $n \to \infty$), subject to an external force.

Using calculations directly from the computer implementation of the transfer matrix (covered in Section 3.6), the expected span per edge was found for SAPs in tube sizes of $(1, 1)$, $(2, 1)$, $(3, 1)$, and $(2, 2)$, for $-10 \le f \le 10$. Figure 5.8 shows how the expected span of a $2n$-edge polygon changes with the tube size, as well as force. Notice that as $f \to \infty$, the size of the tube has little effect on the expected span. This can be thought of as the polygon being fully elongated (so there are only two edges in each section), so the tube restraint has very little effect on the polygon. If a $2n$-edge polygon is fully elongated, it has span $m = \frac{2n-2}{2}$. Thus, as $f \to \infty$, it is expected that

$$\lim_{n\to\infty} \frac{\mathrm{E}(m)}{2n} = \frac{1}{2}. \tag{5.15}$$

Also notice that as $f \to -\infty$, the expected span seems to approach a limit, which seems to differ depending on the tube size. When $f \to -\infty$, the polygon can be thought of as being fully compressed in the tube, such that every vertex is filled (i.e. a compact polygon). Notice that if we have an (L, M)-tube with span m, there are $(L+1)(M+1)(m+1)$ vertices. So if a $2n$-edge

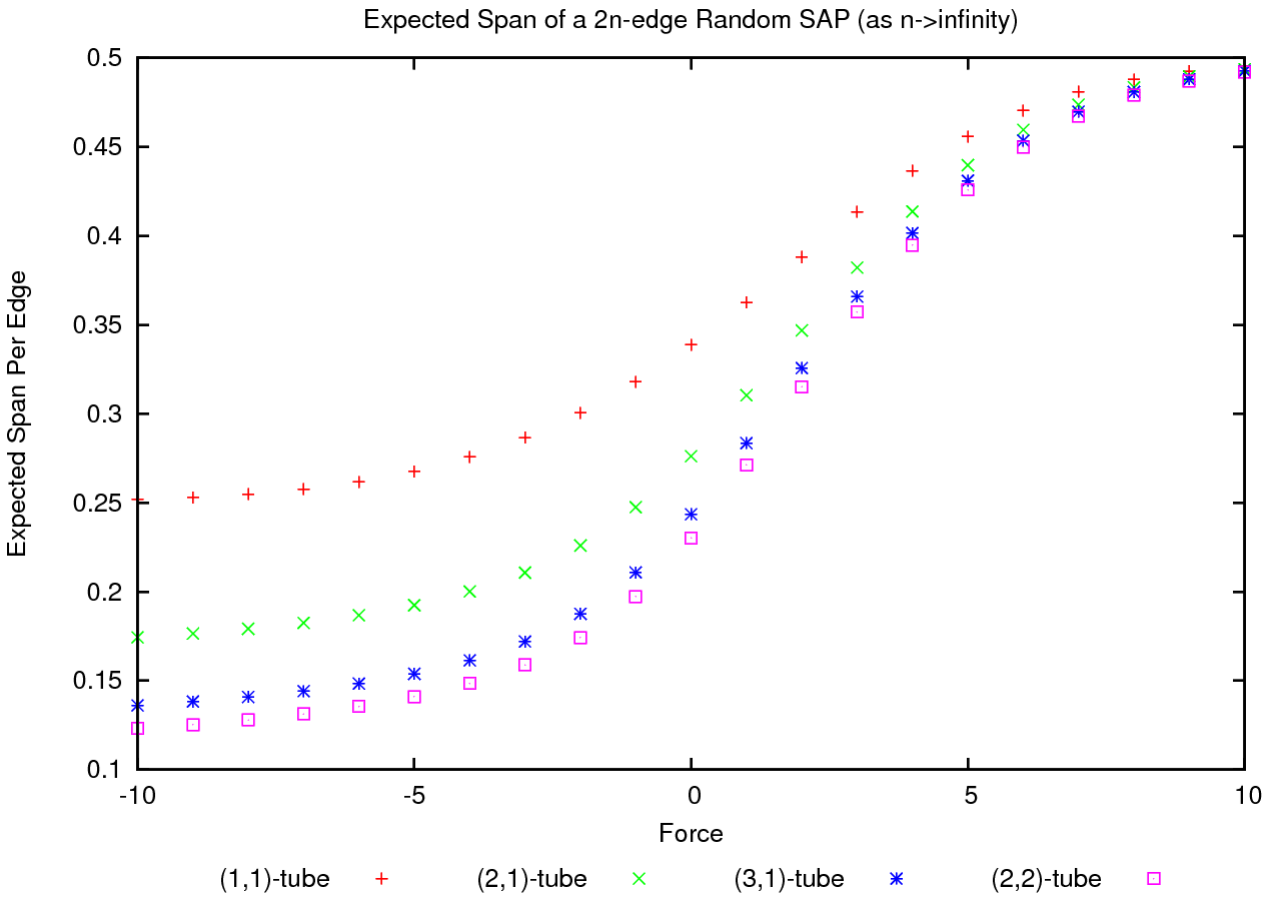

Figure 5.8: Expected span per edge of a random $2n$-edge SAP, as a function of force.

polygon fills every vertex in an (L, M)-tube with span m, ($(L+1)(M+1)(m+1)$ must be an even number), then we know the exact relationship between the polygon length ($2n$) and the polygon span (m) is $2n = (L+1)(M+1)(m+1)$. Solving for m, we have:

$$m = \left(\frac{1}{(L+1)(M+1)} \right) 2n - 1. \tag{5.16}$$

Thus, as $f \to -\infty$, it is expected that

$$\lim_{n \to \infty} \frac{\mathrm{E}(m)}{2n} = \frac{1}{(L+1)(M+1)}. \tag{5.17}$$

Chapter 6

Conclusions and Future Work

6.1 Conclusions

In this thesis, a review was conducted on how a transfer matrix approach resulted in a pattern theorem for SAPs in (L, M)-tubes, and a more general proof than the proof given in [24] was presented. An expression for the expected number of occurrences per edge of a k-span in a random $2n$-edge SAP in an (L, M)-tube (as $n \to \infty$) was found, and it was also shown how an expression for the expected span of a random $2n$-edge SAP in an (L, M)-tube (as $n \to \infty$) could be obtained. The algorithm for creating an appropriate transfer matrix was reviewed, and new numerical results for relatively small tube sizes (obtained from a computer implementation of the transfer matrix) were presented. Regarding compact polygons, a new concatenation theorem for compact polygons was developed and proved, and a transfer matrix approach involving compact k-spans resulted in a new pattern theorem for compact polygons. Using the 2-span information obtained during the transfer matrix generation, a new algorithm for generating polygons in an (L, M)-tube was presented, and compact polygons were generated in $(2, 1)$ and $(3, 1)$-tubes for relatively small spans, with the knot types of the polygons being identified. Lastly, a review of applying an external force to the model was presented, and a new lower bound for negative forces, along with the previously found bounds on the limiting free energy were verified (for relatively small tube sizes).

6.2 Future Work

Due to the memory restriction of computers, transfer matrices were only generated for relatively small tube sizes. Larger tube sizes may be possible by re-defining a k-span to not include order and direction, but instead just include which edges are present, and which edges must "hook up" outside of the k-span. This would reduce the number of k-spans, which would in turn reduce the amount of memory required to (abstractly) store the transfer matrices.

Regarding the generation process, once again, the memory restriction of computers allowed only compact SAPs with small span to be generated. Larger spans are possible by not generating all polygons of a certain span, but instead taking a sample of the polygons with a certain span. This could be done using the transition probabilities from equation (3.57) to choose which 2-span comes next in the generation process. Thus, you could get generate polygons with a larger span by generating a sample of polygons, instead of generating the whole set.

Another area of interest is exploring more about how the probability of a polygon being knotted depends on the force. This could be done by generating all k-spans (for some fixed large enough k) that guarantee a polygon is knotted, and then calculating the sum (over all of these k-spans) of the expected number of occurrences of these k-spans, and observing how this changes as a function of force. This could also be done for other interaction parameters besides force. Some possible interaction parameters include the number/type of right angles or the number of contacts. It could then be examined how these parameters influence the probability that a polygon is knotted.

References

[1] S. Alm and S. Janson. Random self-avoiding walks on one-dimensional lattices. *Communications in Statistics. Stochastic Models*, 6(2):169–212, 1990.

[2] M. Atapour. *Topological Entanglement Complexity of Systems of Polygons and Walks in Tubes.* PhD thesis, University of Saskatchewan, Saskatoon, Saskatchewan, Canada, 2008.

[3] M. Atapour, C. Soteros, and S. Whittington. Stretched polygons in a lattice tube. *Journal of Physics A: Mathematical and Theoretical*, 42(32), 2009.

[4] A. Bates and A. Maxwell. *DNA Topology.* Oxford University Press, New York, New York, United States of America, 2005.

[5] N. Clisby, R. Liang, and G. Slade. Self-avoiding walk enumeration via the lace expansion. *Journal of Physics A: Mathematical and Theoretical*, 40(36), 2007.

[6] P. Cromwell. *Knots and Links.* Cambridge University Press, 2004.

[7] M. Delbruck. Mathematical problems in the biological sciences. *Proc. Symp. Appl. Math.*, 14:55, 1962.

[8] Y. Diao, N. Pippenger, and D. Sumners. On random knots. *Journal of Knot Theory and Its Ramifications*, 3(3):419–429, 1994.

[9] A. Duffy. Asymptotic properties of self-avoiding polygons in (L, M)-prisms, using a transfer matrix approach. Unpublished, 1998.

[10] H. Edelsbrunner and J. Harer. *Computationaly Topology - An Introduction.* The American Mathematical Society, Providence, Rhode Island, United States of America, 2010.

[11] O. Farago, Y. Kantor, and M. Kardar. Pulling knotted polymers. *Europhysics Letters*, 60(1):53–59, 2002.

[12] H. Frisch and E. Wassermann. *J. Am. Chem. Soc.*, 83:3789, 1961.

[13] J Hammersley. The number of polygons on a lattice. *Mathematical Proceedings of the Cambridge Philosophical Society*, 57(3):516–523, 1961.

[14] J. Hammersley. On the rate of convergence to the connective constant of the hypercubical lattice. *Quart. J. Math. Oxford*, 12(2):250–256, 1961.

[15] J. Hammersley and K. Morton. Poor man's monte carlo. *Journal of the Royal Statistical Society. Series B (Methodological)*, 16(1):23–38, 1954.

[16] H. Kesten. On the number of self-avoiding walks. *Journal of Mathematical Physics*, 5, 1963.

[17] N. Madras and G. Slade. *The Self-Avoiding Walk*. Birkhäuser, Boston, Massachusetts, United States of America, 1993.

[18] D. Marenduzzo, C. Micheletti, and E. Orlandini. Biopolymer organization upon confinement. *Journal of Physics: Condensed Matter*, 22(28), 2010.

[19] C. Micheletti and E. Orlandini. Knotting and metric scaling properties of DNA confined in nano-channels: a monte carlo study. *Soft Matter*, 8, 2012.

[20] C. Moraes, S. Srivastava, I Kirkinezos, J. Oca-Cossio, C. vanWaveren, M. Woischnick, and F. Diaz. Mitochondrial DNA structure and function. *International Review of Neurobiology*, 53:3–23, 2002.

[21] E. Rensburg, E. Orlandini, M. Tesi, and S. Whittington. Knotting in stretched polygons. *Journal of Physics A: Mathematical and Theoretical*, 41(1), 2008.

[22] H. Schaefer. *Banach Lattices and Positive Operators*. Springer-Verlag, Berlin, Germany, 1974.

[23] R. Scharein. The knotplot site. http://knotplot.com.

[24] C. Soteros. Knots in graphs in subsets of $\mathbb{Z}^3$. *Institute for Mathematics and Its Applications*, 103:101–134, 1998.

[25] C. Soteros, D. Sumners, and S. Whittington. Entanglement complexity of graphs in $\mathbb{Z}^3$. *Mathematical Proceedings of the Cambridge Philosophical Society*, 111(1):75–91, 1992.

[26] C. Soteros and S. Whittington. Lattice models of branched polymers: Effects of geometrical constraints. *Journal of Physics A: Mathematical and General*, 22(24), 1989.

[27] R. Stanley. *Enumerative Combinatorics*. Wadsworth and Brooks/Cole, 1986.

[28] J. Sulkowska, J. Noel, and J. Onuchic. Energy landscape of knotted protein folding. *Proceedings of the National Academy of Sciences of the United States of America*, 109(44), 2012.

[29] D. Sumners and S. Whittington. Knots in self-avoiding walks. *Journal of Physics A: Mathematical and General*, 21(7), 1988.

[30] C. Vanderzande. *Lattice Models of Polymers*. Cambridge University Press, New York, New York , United States of America, 1998.

[31] A. Vologodskii. Circular DNA. *OnLine Biophysical Chemistry Textbook*, 1999. http://www.biophysics.org/portals/1/pdfs/education/vologodskii.pdf.

Appendix A

Details of the 2-span Generation Algorithm

The algorithm presented in this appendix was developed by Duffy in [9]. This algorithm was used to generate all valid sections and 2-spans in a given (L, M)-tube. This algorithm uses five main functions (or procedures):

- enterhinge()
- leavehinge()
- rowedges()
- coledges()
- recordtemplate()

The function enterhinge() is called by the main program which loops through each possible edge in the first (left) section. That is to say, enterhinge() is called with the location of the edge of entry passed as a parameter. Within the function enterhinge() one can imagine a self-avoiding walk in progress which now has the choice of leaving the hinge, or possibly turning in or out, or turning up or down (See Figure A.1). In the former case, leavehinge() is called, and in the latter cases, rowedges() and coledges() are called, respectively.

In the function leavehinge() the walk can be imagined to be travelling further along (left or right) the (L, M)-tube (outside of the 2-span being generated). If the walk is leaving to the right of the hinge, it must eventually re-enter the hinge since it is part of a closed polygonal walk that started left of the hinge. If the walk is leaving to the left of the hinge, the 2-span is checked if it is a valid 2-span. This check involves making sure there are at least two edges in the right section of the 2-span (to ensure this is not an "end pattern"), as well as making sure the 2-span can "hook up" to ϕ, the pattern defined in Section 3.3. This ensures the generated 2-span can actually occur in a polygon, as there are examples of 2-spans that can never be "closed off" (See Figure A.2). If the generated 2-span is a valid 2-span, then it is recorded using the function recordtemplate(). The function leavehinge() then calls enterhinge() for each available edge in order for the walk to remain self-avoiding and to explore all possibilities.

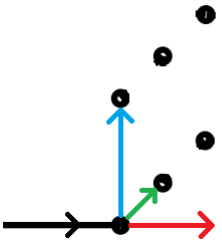

Figure A.1: After entering the hinge, the SAW can leave the hinge, or possibly turn in or out, or up or down. In this case, the SAW has the options of leaving the hinge, turning up, or turning in.

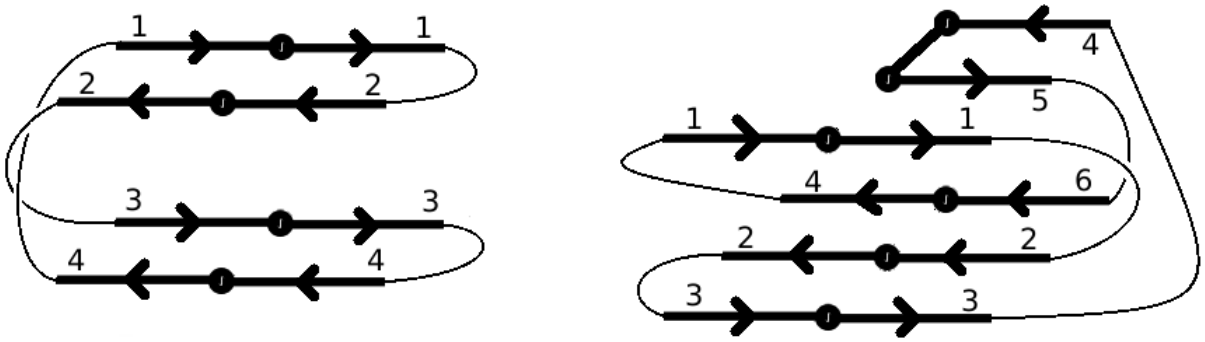

Figure A.2: An example of two invalid 2-spans. The 2-span on the left cannot be closed off on the left, and the 2-span on the right cannot be closed off on the right.

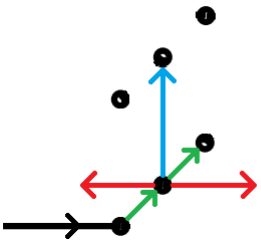

Figure A.3: In this case, enterhinge() was called, followed by rowedges(). Now from within rowedges(), the functions leavehinge(), rowedges(), and coledges() could be called. This ensures all possible SAWs are explored.

If leavehinge is not called and the walk is still in the hinge, then in, out, up, and down turns are explored using the functions rowedges() and coledges(). The algorithm allows for the consideration of all potential 2-spans by then calling leavehinge(), rowedges(), and coledges() from within these functions (see Figure A.3 for an example). Essentially, at each step in the walk all available directions are considered. The following is pseudocode which illustrates how these ideas are implemented:

```
enterhinge
    leavehinge(out opposite side in which entered hinge so as not to trace back)
    rowedges()
    coledges()
leavehinge
    if we have a valid 2-span
        recordtemplate()
    for each available edge
        enterhinge(at available edge)
rowedge
    if vertex toward the inside is free
        move in
        leavehinge(out left side)
        leavehinge(out right side)
        rowedges()
        coledges()
    if vertex toward the outside is free
        move out
        leavehinge(out left side)
        leavehinge(out right side)
        rowedges()
        coledges()
coledge
    if vertex toward the upside is free
        move up
        leavehinge(out left side)
        leavehinge(out right side)
        rowedges()
        coledges()
    if vertex toward the downside is free
        move down
        leavehinge(out left side)
        leavehinge(out right side)
        rowedges()
        coledges()
```

Appendix B

Numbering Sections

Unless stated otherwise, this appendix is based on [9], where Duffy developed a numbering scheme for sections in an (L, M)-tube. Notice that any section of a SAP (or 2-span) can be viewed as a set of an even number of ordered edges that are located in the $(L+1)(M+1)$ possible "slots" of the section, in the yz-plane. *Slots* are the possible spots where an edge could occur in a section. These slots can be ordered lexicographically: let slot i have coordinates (y_i, z_i) and slot j have coordinates (y_j, z_j); then slot $i <$ slot j if:

1. $z_i < z_j$, or
2. $z_i = z_j$ and $y_i < y_j$.

In order to store the configuration of a given section efficiently, a function which assigns a distinct number to a given section such that this number, $N(section)$, obeys the following inequality was used:

$$1 \leq N(section) \leq \sum_{n=1}^{V} \binom{V}{2n} (2n)! \tag{B.1}$$

where V is the number of slots in the section. That is, given an (L, M)-tube, $V = (L+1)(M+1)$. Notice that the upper bound of this inequality is the number of ways to choose an even number of edges from V edges, times the number of ways to order the chosen even number of edges. The number of "valid" sections seems to approach this upperbound as the tube size increases, thus each section will be assigned a distinct number which only requires as much space to store $\sum_{n=1}^{V} \binom{V}{2n} (2n)!$

The arguments to the function, which have been collectively called *section* thus far, are the number of slots V, the number of edges in the given section F, and E_1, E_2, ..., E_F which characterize the positions of the edges in the section as follows:

$$E_i = slot(E_i) - \sum_{n=1}^{i-1} H(slot(E_i) - slot(E_n)) \tag{B.2}$$

where H(n) is the discrete heaviside unit step function:

$$H(n) = \begin{cases} 0 & \text{if } n < 0 \\ 1 & \text{if } n \geq 0 \end{cases} \tag{B.3}$$

and $slot(E_i)$ gives the slot number that edge E_i occupies. The slots are considered to be numbered 1 through V, following the lexicographical ordering described above.

Essentially, the value of E_i is determined by which available slot the i^{th} edge occupies, after all of the previous $i-1$ edges have been put into slots. For example, E_1 is determined by which available slot the first edge occupies. If the first edge is in the ath available slot then $E_1 = a$; Henceforth, this slot is not available to subsequent edges, and there is then one less available slot to subsequent edges. So when E_2 is being determined, the slot which E_1 occupied is essentially ignored, and not counted as an available slot.

The function $N(section)$ is then constructed by first defining the following coefficients:

$$C_k = \begin{cases} 1 + \sum_{n=1}^{k/2} \binom{k}{2n}(2n)! & \text{if } k \text{ is even} \\ k + k\sum_{n=1}^{\frac{k-1}{2}} \binom{k-1}{2n}(2n)! & \text{if } k \text{ is odd} \end{cases}$$

Utilizing these formulas, one obtains C_k for k from 0 through 10:

k	0	1	2	3	4	5	6	7	8	9	10
C_k	1	1	3	9	37	185	1111	7777	62217	559953	5599531

which is sufficient to deal with sections with 10 slots. Therefore, this will work for (L, M)-tube sizes of $(1, 1)$, $(1, 2)$, $(1, 3)$ $(1, 4)$, and $(2, 2)$.

The following intermediate functions are defined next, where $H(n)$ is again the heaviside unit step function:

$$\begin{aligned} N_0 &= H(F - A)(C_1(E_{A-1} - 1) + C_0(E_A - 1) + 1) \\ N_1 &= H(F - A + 2)(C_3(E_{A-3} - 1) + C_2(E_{A-2} - 1) + N_0 + 1) \\ &\vdots \\ N_k &= H(F - A + 2k)(C_{2k+1}(E_{A-(2k+1)} - 1) + C_{2k}(E_{A-2k} - 1) + N_{k-1} + 1) \end{aligned}$$

Finally, the section-numbering function is defined as:

$$N(section) = N_{A/2-1} = H(F - 2)(C_{A-1}(E_1 - 1) + C_{A-2}(E_2 - 1) + N_{A/2-2} + 1) \tag{B.4}$$

Appendix C

Numbering Column States

Unless stated otherwise, this appendix is based on [9], where Duffy developed a numbering scheme for column states in an (L, M)-tube, where $L = 0$ or $M = 0$. Without loss of generality, we will assume $L = 0$ and $M > 0$.

Given a column state with a arcs in a $(0, M = d - 1)$-prism, there are:

$$\sum_{m=1}^{a-1} \frac{d!}{m!(m+1)!(d-2m)!} = \sum_{m=1}^{a-1} \binom{2m}{m} \frac{1}{m+1} \binom{d}{2m} \tag{C.1}$$

column states with less arcs, where d is the total number of vertices (i.e. $d = M + 1$). Now let e index the vertices which are occupied by an edge (end of an arc) define:

$$h_e = \begin{cases} 1 & \text{if the vertex } e \text{ is at the left end of the arc} \\ 0 & \text{if the vertex } e \text{ is at the right end of the arc} \end{cases},$$

where the choice of left and right is irrelevant as long as it is consistent, and such that $h_1 = 1$. Now define:

$$n_s = 2s + 1 - e(s+1), \tag{C.2}$$

where $e(s+1)$ is the value of e for which $h_1 + h_2 + \ldots + h_e$ is equal to $s + 1$. Thus n_s is defined for $1 \leq s \leq a - 1$. This defines a unique sequence $(n_1, n_2, \ldots, n_{a-1})$ for each arc arrangement, which can be arranged lexicographically. The sequence has the property $0 \leq n_1 \leq 1$ and $0 \leq n_i \leq n_{i-1} + 1$ for $1 \leq i \leq a - 1$. This implies that for the column states with the same number of arcs there are

$$\sum_{s=1}^{a-1} \frac{n_{a-s}(2s + n_{a-s} - 1)!}{(n_{a-s} + s)!s!} = \sum_{s=1}^{a-1} \binom{2s + n_{a-s} - 1}{s} \frac{n_{a-s}}{n_{a-s} + s} \tag{C.3}$$

arc arrangements of the column states which are lexicographically less than the arc arrangement under consideration. Now given that the number of arcs is a and the number of vertices is d, there are:

$$\binom{d}{2a} \tag{C.4}$$

possible arrangements of the vertices and arc end points. Thus for each lexicographically less arc arrangement, there are $\binom{d}{2a}$ column states with the given arc arrangement. Thus there are:

$$\binom{d}{2a} \sum_{s=1}^{a-1} \frac{n_{a-s}(2s + n_{a-s} - 1)!}{(n_{a-s} + s)!s!} = \binom{d}{2a} \sum_{s=1}^{a-1} \binom{2s + n_{a-s} - 1}{s} \frac{n_{a-s}}{n_{a-s} + s} \tag{C.5}$$

column states which have the same number of arcs, but a lexicographically less arc arrangement than the one under consideration. Since there are $\binom{d}{2a}$ vertex arrangements for the column state under consideration, there is a one-to-one correspondence with the possible combinations of $2a$

numbers from $(1, 2, 3, \ldots, d)$. Now given a combination which we write $(c_1, c_2, c_3, \ldots, c_{2a})$ with the numbers in accending order and defining c_0 as 0 there will be:

$$\sum_{p=c_{q-1}+1}^{c_q-1} \sum_{q=1}^{2a} \frac{(d-p)!}{(d-p-2a+q)!(2a-q)!} = \sum_{p=c_{q-1}+1}^{c_q-1} \sum_{q=1}^{2a} \binom{d-p}{2a-q} \tag{C.6}$$

column states with vertex arrangements which are lexicographically less than the given one, but with the same number of arcs and same arc arrangement. Putting all the relavent equations together, we have a function which numbers a given column state according to its "lexicographical" ordering in the set of all column states with d vertices. The resulting equation is:

$$\sum_{m=1}^{a-1} \binom{2m}{m} \frac{1}{m+1} \binom{d}{2m} + \binom{d}{2a} \sum_{s=1}^{a-1} \frac{n_{a-s}(2s+n_{a-s}-1)!}{(n_{a-s}+s)!s!} + \sum_{p=c_{q-1}+1}^{c_q-1} \sum_{q=1}^{2a} \binom{d-p}{2a-q}. \tag{C.7}$$

Appendix D

The Existence of Two Mutually Exclusive Classes of Compact k-spans when $(L+1)(M+1)$ is Odd

In this appendix, it will be shown that if $(L+1)(M+1)$ is odd, two mutually exclusive classes of compact k-spans are naturally formed. One class (call it class one) can only occur at odd sections of a polygon, while the other class (call it class two) can only occur at even sections of a polygon (recall what it means for a k-span to occur at a section of a polygon from Definition 3.6). Recall that if $(L+1)(M+1)$ is odd, compact SAPs must have an odd span.

To show this, we show that there are no k-spans for which there is a SAP with the k-span occurring at an odd section and another SAP with it occurring at an even section. Without loss of generality, let π_o be a compact k-span which can occur at an odd section of a compact SAP (let ω_1 be such a SAP). We want to show that π_o cannot occur at an even section of any compact SAP. Suppose to the contrary that π_o occurs at an even section of a compact SAP (let ω_2 be such a SAP). Now take ω_1 and delete π_0, along with all edges to the right of π_o, and call the resulting configuration p_1 (see Figure D.1). Take ω_2 and delete all edges to the left of π_o, and call the resulting configuration p_2 (see Figure D.2). Notice that if p_2 is translated such that it lies immediately to the right of p_1, a new SAP (ω_3) is formed (see Figure D.3).

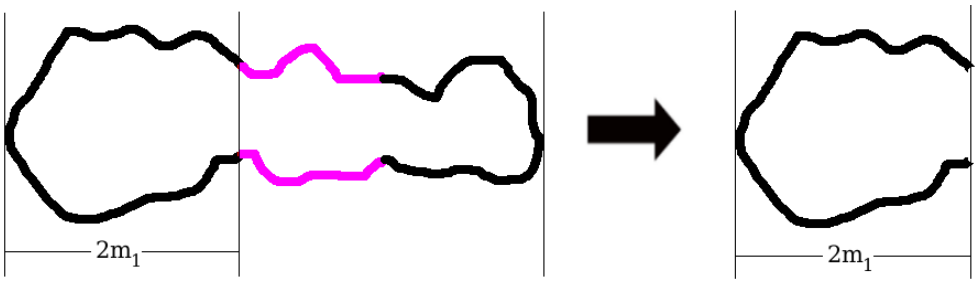

Figure D.1: Obtaining p_1 from ω_1.

Notice that since π_o occurs at an odd section in ω_1, p_1 will occupy an even number of sections ($2m_1$). Also notice that since π_o occurs at an even section in ω_2, p_2 will occupy an even number of sections ($2(m_3 - m_2)$). Thus ω_3 has an even span ($2(m_1 + m_3 - m_2)$), which is a contradiction.

Thus, if $(L+1)(M+1)$ is odd, two mutually exclusive classes of compact k-spans are naturally formed, with one class only occurring at odd sections of compact polygons and the other class only occurring at even sections of compact polygons. Since there are examples of compact polygons with span greater than one, neither of these sets are empty.

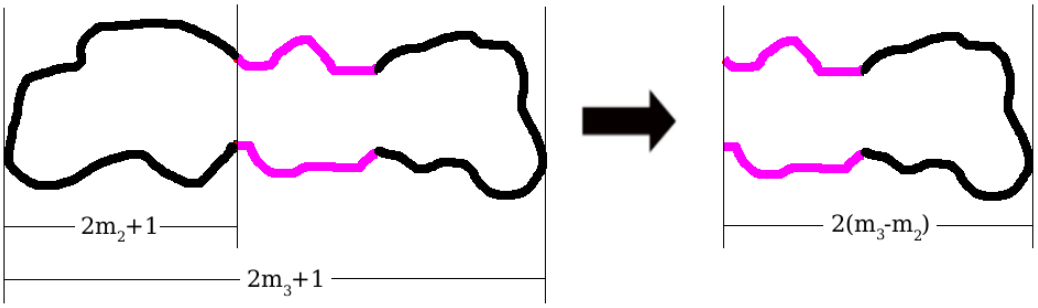

Figure D.2: Obtaining p_2 from ω_2.

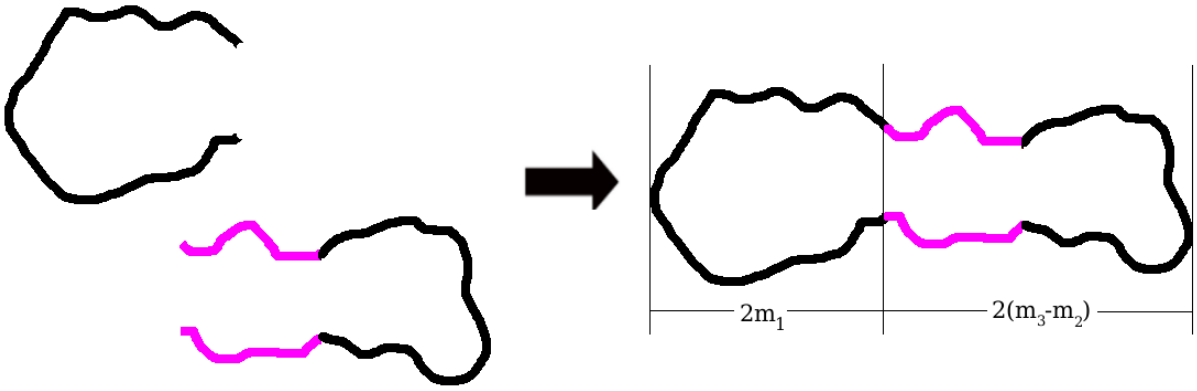

Figure D.3: Combining p_1 and p_2 to create ω_3.